Thesis for the Master's degree in Molecular Biosciences
Main field of study in molecular biology

Tina Hellenes

Mapping the expression of anti-apoptotic proteins and evaluation of the therapeutic potential of TRAIL receptor antibodies in "close-to-patient" melanoma models.

60 study points

Department of Molecular Biosciences
Faculty of mathematics and natural sciences
UNIVERSITY OF OSLO, June 2009

Abstract

Malignant melanoma is a very metastatic and therapy resistant disease, with few therapeutic options in advanced stages. An abnormal apoptosis pathway is considered to contribute substantially to the resistance observed in melanoma patients. In this study, "close-to-patient" melanoma cell models: adherent monolayers in serum-containing media and non-adherent spheroids in stem cell media (which supposedly selects for stem-like melanoma initiating cells), were compared with respect to: the expression of anti-apoptotic molecules from the Inhibitors of Apoptosis Proteins (IAP) family; and sensitivity to the treatment with Tumor Necrosis Factor (TNF) - Related Apoptosis Inducing Ligand (TRAIL), acting through death receptor 4 and 5 (DR4 and DR5), alone or in combination with siRNA-mediated down-regulation of IAPs. Spheroids demonstrated a higher expression of IAPs (in 8 from 15 studied cases), where the IAP livin was up-regulated the most. Also a tendency for up-regulation of DR5 was shown, and the spheroid cells were more sensitive to the DR5-mediated treatment than the monolayer cells, indicating that this strategy might affect tumor initiating cells present in melanoma spheres. The treatment via DR4 had only a negligible effect. Although down-regulation of XIAP showed a small additive effect, the contribution of the XIAP or survivin knock-down to the reduced cell viability or spheroid forming capacity, was very low.

Acknowledgements

This work was preformed at the Gene therapy-group, Department of Tumor Biology, Institute for Cancer Research, Radiumhospital, Oslo University Hospital, in collaboration with the University of Oslo in the period February 2008 to May 2009.

First of all I would like to thank my supervisor Lina Prasmickaite. Your patience has helped me tremendously through the periodic frustration during my practical work, and throughout long lists of questions concerning the theoretical aspect of my experiments. I really appreciate your knowledge and your ability to solve practical problems. Second, I would like to express my gratitude to Birgit Engesæter, my second supervisor, who contributed with knowledge and a critical view. You introduced me to the Gene therapy–group and your project, which gave me an extra motivation before starting my master thesis. Both of you have thought me patience, which I now understand, is one of the most important properties a scientist should have.

I will also take the opportunity to thank supervisor Gunhild M. Mælandsmo for introducing me to the Department of Tumor Biology, and for contribution with objective comments. Additionally, I will thank all members of the Gene Therapy – group for providing a really good work environment. All of you have helped me scientifically, as well as making every day - a good one. Menaka, Geir and Hilde – you could always make me smile!

Last, I will thank my family and Ola, my boyfriend, for patience and helping me think of other things in life than science. Thanks go also to my class mates, especially Guro, who always gives her support and make me think positive.

Tina Hellenes

May 2009

Content

Abbreviations

Ab	Antibody	ILP-2	IAP-Like Protein-2
APS	Ammonium PerSulfate	LDS	Lithium Dodecyl Sulfate
Bcl-2	B-cell lymphoma-2	LP2000	Lipofectamine 2000
BFB	Brom Fenyl Blue	LPMAX	Lipofectamine RNAi MAX
bFGF	basic Fibroblastic Growth Factor	MEF	Mouse Embryonic Fibroblasts
BIRC	Baculovirus IAP repeat containing	miRNA	micro RNA
Bruce	BIR repeat-containing ubiquitin-conjugating enzyme	mono	monolayer
BSA	Bovine Serum Albumin	MOPS	3-(N-morpholino)propanesulfonic acid
BSN	Bjerrum Scāfer Nilsen	mRNA	messenger RNA
CAD	Caspase Activated DNase	MTS	3-(4,5-dimethylthiazol-2-yl)-
CARD	Caspase Recruitment Domain		5-(3-carboxymethoxyphenyl)-
cDNA	complimentary DNA		2-(4-sulfophenyl)-2H-tetrazolium
cFLIP	cellular FLICE-Inhibitory Protein	NAIP	Neuronal Apoptosis Inhibitory Protein
cIAP-1	cellular IAP - 1	PBS	Phosphate Buffered Saline
cIAP-2	cellular IAP - 2	PCR	Polymerase Chain Reaction
CSC	Cancer Stem Cell	PI	Propidium Iodide
Ct	Threshold cycle	PMSF	phenylmethylsulphonylfluoride
DcR1	Decoy Receptor 1	qPCR	quantitative PCR
DcR2	Decoy Receptor 2	RING	Really Interesting New Gene
DIABLO	Direct IAP-binding protein with low pI	RISC	RNA-Induced Silencing Complex
DMEM	Dulbecco's modifed Eagle's medium	RNA	Ribonucleic acid
DNA	Deoxyribonucleic acid	RNAi	RNA interference
DR4	Death Receptor 4	RPLPO	Large Ribosomal Protein
DR5	Death Receptor 5	rpm	rounds per minute
DTIC	Dacarbazine	RPMI	Roswell Park Memorial Institute
ECL	Electrochemiluminescence	RQ	Relative Quantification
EDTA	ethylenediaminetetraacetic acid	RSF	Relative Spheroid Formation
ER	Endoplasmatic Reticulum	SDS	Sodium Dodecyl Sulfate
FAM	Carboxyfluorescein	SDS-PAGE	SDS-Polyacryl Amide Gel Electrophoresis
Fbb	Flow blocking buffer	SFC	Spheroid Forming Capacity
FCS	Fetal Calf Serum	siRNA	small interfering RNA
FITC	Fluorescein isothiocyanate	SPH	spheroids
FSC	Forward Scatter	SSC	Side Scatter
hESCM4	human Embryonic Stem Cell Media 4	TBP	TATA Binding Protein
HGS	Human Genom Sciences	TBST	Tris-Buffered Saline + Tween 20
HMW-MAA	High Molecular Weight melanoma-associated antigen	TEMED	Tetramethylethylenediamine
HRP	Horseradish Peroxidase	TNF	Tumor Necrosis Factor
HSA	Human Serum Albumin	TRAIL	TNF Related Apoptosis Inducing Ligand
IAP	Inhibitors of Apoptosis Proteins	UV	Ultra Violet
IgG	Immunoglobin G	XIAP	X-chromosome IAP

1. Introduction

1.1 Cancer

In 2007 the Word Health Organization reported 7.9 million deaths globally from cancer. Cancer Registry of Norway estimates that one out of three Norwegians will be diagnosed with cancer before the age of 75, and that the overall survival rate after 5 years averagely would be ~60% [1].

When a cell obtains genetic or epigenetic changes that result in proliferation without normal restraints, or reduced ability to die, it will be defined as a cancer cell[2]. Cancer cells may invade nearby tissue, and they may spread through the bloodstream and lymphatic system to other parts of the body. Generally, several independent alterations, like loss of tumor suppressor genes or gain of oncogenes, are needed to form a cancer cell, consistent with, that cancer incidence correlates with age. Both inheritable factors and environmental factors (like chemical carcinogens, ionizing radiation and virus) could influence tumor formation[2,3]. However, 80-90% of cancer incidences are thought to result from environmental factors (www.kreft.no).

A benign tumor consists of abnormal cells growing in a distinct area incorporated in a connective tissue, and is usually curable by surgery. If a tumor consists of cells with invasive properties, it is defined as malignant, and, if not treated, might form metastases at a distant site, i.e. a secondary tumor. A metastatic cancer is often related to a poor outcome[1,2].

Standard therapies of cancer like radiotherapy and chemotherapy, often do not lead to cure due to the presence of therapy resistant cancer cells within a tumor (FIG. 1.1). This will often result in a relapse and formation of a new more resistant tumor.

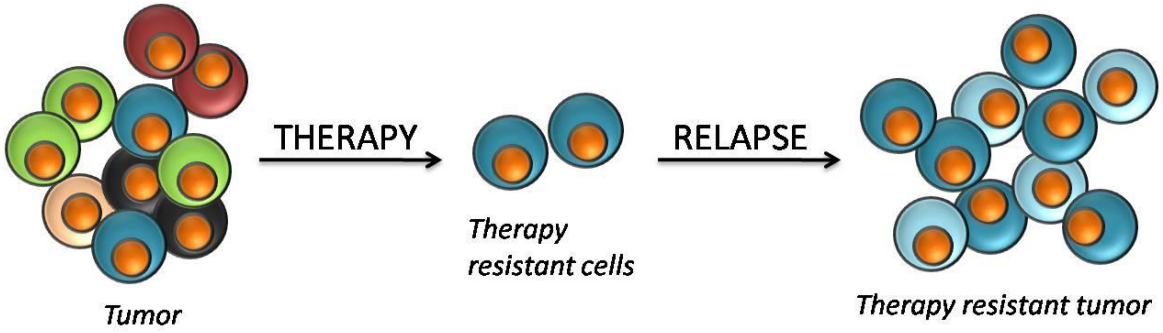

FIG. 1.1: A tumor often consists of heterogeneous cells, where some cells are resistant to therapy and may lead to relapse, forming a new therapy resistant tumor after therapy completion.

1.1.1 Melanoma

Melanoma is a cancer deriving from melanocytes, the pigment melanin producing cells found predominantly in skin[4,5]. Under normal conditions, homeostasis of melanocytes is tightly regulated by keratinocytes. UV radiation triggers keratinocytic stimulation of melanocytes, leading to their proliferation, differentiation and melanin production[5]. In melanoma, this regulation is lost. The classical melanoma progression model emphasizes a stepwise transformation of normal melanocytes to malignant melanoma through several intermediate stages as illustrated in FIG. 1.2[4,6].

Melanoma is the most deadly form of skin cancer and it is considered to be among the most aggressive types of human cancer. The incidence of melanoma is rising in industrialized countries, leading to more than 1 100 Norwegians diagnosed with this disease every year[1,4]. If melanoma is discovered in an early phase, removal of cancerous tissue by surgery is very effective, reflected by good prognosis of 90% survival 5 years after diagnosis (oncolex.no). However, melanoma is highly metastatic and metastasized cells are markedly resistant against all chemotherapeutic drugs[4]. The metastatic disease is incurable in most patients. The median survival of these patients is only 6 months and the 5-year survival rate less than 5 % [4]. The alkylating agent Dacarbazine (DTIC), is the only chemotherapy approved in Norway against advanced melanoma, with no significant effect on overall survival[7].

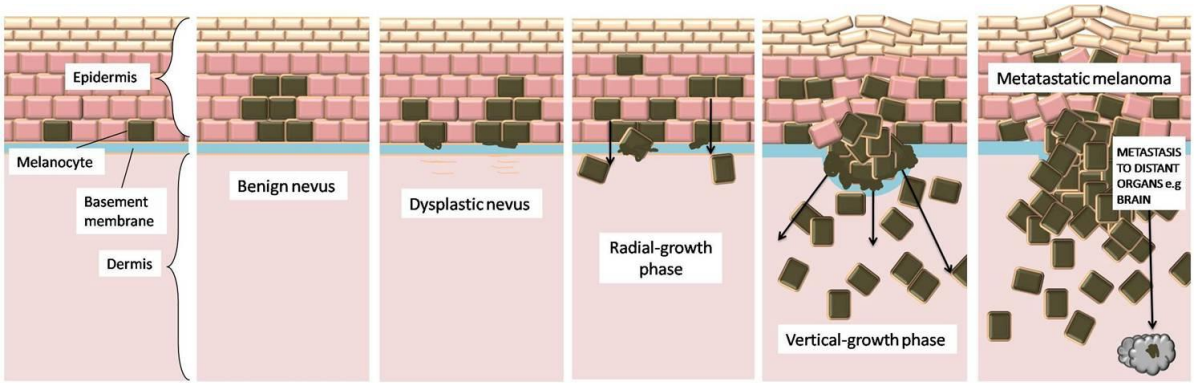

FIG. 1.2: A classical model of melanoma progression through several steps: a benign nevus followed by phases invading the basement membrane, resulting in aggressive metastatic melanoma.

Various combinatorial treatments towards metastatic melanoma are tested in clinical trials, often demonstrated to improve the tumor response rate, but unfortunately not the overall survival of the patient[8,9]. One such promising treatment involves the anti-apoptotic protein Bcl-2 (FIG. 1.4), which is involved in a large trial, which will be finish in 2011 (www.clinicaltrials.gov). A lot of poor responses in clinical trials could be related to the extremely low threshold to give permission for new treatment modalities in melanoma trials[9]. This is of course related to the desperate need for better therapy for patients in advanced stages. A more personalized treatment would very likely be more efficient than therapies used today. If scientists find markers describing cancer stem cells in melanoma (discussed in chapter 1.1.2), this could be the new angle of attack, and contribute to the discovery of novel treatments.

1.1.2 Tumor-initiating cells (Cancer stem cells)

Cells constituting a tumor are heterogeneous, they have different tumor initiating abilities, metastatic potential, sensitivity to therapies etc.[10]. Hence, identification and targeting of the most tumorigenic cells are of great importance in cancer therapy. Traditionally, cancer development has been explained by the clonal evolution model (shown in FIG. 1.3 A) postulating that this is a random process where all cells have an equal probability to be a tumor initiating cell. Selection of the tumorigenic cell best fitted for the given microenvironment would expand and give rise to a tumor[11].

Lately it has been shown that some cancer cells show properties of normal stem cells, e.g.: they can self renew, differentiate and have enhanced resistance mechanisms, (reviewed in[12,13,14]). It has been hypothesized that such rare tumor cells with stem cell properties, often called cancer stem cells (CSC), are responsible for tumor initiation (FIG. 1.3 B). Post-therapy tumor relapse (as shown in FIG. 1.1) or development of metastases also might originate from a CSC, though not necessarily identical to the CSC initiating the primary tumor[15, 13, 16].

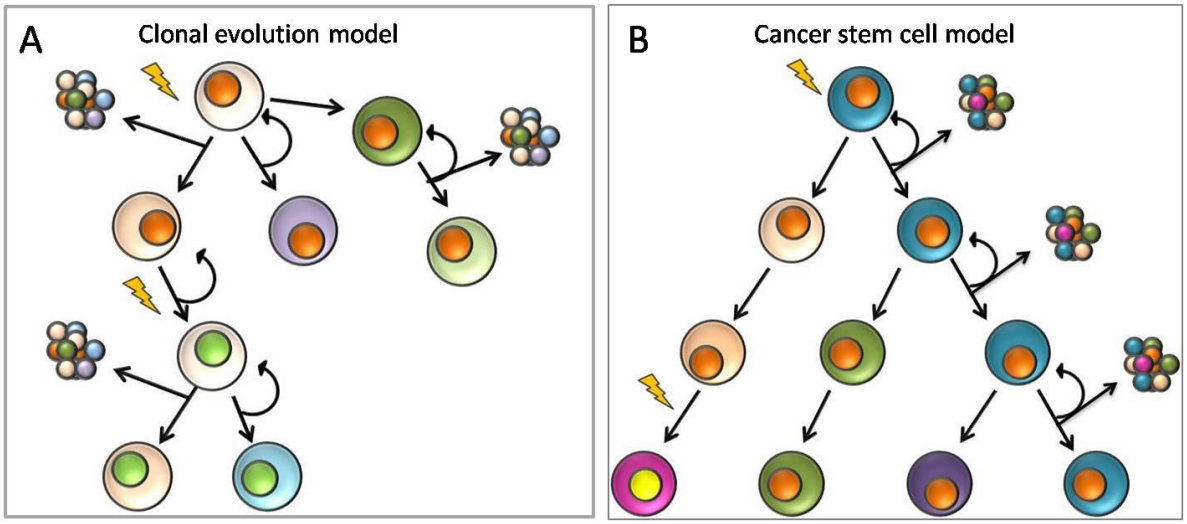

FIG. 1.3: The two models used to explain tumor heterogeneity and proliferation are (A) the clonal evolution model and (B) the cancer stem cell model. The clonal evolution model is based on a random selection of the cell best fitted for the given microenvironment. The cancer stem cell model is based on a non-random cell with certain predetermined properties (stem cell properties) necessarily for tumor initiation. Tumor cells with different phenotypes are presented in different colors, a curved arrow indicates self renewal properties, and an oncogenic hit is marked with a lightning.

Malignant melanoma cells resemble stem cells in many ways, i.e. they show great therapeutic resistance and easy adaptation to various microenvironments (metastatic site), are very heterogeneous and plastic, can differentiate into multiple lineages and expresses developmental genes. Therefore, it was suggested that stem-like cells might be present in melanoma and might play a role in its progression[17,18]. Several studies

have attempted to identify candidate melanoma CSC, and cell surface molecules like CD20, CD133, ABCG2 or ABCG5 were suggested as CSC markers, but no consistent conclusions have been drawn yet[19,20,21,15,22]. Furthermore, it has been shown that by growing cells in media without serum, (which supports sphere-formation), the media will enrich for stem cell properties, and consequently, CSC[23] (described further in chapter 1.3.1).

Given that the clonal evolution model is the basis for most existing therapies, which targets the bulk of a tumor, and that relapse after treatment still is a problem in most solid cancers, CSC theory could represent a more accurate foundation for drug development. However, targeting CSC is not an easy task, and it has been reported that majority of conventional therapies do not affect stem-like tumor cells[24]. Though, several therapeutic approaches targeting CSC have been tested. In melanoma, e.g. treatment with monoclonal Ab against the multidrug resistant protein ABCB5, which according to Schatton et. al. identifies melanoma initiating cells, resulted in tumor-inhibitory effects *in vivo*[15]. Thus, growing evidence indicates that it might be important to focus on the tumor initiating cells when creating future therapies, and, therefore more knowledge about these cells is needed.

1.2 Apoptosis

Apoptosis is defined as controlled cell death, and many therapeutic anti-cancer strategies are based on this process (reviewed by e.g. Jacobson et. al.[25]). Apoptosis leads to shrinkage and fragmentation of the cell and the nucleus, degradation of chromosomal DNA by e.g. caspase activated DNase (CAD) [26], and cytoskeleton degradation. Reduced ability to induce apoptosis is often considered to be one of the hallmarks of cancer[27].

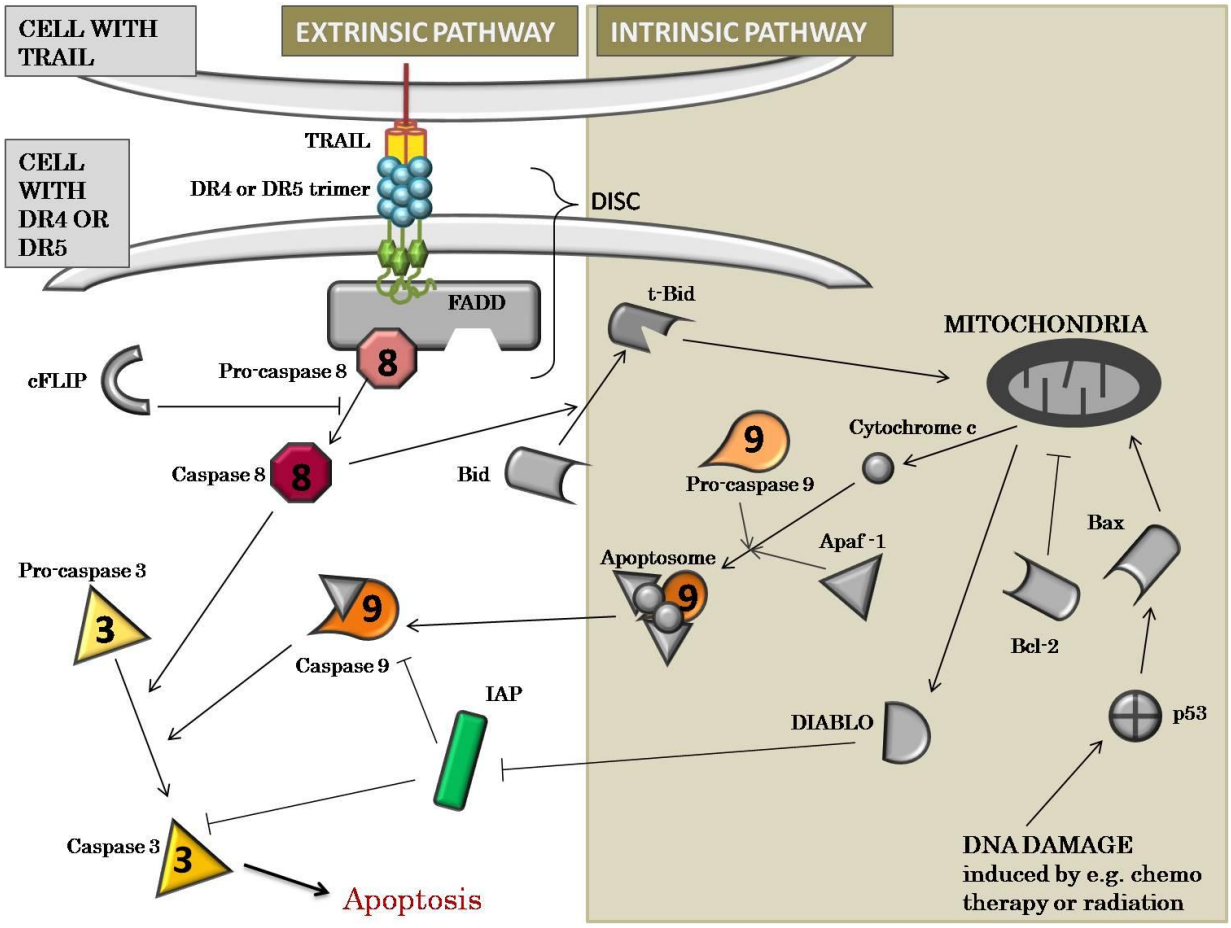

FIG. 1.4: The main actors in the intrinsic and extrinsic apoptotic pathway, here illustrated by receptor induced apoptosis by TRAIL. TRAIL binding to DR4 or DR5 leads to receptor trimerization, Fas-associated death domain protein (FADD) binding, and pro-caspase 8 association. The complex formed is called death-inducing signalling complex (DISC). In DISC, pro-caspase 8 is cleaved to form caspase 8, which cleaves pro-caspase 3 to active caspase 3, resulting in apoptosis. IAPs inhibit the apoptotic stimuli primarily by blocking active caspase 3 and/or caspase 9. Caspase 8 also cleaves Bid to active truncated, t- Bid, which links the extrinsic and intrinsic pathway together. Cytochrome c and DIABLO release from the mitochondria may result from e.g. t-Bid or Bax stimulation, and could be inhibited by anti-apoptotic members of the Bcl-2 family. Pro-caspase 9 associates with cytosolic cytochrome c and Apaf-1 to form the apoptosome. The apoptosome processes pro-caspase 9 into the active version of caspase 9, which further stimulate pro-caspase 3 cleavage. The intrinsic pathway could be activated via p53 by e.g. DNA damage. See chapter 1.2.1 and 1.2.2 for relevant abbreviations.

Cystein proteases called caspases, are the central players in the apoptotic pathway, where they upon activation cleaves nearly 100 different proteins in the cytoplasm (reviewed by Hengartner[28]). Caspases are produced as zymogens and becomes processed in the cytoplasm by other caspases or by autocatalysis. The initiator caspases includes caspase 8 and 9, and are activated by cellular stress, like death receptor activation (extrinsic pathway), DNA damage (intrinsic pathway) or ER stress [28,29]. Executor caspases, like caspase 3, are activated by the initiator caspases, and are responsible for cleavage of downstream effectors. FIG. 1.4 presents an overview of the apoptotic pathway, focusing on the proteins relevant in this study. The apoptotic pathway is demonstrated to be important, when understanding malignant melanoma: e.g. the caspase 8 inhibitor cFLIP is up-regulated in malignant melanoma, when compared to benign nevus[30].

1.2.1 TRAIL induced apoptosis via death receptor 4 and 5

A member of the tumor necrosis factor (TNF) super family, called TNF related apoptosis inducing ligand (TRAIL), was discovered in 1995 by the help of bioinformatics[31]. This membrane-bound ligand is expressed by cells in the immune system[32], like natural killer cells, B and T lymphocytes. The natural target cell of TRAIL is oncogenic cells or pathogen infected cells, and was therefore early posted to have promising effects in cancer therapy. TRAIL binds to receptors on the target cell (FIG. 1.5), resulting in apoptosis induction by signalling through the extrinsic pathway[31], as illustrated in FIG. 1.4. TRAIL is able to bind five different receptors. death receptor 4 and 5 (DR4 and DR5) are the functional transducers in the target cell, which need TRAIL binding and receptor trimerization to be active [33,34]. The decoy receptors DcR1 and DcR2 and the plasma protein osteoprotegerin can associate with TRAIL, but can not activate the apoptotic pathway, and have a more uncharacterized function than DR4 and DR5[35,36,37].

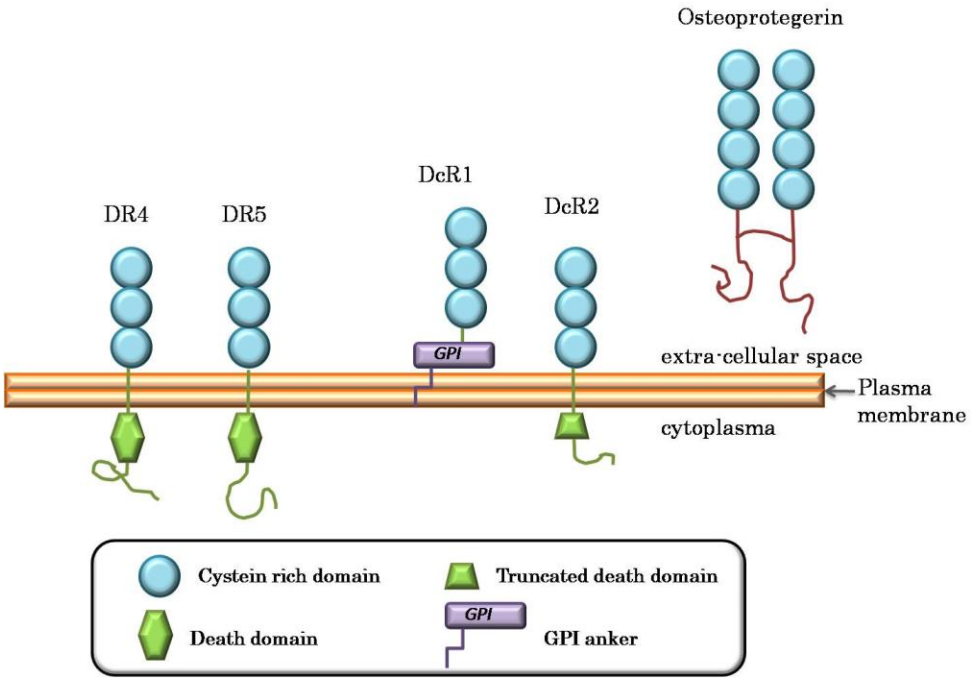

FIG. 1.5: Receptors binding TRAIL presented in their monomeric form. DR4 and DR5 have a functional cytoplasmic death domain, while the decoy receptors DcR1, DcR2 and osteoprotegerin are unable to signal through the extrinsic apoptosis pathway.

DR4 and DR5 are reported to be up-regulated in several cancer tissue[38], whereas the receptor deficient mice are proven to be more exposed to lymph node metastasis[39]. Despite DR4 and/or DR5 expression in cancer cells, resistance to TRAIL is reported by several groups, and is often a result of alterations in the extrinsic pathway[40]. In melanoma, about one third of melanoma cell lines are TRAIL resistant, despite high levels of DR5[41,42]. Generally melanoma has a higher level of DR5 then DR4[43], and a patient has a greater chance of disease free survival if DR5 positive melanoma cells are greater than 90%[44]. Primary melanomas show an increased DR5 level when compared to nevi or metastatic tissue, indicating that DR5 down-regulation could be involved in therapy resistance in metastatic tissue[44].

There are several options for apoptosis induction via DR4 or DR5. Recombinant TRAIL peptides, proto-agonistic Ab (Ab activating both DR4 and DR5), TRAIL receptor antibodies and gene therapy vectors (i.e. plasmids, adenovirus and adeno-associated virus (AAV)) coding for TRAIL, have been tested *in vitro* and *in vivo*,

alone or in combination with other therapeutic substances, as reviewed in [45,46]. In this study, TRAIL receptor Abs from Human Genome Sciences (HGS), (HGS-ETR 1 (Mapatumumab) directed towards DR4, and HGS-ETR 2 (Lexatumumab) directed towards DR5), are employed to initiate the extrinsic pathway in melanoma cells.

Clinical studies so far, indicate that TRAIL-mediated DR4/DR5 activation alone could result in longer progression free survival, but not longer overall survival in several cancer types. Thus, a combination of drugs is probably needed to achieve a complete treatment response.

1.2.2 Inhibitors of Apoptosis Proteins

In 1993 Crook et al. discovered a baculovirus gene that coded for a protein able to inhibit apoptosis in insect cells, i.e. inhibitor of apoptosis protein (IAP)[47]. To this date, eight human homologs are identified as baculovirus IAP repeat containing (BIRC) proteins, i.e. IAPs, as reviewed by LaCasse[48] and Srinivasula[49]. In addition to the seven IAPs used in this study (Table 1.1), there is discovered an IAP named IAP-like protein-2 (ILP-2)/BIRC8[50,51].

Table 1.1: Overview of the IAPs used in this study with BIRC pseudonyms, number of amino acids in the main splicing form, and domains essential for their function. All IAPs contain at least one baculovirus IAP repeat (BIR) domain. Livin, XIAP, cIAP-1and cIAP-2 contains a domain called really interesting new gene (RING), and cIAP-1 and cIAP-2 has a caspase-recruitment domain (CARD). (Nucleotide-binding and oligomerization domain (NOD), leucin-rich repeat (LRR) domain, ubiquitin-conjugation (UBC) domain[48].) See text for abbreviations of IAPs.

IAP:	BIRC nr:	# amino acids:	Domains:
Survivin	BIRC5	142	
Livin	BIRC7	298	
XIAP	BIRC4	497	
cIAP 1	BIRC2	604	
cIAP 2	BIRC3	618	
NAIP	BIRC1	1403	
Bruce	BIRC6	4830	

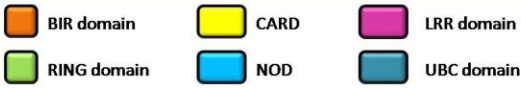

The BIR domains function primarily in protein-protein interactions between the IAPs, or between an IAP and a caspase in the apoptotic pathway, resulting in inhibition of caspase activity (FIG. 1.4). Neuronal apoptosis inhibitory protein (NAIP) and BIR repeat-containing ubiquitin-conjugating enzyme (Bruce) contain additional domains not essential in the apoptotic process.

The apoptotic roles of the IAPs are not fully understood, nevertheless, X-linked IAP (XIAP) seems to be one of the central players with direct caspase 3, 7 and 9 blocking capacity[52]. The other IAPs seem to inhibit the caspases indirectly by releasing XIAP from IAP inhibitors as DIABLO, or marking the caspases for protein degradation by their E3 ubiquitin ligase domain, RING. The RING containing IAPs could also regulate each others levels, as seen for e.g. cellular IAP-2 (cIAP-2) and XIAP degradation by cellular IAP-1 (cIAP-1)[53,54]. IAPs have also been shown to participate in signalling associated with cell division and signal transduction[49]. Apoptosis resistance in cancer is in some cases influenced by IAP[48], and several cancers are reported to have an elevated IAP level[55].

Several studies have reported about survivin expression in all stages of melanoma, whereas no survivin was expressed in normal melanocytes[56,57]. This matches observations where survivin level is significantly correlated with disease outcome in melanoma patients[58,59]. Several studies show that nuclear survivin detection in melanoma can be used as a factor to predict poor survival[60,61,62].

By down-regulating XIAP and inducing apoptosis by TRAIL, Chawala-Sarkar et al. demonstrated apoptotic induction in originally TRAIL resistant melanoma cells *in vitro*, and Vogler et al. induced apoptosis in pancreatic cancer cells in mice models[63,64]. Both XIAP and survivin down-regulation in cancer are under clinical investigation, as reviewed by LaCasse et al. 2008, where phase 2 studies show promising results so far[48]. A great amount of evidence indicate that IAP inhibition have the potential as a good therapeutic target in cancer.

1.3 Methodological background

1.3.1 Model systems

In vitro cell cultures like adherent monolayers in serum-containing media is a usual model system used in cancer research. However, long-term culturing under such conditions will lead to cell differentiation and adaptation to the two-dimensional (2D) growth, thus these cells might have a different phenotype/genotype than the original cells taken from the patient[23]. Culturing the cells as non-adherent spheroids in serum-free media supplemented with growth factors (i.e. media for normal embryogenic stem cells), preserve the phenotype/genotype of the original tumor[65,23], suggesting that, spheroids are a better model to mimic clinical samples[66]. Furthermore, it has been shown, that spheroid cultures allow the persistence of stem cell properties, and, consequently, spheroids seem to be enriched for CSC[23,65]. Fang et. al. has shown that melanoma spheroids contained cells with stem cell properties and, that spheroid cells demonstrated higher tumorigenic abilities in mice than the monolayer cells[19]. An independent study by Prasmickaite et. al. (manuscript in preparation), comparing tumor initiating abilities of monolayer and spheroid cells from "close-to-patient" cell cultures called Melmets (FIG. 1.6), generally confirmed the observations by Fang et. al. All together, this encouraged the here presented study on therapy resistance associated molecules, IAPs, and response to pro-apoptotic stimulus via DR4 and DR5 in melanoma spheroids *versus* monolayers.

In the present study, three different Melmet cell lines were studied: Melmet 1, Melmet 5 and Melmet 79. Melmet cultures represent "close-to-patient" early-passage material and, therefore, are superior to the long-established commercially available melanoma cell lines cultured *in vitro* for years, when studying melanoma resistance and evaluating new therapeutic strategies.

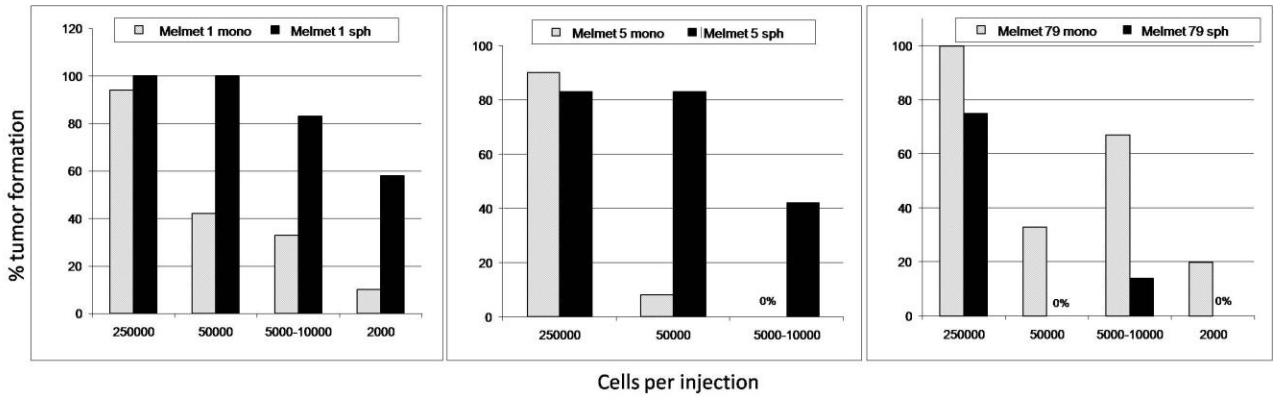

FIG. 1.6: Efficiency of tumor initiation in nude mice by Melmet 1, Melmet 5 and Melmet 79, respectively. Number of cells per injection is plotted against percent tumor formation. Monolayer is abbreviated (mono) and spheroids (sph). (Figure borrowed with permission from Prasmickaite).

The Melmets were tested for the sensitivity to the reference chemotherapeutic drug DTIC, and demonstrated a low response when grown as monolayers (FIG. 1.7, Engesæter, unpublished), reflecting the true chemo-resistant nature of malignant melanoma.

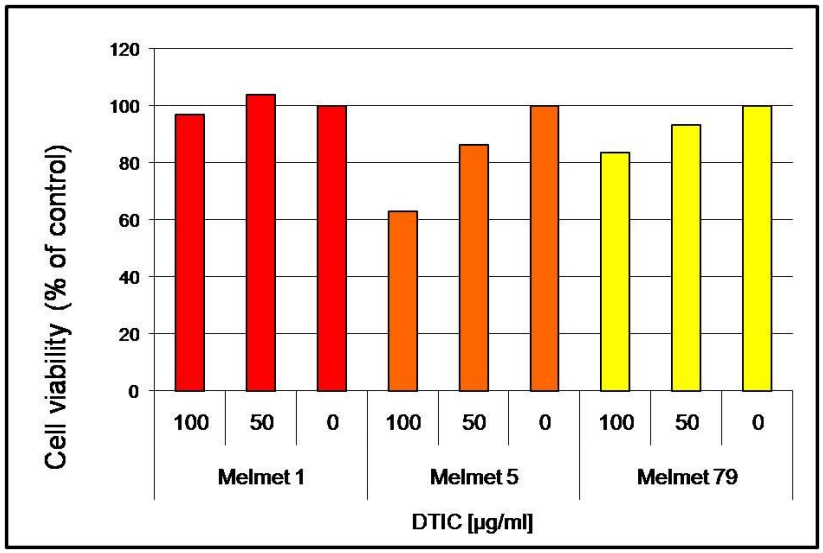

FIG. 1.7: Melmet 1, 5 and 79 treated with DTIC at the concentrations 50µg/ml and 100µg/ml. Cell viability are related to untreated control cells. (Figure borrowed with permission from Engesæter).

1.3.2 Oligonucleotide transfection

There are several ways to introduce nucleotides transiently into cells *in vitro*, reviewed by Colosimo et. al.[67]. Protein up-regulation could be achieved by e.g. introduction of mRNA or DNA, and protein down-regulation could result from e.g. introduction of siRNA (described in chapter 1.3.3). Oligonucleotides by themselves are poorly taken up by the cells. To improve the uptake, the oligonucleotides are often complexed with various transfection agents. Liposomes, like Lipofectamine 2000™ and Lipofectamine RNAi MAX™, in complex with oligonucleotides are generally effectively taken up by eukaryotic cells by endocytosis and/or membrane fusion[68]. Disadvantages of these cationic lipids are a varying degree of toxicity[69].

1.3.3 mRNA down-regulation by RNA interference

RNA interference (RNAi) was revealed in 1998 by Fire and Mello[70]. By using *Caenorhabditis elegans* as model system, they demonstrated that by introducing double stranded RNA, with a homologous sequence to an mRNA, this specific mRNA would be degraded. This system is now discovered in almost all eukaryotes, and has been associated with functions as viral defence, mobile element silencing, mRNA regulation (by microRNA) and chromatin condensing[71].

The general mechanism of the RNAi system used by endogenous gene regulatory RNA is reviewed in[72,73]. When the mechanism is exploited artificially by small interfering RNA (siRNA), the antisense strand of siRNA incorporates into the RNA-induced silencing complex (RISC) (FIG. 1.8). RISC associated proteins perform mRNA degradation when the antisense strand has 100% complementary to the mRNA.

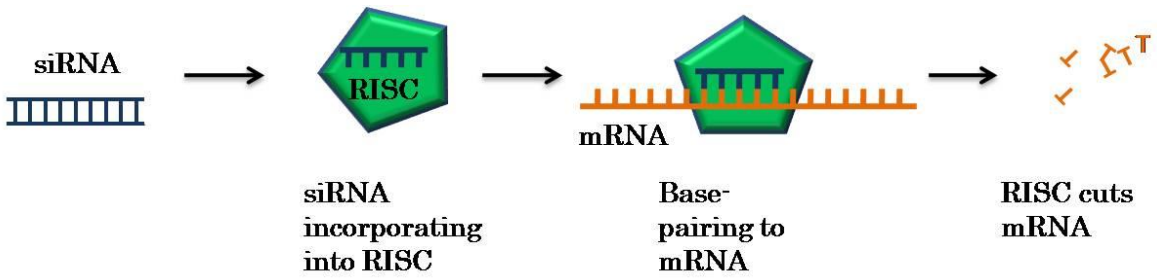

FIG. 1.8: When the RNAi mechanism is used artificially, the antisense strand from the siRNA will be incorporated into RISC. When the antisense sequence is 100% complimentary to an mRNA molecule, the endonuclease activity of RISC cleaves the target mRNA.

The RNAi mechanism is an excellent tool in research, giving the opportunity to down-regulate the expression from specific genes and thereafter evaluating phenotypic effects (reverse genetics). There are also reports from *in vivo* studies, highlighting a promising future for siRNA as therapy in humans[74,75]. In cancer research, RNAi could theoretically be used to knock-down oncogenes, though, problems related to stability in blood and delivery to target cells, limits the practical benefit to this date. Clinical trials using siRNA were first initiated in 2004, and in 2008, several trials were ongoing, e.g. two phase II studies involving an eye disease[76]. Given the theoretical potential and the rapid development in the field, the RNAi mechanism will most likely be central in future therapy of human diseases.

Aim of the study

The overall aim of the present study was to characterize "close-to-patient" malignant melanoma cell cultures, Melmets, in respect to apoptotic resistance-associated molecules, IAPs, and pro-apoptotic molecules, DR4 and DR5. Furthermore the effect of a therapeutic strategy based on RNAi mediated down-regulation of IAPs combined with activators of the apoptotic pathway via DR4 and DR5 was investigated. The focus of the study was a comparison of different *in vitro* Melmet models: monolayers *versus* spheroids (supposedly enriched for melanoma stem cells), with regard to:

1) Expression of IAPs (survivin, livin, XIAP, cIAP-1 and cIAP-2) at protein and mRNA level

2) Expression of DR4 and DR5 at protein level

3) Cell viability and spheroid formation after treatment with TRAIL receptor antibodies targeting DR4 and DR5

4) Cell viability and spheroid formation after treatment with TRAIL receptor antibodies in combination with siRNA targeting selected IAPs: XIAP or survivin.

By studying these aspects, we aim to reveal resistance-associated properties of aggressive melanoma cells and to get an implication for future therapeutic strategies.

2. Materials and methods

2.1 Cell lines

Metastatic melanoma cell lines, generally named Melmets, were established from biopsies of metastatic melanoma patients at the department of Tumor Biology, the Norwegian Radiumhospital. The establishment of Melmet 1, Melmet 5 and Melmet 79 cultures as monolayers and spheroids is described by Prasmickaite et. al. (manuscript in preparation)(background information summarized in table 1.2). In brief, monolayer cultures were established isolating melanoma cells by the immunomagnetic bead-based method as described below (chapter 2.3), and growing the isolated cells in serum-containing media RPMI ++ (described in chapter 2.2). Melmet 1 and Melmet 5 spheroid cultures were established from the low-passage (passage 9 and 8, respectively) corresponding monolayer cultures, growing the cells in the specialized serum-free human Embryonic Stem Cell Media 4 (hESCM4) (composition described in the appendix), which supports sphere formation[19]. The Melmet 79 spheroid culture was established directly from the lymph node biopsy, omitting the immunomagnetic bead-based step and the monolayer step, but culturing the cells directly in hESCM4.

Table 1.2: Summary of the background information of Melmet 1, 5 and 79.

	Melmet 1	Melmet 5	Melmet 79
Source:	Female / 36 years	Male / 56 years	Female / 63 years
Tissue :	Subcutanous	Lymph node	Lymph node
Distant metastases:	Brain, lung, breast, skin	Brain, lung, liver, abdomen	No
Spheroids culture established from serum growing cells:	Yes	Yes	No
Tumorigenic in mice:	Yes	Yes	Yes

2.2 General cell work.

All reagents, materials and instruments used in cell related work are listed in table 2.2. Cells cultured as monolayers were grown in cell flasks in RPMI 1640 media supplemented with 8% FCS and 2mM L-glutamine (further referred as "RPMI++"). Cells cultured as spheroids were grown in petridishes in hESCM4. Cells were cultured in an antibiotic free environment, in a 5.0% CO_2 atmosphere at 37°C. EDTA was used to detach monolayer cells from a flask, and to disintegrate spheroids into single cells. When making a new passage of spheroids, single cells were seeded at a low concentration (i.e. 1000 cells/ml), to make sure the spheroids formed originate from one cell, and not a cell aggregate. 2µl trypanblue was added to 10µl cell suspension to label dead cells so that only the viable cells were counted. The cells were tested for mycoplasma infection every sixth week. All cell cultures used in this work were mycoplasma-free.

Dry pellets were made for various analyses described in chapter 2.4 and 2.5. When dry cell pellet was made from monolayer cultures, the cells were washed once in cold PBS. New PBS was added, and a cell scrape was used to harvest the cells. Cell suspension was centrifuged for 8min at 1200rpm at 4°C. Supernatant was removed and the dry cell pellet was stored at -80°C.

When dry cell pellet was made from spheroid cultures, the spheroids were sedimented, the spheroid pellet was washed once with cold PBS and disintegrated into single cells with 50µl EDTA. 5ml RPMI++ was added to the single cell suspension which was centrifuged for 8min at 1200rpm. Cold PBS was added to the cell pellet and centrifuged again for 8min at 1200rpm. Supernatant was removed and the dry cell pellet was stored at -80°C.

Table 2.2: Materials and instruments used in general cell work.

Materials/instruments:	**Company:**	**Cat#:**
12 well plates	NUNC™, Denmark	150200
15 ml tubes	Sarstedt, Nümbrecht	62.554.502
2, 5, 10 and 25ml pipettes	Sarstedt, Nümbrecht	
50 ml tubes	Sarstedt, Nümbrecht	62.547.254
6 well plates	NUNC™, Denmark	150239
96 well plates	BD Falcon™, USA	
basic Fibroblastic Growth Factor (bFGF)	Invitrogen	13256-029
Biofuge primoR, for eppendorf tubes	Heraeus	
Bovine Serum Albumin (BSA)	Sigma Aldrich, Switzerland	A-3059
Cell flasks, EasYFlasks™ with filter	NUNC™, Denmark	
Cell scraper	Sarstedt, Nümbrecht	83.1831
Centrifuge 5810R, for 10ml tubes	Eppendorf	
EDTA, Versene	BioWittaker®, Belgium	12-711A
Eppendorf tubes	Trefflab, Switzerland	
Fetal Calf Serum (FCS)	PAA Laboratories, Austria	A15-101
Filter tips	Molecular Bio Products®	
Knock Out™ DMEM-F12	Gibco®, Invitrogen	12660
KnockOut™ Serum Replacer	Invitrogen	10828-028
L-Glutamine	GibcoBRL, UK	25030
Microscope for general cell work	Leica DMIL	
Mouse Embryonic Fibroblast, P3 strain CF-1	Chemicon Embryomax®	PMEF-CF
Mycoplasma PCR detection kit	Venor®GeM, Minerva biolabs	11-1025
Non essential amino acids	Gibco®, Invitrogen	11140-035
Phosphate Buffered Saline (PBS)	BioWittaker®, Belgium	17-516F
RPMI 1640 media	BioWittaker®, Belgium	12-167
Trypanblue	Sigma Aldrich, Switzerland	T-0887
β-mercaptoethanol	Sigma Aldrich, Switzerland	7522

2.3 Isolation of tumor cells with immunomagnetic beads

The immunomagnetic bead-based technique has been used for isolation of metastatic melanoma cells from patient biopsies and from various organs (like brain, lung, bone marrow, spinal cord and eyes) of rats with experimental metastases. Materials and instruments used for immunomagnetic isolation of tumor cells are listed in table 2.3. Magnetic beads were coated with the 9.2.27 Ab, which binds to the High Molecular Weight melanoma-associated antigen, HMW-MAA, and in this way, allows separation of melanoma cells from the rest of the cells by using a magnet[77,78]. PBS supplemented with 1% HSA, (to prevent unspecific binding, further referred as "PBS+") was used in all steps when isolating cells with immunomagnetic beads. All the procedures were performed at 4°C. Lymph node biopsies or samples from rat brain, lung or eyes were disintegrated into small pieces in cold PBS+ by using scalpels, and filtered through a 70µm filter to remove big clumps. Cells from rat tibia or columna were isolated by flushing these organs with PBS+ by the help of a syringe and a needle. The obtained cell suspension was filtered as described above and centrifuged for 5min at 1100rpm. Supernatant was discarded and the ACK Lysing buffer was added to the cell pellet at the volume ratio of 1:1 to disrupt red blood cells. After incubation for approximately 2-3min, 10ml of cold PBS+ was added before centrifugation for 5min at 1100rpm. Pellet was resuspended in 0.5ml PBS+ and mixed with 25µl of a magnetic bead suspension containing $2x10^8$ antibody coated beads/ml. It is important to have an excess of beads with respect to the number of cells. After incubation under constant rotation for 30min at 4°C, 10µl of suspension was dripped onto a cover slip glass and examined under a microscope. A cell with ≥5 beads was considered as "positive" i.e. melanoma cell (FIG. 2.1).

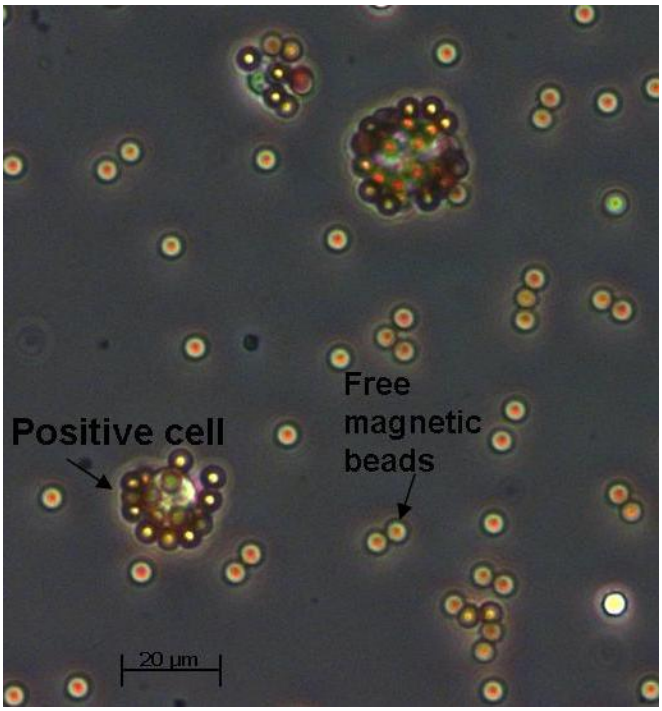

FIG. 2.1: Melanoma cells binding 9.2.27-coated magnetic beads.

To separate melanoma cells from the rest of the cells, the tube with the cell and bead suspension was put into a special holder with a magnet, and the supernatant was discarded. The magnet-bound cells were gently washed with 500µl PBS+, and resuspended in appropriate buffer. Then the tube with the "cells + beads" was taken of the magnet. The cells binding the beads were further used for preparation either protein lysate or RNA lysate as described below. To make protein lysate for protein analysis, 100µl of lysis buffer with inhibitors (specified in appendix, materials listed in chapter 2.4.2) was added to the "cells + beads", and the resulting suspension was put in -80°C. After thawing, the beads were removed with the magnet as described above, and the remaining lysate was sonicated (as described in chapter 2.4.2). To make RNA lysate for gene expression analysis, RNA lysate buffer containing β-mercaptoethanol was added to the "cells + beads", and the beads were discarded by the help of the magnet. The obtained lysate was used for isolation of RNA as described in chapter 2.5.1.

Table 2.3: Materials and instruments used when isolating tumor cells with the magnetic bead technique.

Materials/Instruments:	**Company:**	**Cat#:**
ACK lysing buffer	BioWhittaker®, Lonza	10-548E
Cell Strainer, 70µm filter	BD Falcon™, USA	352340
Human Serum Albumin (HSA)	Octapharma, Sweden	(MT.nr.) 03-2156
Mouse anti-human 9.2.27 antibody	Reisfeld R., La Jolla,CA	
Scalpels	Swann-Moston®,	
Sheep anti-mouse(SAM) M450 IgG magnetic beads	Dynal, Invitrogen	110.31
Syringes and needles	Tamro	

2.4 Protein analysis by SDS-polyacrylamide gel electrophoresis (SDS-PAGE) and western blotting

SDS-PAGE is a method based on separation of proteins based on their size: a large protein will travel a shorter distance than a smaller protein in an unfolded state in a given polyacrylamide gel. Western blotting is a method for transmitting proteins from a gel to a membrane using an electrical gradient. The proteins of interest are visualized by using specific antibodies. FIG. 2.2 illustrates a theoretical overview of SDS-PAGE and western blotting. SDS-PAGE was preformed by using either home-made gels prepared with reagents from BIO-RAD (see chapter 2.4.1) or commercial gels from Invitrogen. Materials used to make general buffers are listed in table 2.4.

Table 2.4: Materials used to make general buffers used in SDS-PAGE and western blot.

Materials:	**Company:**	**Cat#:**
Glycin	Merck KGaA, Germany	104201
NaCl	Merck KGaA, Germany	106404
Sodium Dodecyl Sulfate (SDS) 20%	BIO-RAD laboratories	161-0416
Tris HCl	Merck KGaA, Germany	108382
Tween 20	Merck KGaA, Germany	822184
Milk powder, low fat	Nestlê Molico	

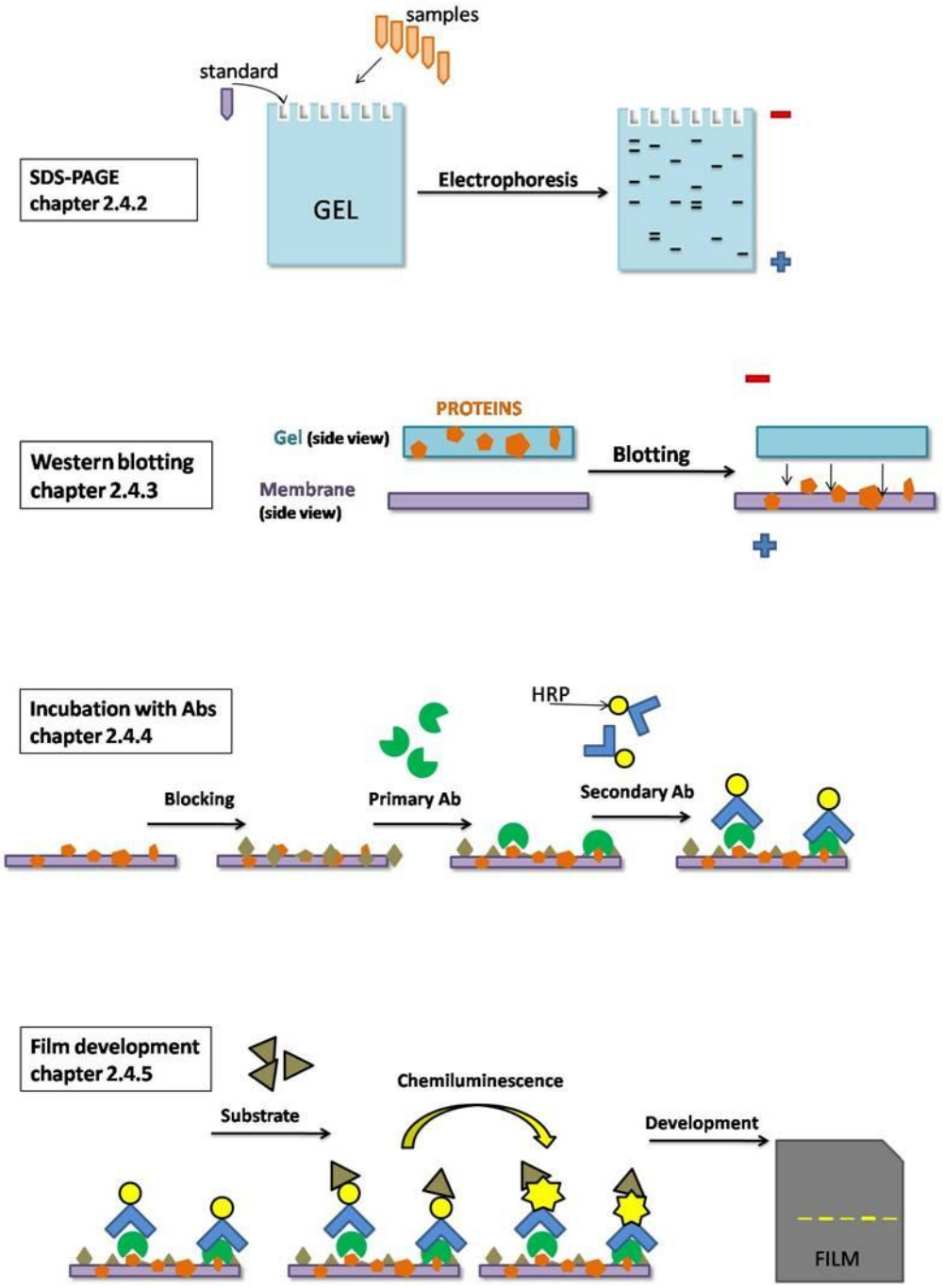

FIG. 2.2: Theoretical overview of SDS-PAGE and western blot. Positive and negative circles illustrate an electrical gradient. Different chapters indicated on the left side, describe the theory and performance in more detail. (Ab – antibody, HRP – Horseradish peroxidase).

2.4.1 Gel casting: home-made gels

The gels consist of two parts: the lower separating part and the upper concentrating part. The gel-parts were prepared from materials in amounts listed in table 2.5. Materials and instruments used in gel casting are listed in table 2.6.

First the separating gel, containing 8% acryl amide, was mixed and poured into an assembled gel casting apparatus. After approximately 30min, the gel was polymerized, and a concentrating gel containing 5% acryl amide, was poured on top of the separating gel. The concentrating gel was left for polymerization for approximately 30min.

Table 2.5: Volumes of different materials used in SDS-PAGE gel casting.

Material:	**Separating gel:**	**Concentrating gel:**
Acryl amide/bis	5.4ml	1.34ml
Tris pH 8.8	7.5ml	-
Tris pH 6.8	-	1ml
SDS	100µl	40µl
APS	200µl	80µl
ddH_2O	6.7ml	5.4ml
TEMED	12µl	8µl

Table 2.6: Materials and instruments used to make home-made gels from BIO-RAD.

Materials:	**Company:**	**Cat#:**
Acryl amide/bis 30%	BIO-RAD laboratories	161-0158
Ammonium PerSulfate (APS) 10%	BIO-RAD laboratories	161-0700
Gel casting equipment (Mini Trans-Blot Cell)	BIO-RAD laboratories	170-3935
TEMED	BIO-RAD laboratories	161-0801

2.4.2 SDS-PAGE

To get access to all proteins in a cell, the cells must be lysed. Materials and instruments used for lysation and when performing SDS-PAGE, are listed in table 2.7. A lysis buffer with protease inhibitors was added to cell pellets (harvested as in chapter 2.2), and incubated on ice for an hour, vortexing every 15min. The samples were then sonicated 3 times for 5 seconds and centrifuged for 15min at 12000rpm at 4°C. The supernatant, i.e. the cell lysate, was transferred to a new tube and frozen at -80°C.

The protein concentration of the cell lysate was determined by using the Bio-Rad protein assay in accordance with the producer recommendations. The kit is a colorimetric assay that is based on the color change of Coomassie Brilliant Blue dye in response to various concentrations of proteins. The absorption was measured at 595nm and is proportional to the amount of the protein in the sample. The protein concentration was calculated from a standard curve based on absorption of the known amounts of protein in Protein standard 1.

When home-made gels were used, 4µl of 6x sample buffer, to denature the proteins and give them a negative charge, were added to 40µg protein lysate. Lysis buffer without inhibitors (specified in appendix) was used to dilute samples to a total sample volume of 20µl. Samples were denatured at 95°C for 5min before application on a gel. In parallel, 4µl sample buffer was added to 6µl of the Standard ladder, denatured as above and applied in at least one well. A ladder contains proteins with known molecular weight, and is used to confirm that the band detected, has approximately the same weight as the protein of interest. The gel was run in a running buffer (specified in appendix) for approximately 2 hours at 30mA.

When commercial gels were used 1µl of 10x reducing agent and 2.5µl of 6x LDS sample buffer was added to 22µg protein. ddH_2O was used to dilute samples into a total sample volume of 10µl. Samples were denatured at 70°C for 10min before

application on a gel. 2.5µl See blue standard was applied in at least one well. The gel was run in 1x MOPS for approximately 60min at 150V, to obtain good separation of the proteins.

Table 2.7: Materials and instruments used in SDS-PAGE.

Materials/instruments:	**Company:**	**Cat#:**
Aprotinin	Sigma Aldrich, Switzerland	A4529
Bromophenol blue	Merck, Germany	8122
Glycerol	Sigma Aldrich, Switzerland	G7893
Leupeptine	Sigma Aldrich, Switzerland	L2884
NONIDET®P40	Usb, corporation, USA	19628
Bio-Rad protein assay kit	BIO-RAD laboratories	500-0006
NuPAGE® LDS sample buffer (4x)	Invitrogen	NP0008
NuPAGE® MOPS SDS Running Buffer (20x)	Invitrogen	NP0001-02
NuPAGE® Novex® 4-12% Bis-Tris Midi Gel	Invitrogen	WG1403BOX
NuPAGE® Sample Reducing agent (10x)	Invitrogen	NP0004
Pepstatine A	Sigma Aldrich, Switzerland	P4265
Phenylmethanesulfonylfluoride (PMSF)	Sigma Aldrich, Switzerland	P7626
Precision Plus Protein™ Dual Color Standards	BIO-RAD laboratories	161-0374
Protein standard 1.	BIO-RAD laboratories	500-0005
See Blue® Plus 2 Prestained Standard (1x)	Invitrogen	LC5925
β-mercaptoethanol	Sigma Aldrich, Switzerland	M7522
Ultrasonic Homogenisator/ Sonicator		

2.4.3 Western blotting

The separated proteins were transferred from the gel to a filter, before protein detection using Abs. All materials and instruments used for western blotting are listed in table 2.8. Home-made gels were washed in Bjerrum-Scäfer-Nilsen (BSN) buffer (specified in appendix) for 10min. In parallel, an Immobilon-P Transfer Membrane was activated in methanol, before a wash in ddH_2O, and 10min of neutralizing wash in the BSN buffer. All pads and filter papers were soaked in the BSN buffer. A gel-membrane sandwich was assembled as shown in FIG. 2.3.

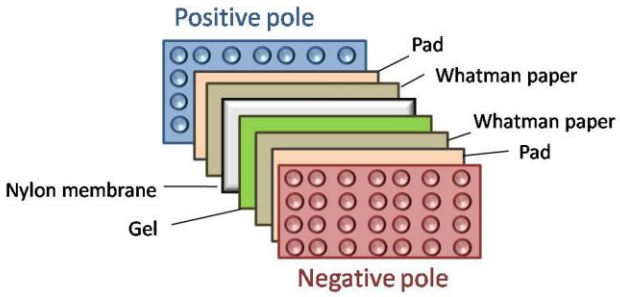

FIG. 2.3: Assembly of pads, filter papers, a membrane and a gel.

Home-made gels were blotted in the BSN buffer with a cooler element and a magnetic stirrer over night at 4°C at 30V, or at room temperature for 90min at 90V. To visualize the protein bands, the membrane was thereafter incubated in amidoblack solution (specified in appendix) for 5min, and washed in destaining solution (specified in appendix) for 2 x 10min. Since amidoblack stains all proteins in the membrane, it is possible to get an indication about the quality of a loading and a transfer (see FIG. 2.4).

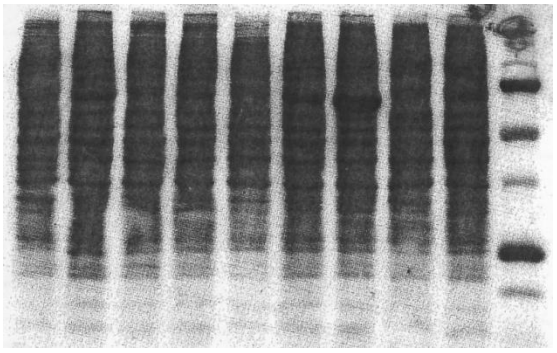

FIG. 2.4: An example of a filter stained with amidoblack, where 9 samples and one standard (the right line) were applied.

Commercial gels were blotted onto a nitrocellulose membrane in iBlot™ blotting apparatus from Invitrogen for 10min, in accordance with the protocol of the supplier. Since the membrane used with commercial gels is nitrocellulose-based, it could not be stained with the methanol-containing amidoblack solution, since methanol would dissolve the membrane.

Table 2.8: Materials and instruments used in western blotting.

Materials/instruments:	**Company:**	**Cat#:**
Acetic Acid	Merck, Germany	100063
Blotting equipment	BIORAD laboratories	170-3935
Gel Blotting paper/ Whatman paper	Schleicher & Schuell	10426694
iBlot™ blotting machine	Invitrogen™	IB1001EU
iBlotTM Gel Transfer Stacks Nitrocellulose	Invitrogen™	IB3010-01
Immobilon-P Transfer Membrane	Millipore	IPVH00010
Methanol	VWK	20834-325
Naphtol Blue Black	Sigma Aldrich, Switzerland	N-3005

2.4.4 Incubation with antibodies

To detect the protein of interest, the filters were incubated with different primary Abs specific for the various proteins studied. Secondary Abs link primary Abs to a detectable signal (explained in chapter 2.4.5). This step of the western analysis is identical for both gel-types.

Table 2.9: Antibodies used for protein detection, western analysis.

primary antibody	Bruce	cIAP-1	cIAP-2	Livin	NAIP	Survivin	XIAP	alfa-tubulin	
Host	Rabbit	goat	goat	goat	rabbit	rabbit	goat	mouse	Primary
pseudonymes	BIRC 6	BIRC 2	BIRC 3	BIRC 7	BIRC 1	BIRC 5	BIRC 4		
company	abcam	R&D	R&D	Calbiochem®	abcam	R&D	R&D	Calbiochem®	
Cat.nr	ab19609	AF8181	AF8171	PC724	ab25968	AF886	AF8221	CP06	
Weight	528kD	69kD	68kD	38kD	160kD	19kD	55kD	51kD	
buffer type	cell signaling	R&D	R&D	low TBST	cell signaling	R&D	R&D	TBST	
blokcing milk	10 %	10 %	10 %	10 %	10 %	10 %	10 %	10 %	
milk for primary Ab	5 %	2 %	2 %	5 %	5 %	2 %	2 %	5 %	
storage	4°C	-80°C	-80°C	-20°C	4°C	-80°C	-80°C	4°C	
dilution	1 to 6000	1 to 2000	1 to 2000	1 to 1000	1 to 2000	1 to 2000	1 to 2000	1 to 2000	
secondary antibody	anti rabbit	anti goat	anti goat	anti goat	anti rabbit	anti rabbit	anti goat	anti mouse	Secondary
company	Dako	Dako	Dako	Dako	Dako	Dako	Dako	Dako	
Cat.nr	P0448	P0160	P0160	P0160	P0448	P0448	P0160	P0260	
milk for secondary Ab	5 %	2 %	2 %	5 %	5 %	5 %	5 %	5 %	
storage	4°C	4°C	4°C	4°C	4°C	4°C	4°C	4°C	
dilution	1 to 5000	1 to 5000	1 to 5000	1 to 2000	1 to 5000	1 to 5000	1 to 5000	1 to 5000	

Ab dilutions, buffer types and composition of the milk solutions were optimized for each Ab and are listed in the table 2.9, and specified in the appendix. Generally, a membrane was blocked in a milk solution for one hour and incubated with a primary

Ab over night at 4°C. After 3 x 10min washing in the buffer, the membrane was incubated with a secondary Ab for one hour at room temperature. Then the membrane was washed 3 x 10min in the buffer before development.

2.4.5 Film development and membrane stripping

The secondary Abs used in chapter 2.4.4, are covalently bound to the enzyme Horseradish Peroxidase (HRP). HRP react with a substrate, and the product formed produces chemiluminescence, which could be detected by a film or an image station. Materials and instruments used during film development and membrane stripping are listed in table 2.10. A substrate solution was made by mixing equal amounts of the two solutions from the SuperSignal®West Dura Extended Duration Substrate kit. The membrane was incubated in the Substrate solution for 2-5min before development, which was performed first on the computer based Kodak image station, and then on the more sensitive film-based AGFA CURIX 60 developer.

If the membrane was reused for subsequent incubation with a different primary Ab, the membrane had to be stripped removing the previous Abs. The membrane was washed with a buffer to remove excess of substrate and incubated in 1M Glycine pH 2.2 for 30min removing the Abs, followed by neutralization for 10min in the buffer suitable for the next Ab. Then, the membrane was blocked in a milk solution and incubated with a subsequent primary Ab followed by the secondary Ab as explained in chapter 2.4.4.

Table 2.10: Materials and instruments used to develop a film from a membrane, and strip a membrane, during western analysis.

Material/instrument:	**Company:**	**Cat#:**
Glycine 1M, pH 2.2	Merck, Germany	04201
SuperSignal®West Dura Extended Duration Substrate	Thermo Scientific	34076
AGFA CURIX 60 developer	AGFA	
Kodak image station 2000R	Kodak	

2.5 Quantitative Polymerase Chain Reaction – qPCR

Quantitative PCR, also called real time PCR, is a method used to amplify and simultaneously quantify a target DNA sequence in a given sample. This method is often used to quantify the mRNA level in cells. First, purified RNA is transcribed into complementary DNA (cDNA), which is further amplified by PCR. This enables quantification of a target mRNA level (i.e. gene expression). In this work, real time PCR was performed by employing a sequence-specific fluorogenic (TaqMan) probe resulting in an increase of fluorescence intensity proportional to the amount of an accumulating PCR product matching the probe. Materials and instruments generally used in qPCR are listed in table 2.11.

Table 2.11: Materials and instruments generally used in qPCR.

Material/instruments:	**Company:**	**Cat#:**
iCycler PCR machine	BIO-RAD laboratories	170-8703
Nuclease free water	BIO-RAD laboratories	10623
PCR plates, 96 well for iCyclerIQ™	BIO-RAD laboratories	223-9441

2.5.1 RNA isolation and purification of RNA samples

To isolate cellular RNA, the cell must be lysed, and the cell lysate must be purified. Materials, instruments and software used for RNA isolation and RNA sample purification are listed in table 2.12. RNA was isolated from cell pellets (harvested as in chapter 2.2) by using the column based RNA isolation kit from Sigma. RNA concentrations, the 260/280 ratio and the 260/230 ratio were measured by the Nanodrop 1000 instrument and recorded by the ND-1000 program, as shown in FIG. 2.5.

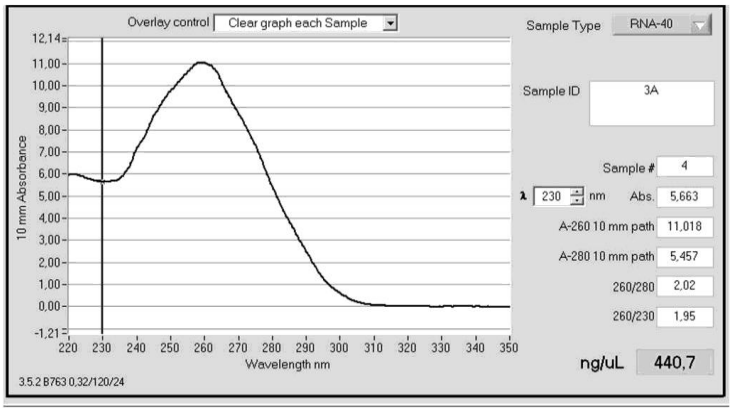

FIG. 2.5: RNA absorption curve. This sample had a high RNA concentration = 440,7ng/µl, and the 260/280 and 260/230 ratios are satisfactory.

If 260/280 (describing the RNA/protein relation) and 260/230 (describing the RNA/ organic contaminant relation) ratios were lower than 2.0 and 1.7, respectively, ethanol precipitation was performed to purify the RNA sample as follows: 3M NaAc pH 5.2 was added to the RNA sample at the volume ratio of 0.1:1 and mixed well before the addition of 2.5 volumes of absolute ethanol. The sample was mixed well, kept on ice for at least 10min, and centrifuged for 20min at 4°C at 12000g. The pellet was washed with 100µl 70% ethanol and centrifuged as before. Supernatant was discarded, while the RNA pellet was dried on ice for about 5min. 50µl RNA Storage buffer was added to the RNA pellet and the RNA concentration was measured by the Nanodrop 1000 instrument. RNA solutions with a satisfactory quality (i.e. 260/280 and 260/230 ratios) were diluted to a concentration of 200ng/µl with a RNA storage buffer and stored at -80^{o}C.

Table 2.12: Materials, instruments and software used for RNA isolation and RNA sample purification.

Materials/instruments/Software:	**Company:**	**Cat#:**
Ethanol/ Absolutt Alkohol Prima	Arcus	
GenElute™ mammalian total RNA miniprep kit	Sigma Aldrich, Switzerland	RTN350
Nanodrop 1000	Thermo Scientific	
ND-1000 program, Version 3.5.2	Nanodrop	
RNA storage buffer	Ambion	AM7001
Sodium Acetate 3M (NaAc) pH 5.2	Novagen	69718

2.5.2 From RNA to complementary DNA: cDNA synthesis

To synthesize cDNA from RNA, 5µl of a 200ng/µl RNA sample was mixed with 10µl nuclease free water, 4µl 5x iScriptTM reaction mix and 1µl Reverse transcriptase iScript TM to give a total volume of 20µl (materials listed in table 2.13.). The cDNA synthesis program was as follows: 22°C for 5min, 42°C for 30min, 85°C for 5min and 4°C as a hold temperature. Then, 80µl nuclease free water was added to each cDNA sample, which was stored at -80°C.

Table 2.13: Materials used in cDNA synthesis.

Material:	**Company:**	**Cat#:**
5x iScriptTM reaction mix	BIO-RAD laboratories	10651
Reverse transcriptase iScript TM RT	BIO-RAD laboratories	10650

2.5.3 Real time PCR

To quantify the expression of the selected gene, real time PCR was preformed using TaqMan probes. Materials, instruments and software used in real time PCR are listed in table 2.14. The reaction mixture for each well was as follows: 7.25µl nuclease free water, 1.25µl TaqMan primer/probe targeting the desired gene and 12.5µl TaqMan Master Mix were mixed. The mix was transferred to a 96-well PCR plate, before 4µl of cDNA template was added. In the negative controls, 4µl nuclease free water was added. The samples were run 40 cycles for 15s at 95°C and 1min at 60°C, after 5min initial denaturation at 95°C. The iCYCLER IQ program was used to record the data.

Relative quantification of gene expression was performed by the Genex software in Microsoft excel using the ΔΔCt method, where Ct (threshold cycle) is defined as the cycle number at which the samples fluorescence passes the threshold value[79]. Relative quantification enables comparison of a level of a target mRNA (i.e. expression of a target gene) in a test sample relative to another reference sample. First, the C_t values of all samples are normalized to an endogenous housekeeping

gene, here TBP and/or RPLPO, which gives the samples ΔCt-values. Then, the difference between ΔCt (test sample) and ΔCt (reference (here by Melmet 79 monolayer)), gives the ΔΔCt-values for each test sample. Relative Quantification (RQ), was calculated as $RQ = 2^{-\Delta\Delta Ct}$.

Table 2.14: Materials, instruments and software used in real time PCR.

Materials/Instruments/Software:	**Company:**	**Cat#:**
Bruce Primer/Probe	Applied Biosystems	HS00212288
cIAP-1 Primer/Probe	Applied Biosystems	HS00357350
cIAP-2 Primer/Probe	Applied Biosystems	HS00154109
Genex software v1.10 ©2004	BIO-RAD laboratories	
iCYCLER IQ™, version 3.1	BIO-RAD	
Large Ribosomal protein -RPLPO Primer/Probe	Applied Biosystems	4333761-0701012
Livin Primer/Probe	Applied Biosystems	HS00223384
NAIP Primer/Probe	Applied Biosystems	HS00244967
Survivin Primer/Probe	Applied Biosystems	HS00153353
TaqMan®Gene Expression Master Mix	Applied Biosystems	4369016
TATA Binding Protein - TBP Primer/Probe	Applied Biosystems	4333769-0704010
XIAP Primer/Probe	Applied Biosystems	HS00236913

2.6 Complexation and transfection of siRNA

To introduce foreign nucleic acids in mammalian cells by transient transfection, cationic lipid based transfection agents, such as Lipofectamine 2000 (LP2000) and Lipofectamine RNAi MAX (LPMAX), could be used. Lipids in complex with siRNA will theoretically be taken up by endocytosis, follow the endocytic pathway, and result in siRNA release into the cytosol. Materials used in complexation and transfection of siRNA are listed in table 2.15. Which type of siRNA used, varied in different assays, but final concentration of siRNA was always 25nM. Information about the siRNAs is listed in the different assay used.

Transfection solution with LP2000 was made as follows (see FIG. 2.6 for illustration): 250µl RPMI without FCS (RPMI+) was mixed with 2.5µl LP2000 and

incubated for 5min (volume of LP2000 could vary between experiments). Then the LP2000-solution was carefully dripped into 250µl RPMI+ mixed with 2.5µl siRNA, and incubated for 20min to form siRNA/LP2000 complexes. The 500µl transfection solution was added gently into well containing cells in 500µl fresh media (RPMI++ in monolayer and hESCM4 in spheroids). Incubation time varied between experiments

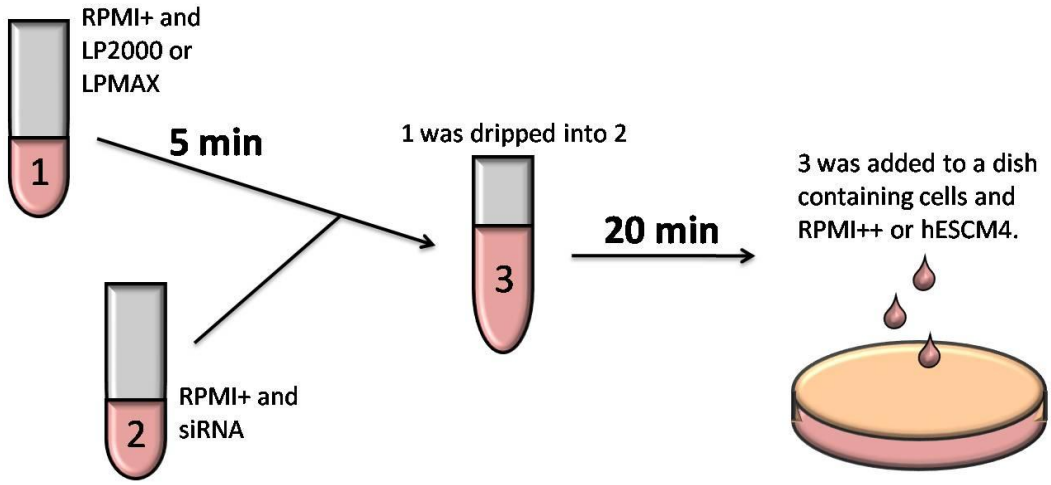

FIG. 2.6: *General preparation of siRNA complexes for transfection of cells. (See text for explanation).*

Transfection solution with LPMAX was made as follows (see FIG. 2.6 for illustration): 2.5µl LPMAX was mixed with 100µl RPMI+ and incubated for 5min (LPMAX volumes could vary between experiments). An siRNA solution containing 100µl RPMI+ mixed with 3µl siRNA, were made, and the LPMAX solution was added. After 20min, 200µl transfection solution was added gently into well containing cells in 1000µl fresh media (RPMI++ or hESCM4). Incubation time varied between experiments.

Table 2.15: Materials used in complexation and transfection of siRNA.

Materials:	**Company:**	**Cat#:**
Lipofectamine™ 2000, 1µg/ml	Invitrogen, CA	P/N 52887
Lipofectamine™ RNAiMAX	Invitrogen, CA	13778-075

2.7 Flow cytometry

Flow cytometry is a method, which allows multi parameter analysis of the physical and/or chemical parameters of single cells. It enables identification of cell populations with certain qualities, based upon the specific light scattering and fluorescent characteristics of the individual cells. Materials, instruments and software generally used in Flow cytometry are listed in table 2.16. Forward scatter (FSC) reflects the cell size, while side scatter (SSC) reflects the complexity/granularity of a cell. Here, FCS and SSC parameters have been used to select, (i.e. to gate), a main cell population[80] (FIG. 2.7 A). Single cells have been discriminated from duplets by gating on SSC width against SSC area (FIG. 2.7 B). Propidium Iodide (PI) is able to penetrate the cell membrane of dead/dying cells, but is not taken up by healthy cells. Thus, PI-staining can be used to exclude dead cells from the analysis. Prior to analysis, PI was added (1µg/ml, final concentration) and the gate was set to only include the viable cells (FIG. 2.7 C).

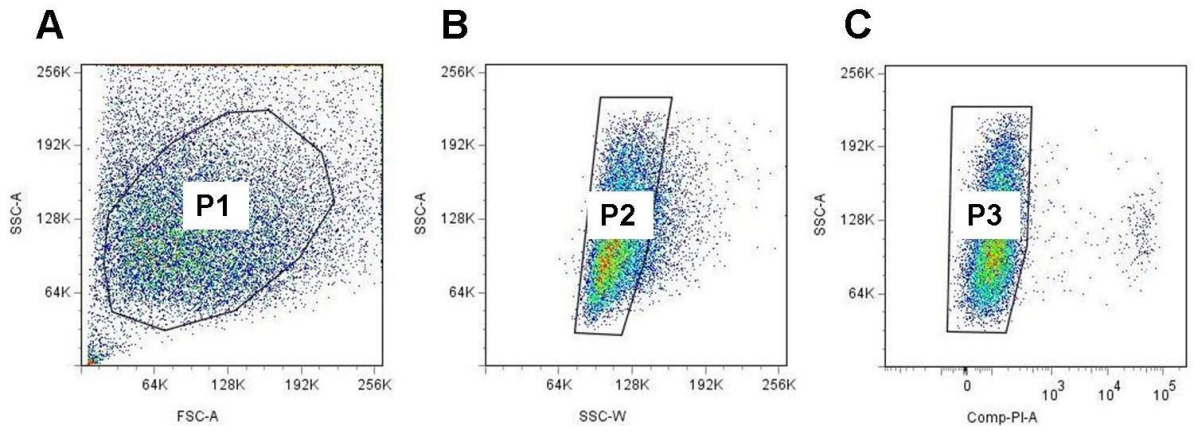

FIG. 2.7: Representative dot plots from the flow cytometry analysis. Samples were analyzed by sequential gating including: main population (P1) in (A), single cells (P2) in (B) and living cells (P3) in (C).

The cells from the P3 gate, i.e. viable single cells, were further analyzed for the fluorescence signals. The fluorescent dyes like FAM, Alexa 488 and FITC were identified after excitation with a blue argon laser (488 nm), while Alexa 647 was identified after excitation with a red diode laser (635 nm). The cells

containing/binding a fluorescent dye were identified by comparing the fluorescent signals in the test samples versus the unstained control samples in dot plots (FIG. 2.8 A) or in histograms (FIG. 2.8 B).

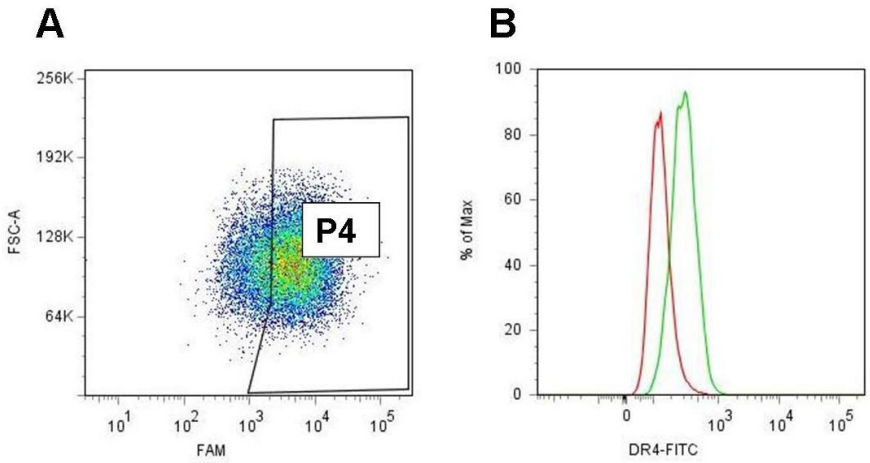

FIG. 2.8: (A) A representative dot plot indicting cells positive for the fluorescent molecule FAM, shown in the P4 gate. The P4 gate was set adjacent to the control (i.e. cells without a fluorescent dye). (B) A representative histogram indicating a clear shift of the FITC-dye signal in the fluorescent test sample, in green, as compared to the unstained control sample, in red.

Between 10000 and 20000 events were recorded for each sample. BD FACSDiva™ software was used to control flow cytometer settings and sample analysis, and FlowJo Software was used to process the data.

Table 2.16: Materials, instruments and software generally used in Flow cytometry.

Materials/instruments/Software:	**Company:**	**Cat#:**
BD FACSDiva™ software, version 5.0.3	Becton Dickinson (BD)	
Flow cytometer - BD LSRII	Becton Dickinson (BD)	
Flow tubes	BD Falcon	352235
FlowJo 7.2.5 software	Tree Star Inc, Oregon	
Propidium iodide (PI)	Sigma Aldrich, Switzerland	70335

2.8 Uptake of siRNA-FAM by microscopy and Flow cytometry

To test whether Melmet cells grown as monolayer or spheroids could be efficiently transfected with siRNA in complex with the transfection agent LP2000, we employed fluorescently labeled siRNA, which could be detected by Flow cytometry using a 488nm excitation laser or by microscopy using an Hg-lamp and a 488nm filter. (siRNA sequence: 1.strand: 6-FAM(carboxyfluorescein)-5`-AUU-CUU-CCC-CUC-UCU-ACA-AdTdT-3`, 2.strand: 5`-UUG-UAG-AGA-GGG-GAA-GAA-GAA-UdTdT-3`). Unlabeled siRNA was used as a negative control. Materials, instruments and software used to study uptake of siRNA-FAM were listed in table 2.17.

Approximately $2.0x10^5$ monolayer cells were seeded into a well of a 6-well plate on day one, transfected with siRNA complexes on day two and analyzed on day three. Spheroids transferred into a well of a 12-well plate were transfected with siRNA complexes on day one and measured on day two. One well of a 6-well plate contained 1000µl, and one well of a 12-well plate contained 500µl of transfection solution. LP2000 concentration was 2.5µl/1000µl media, and the transfection solutions were made as described in chapter 2.6. The plate was covered in aluminum foil for light protection.

Spheroids were treated similarly to monolayer cultures, but with transfection solutions in half the amounts.

2.8.1 Detection by microscopy

Monolayer cultures: On day three, the transfection media was removed, the cells were washed once with PBS and 1ml RPMI++, before pictures were taken by microscopy. Cell pictures were taken by using the AxioVision software. Fluorescence pictures were taken by using a FITC filter and merged with a phase contrast pictures by using Adobe Photoshop software.

Spheroids: On day two, spheroids were disintegrated as described above and the single cell solution was transferred to a new well in a 12-well plate. The cells were allowed to attach for 3-4 hours before the picture were taken and processed as described above.

2.8.2 Detection by Flow cytometry

Monolayer cultures: On day three, the transfection media was discarded, the cells were washed once with PBS and incubated with Trypsin. 4ml RPMI++ was added to inhibit Trypsin, and the cell suspension was centrifuged for 5min at 1200rpm. Pellet was washed once with RPMI++ and centrifuged for 5min at 1200rpm. The cell pellet was resuspended in 500µl RPMI++, filtered trough a flow-tube filter and collected in a flow tube. The samples were kept on ice in the dark until analysis by the flow cytometer as described in chapter 2.7.

Spheroids: On day two, the spheroids were sedimented in media once, and in PBS twice, to separate big spheroids from the single cells and small cell clumps, which stayed in the solution and could be discarded. Then the pellet of the big spheroids was treated with 100µl Trypsin until the spheroids were dissembled into single cells. RPMI++ was added and the cell suspension was centrifuged for 5min at 1200rpm. The pellet was washed with RPMI++, centrifuged again, resuspended in 500µl RPMI++ and transferred into a flow tube and analyzed by the flow cytometer as described above and in chapter 2.7.

Table 2.17: Materials, instruments and software used by Flow cytometry and microscopy, investigating uptake of siRNA-FAM.

Materials/Instruments/Software:	**Company:**	**Cat#:**
Adobe Photoshop CS2, software		
Aluminum foil		
AxioVision Rel 4.6, software		
Lipofectamine™ 2000, 1µg/ml	Invitrogen, CA	P/N 52887
Microscope Axiovert 200M	Zeiss	
siRNA Silencer® Negative Control	Ambion	AM4611
siRNA-FAM 20µM	OliGold	
Trypsin EDTA	BioWittaker®, Belgium	17-161E

2.9 Detection of DR4 and DR5 level by Flow cytometry

The levels of DR4 and DR5 were determined by flow cytometry in Melmet cells grown as monolayers or as spheroids. Materials used when detecting DR4 and DR5 levels are listed in table 2.18. Since the primary DR5-specific Ab did not have a fluorescent label, the use of a secondary Ab labeled with a fluorescent dye was necessary. Therefore DR5 primary Abs were used in combination with Alexa 488- or Alexa 647-labeled secondary Abs that could be detected by the flow cytometer following excitation with a blue or a red laser, respectively. Samples treated with the mouse IgG_1, which should not bind any specific surface molecule, was used as a control and to set the gates to identify DR5 positive cells. DR4 primary Ab was labeled with Alexa 488 and, therefore, did not require a secondary Ab. Mouse IgG_1 FITC was used as an isotype control. Various concentrations of DR5 and DR4 Abs were tested to stain ~$350x10^3$ cells. HeLa and HCT116 cells were used as positive controls, as recommended by the manufactures (data not shown).

Monolayer cells were EDTA treated and diluted with RPMI++. Spheroids were sedimented, washed in PBS, sedimented again, treated with EDTA to disintegrate the spheroids and diluted in RPMI++. Cells were counted to determine cell concentration

in the suspension. The cell suspension was centrifuged for 8min at 1500rpm and pellet was washed in PBS with 2% FCS, before centrifugation for 8min at 1500rpm. The cell pellet was resuspended in Flow blocking buffer (Fbb) until the final concentration of ~350x10^3 cells in 50µl buffer. 50µl cell suspension was transferred into each test tube containing 50µl Fbb with the desired concentration of primary Ab and mixed gently. After incubation for 30min on ice, 900µl PBS with 2% FCS were added, and the tubes were centrifuged for 8min at 1500rpm. Samples stained with the fluorescently labeled anti-DR4 were resuspended in 500µl PBS with 2% FCS and pipetted through a filter into a flow tube. The tubes were kept on ice in the dark before analysis. Samples stained with the unlabeled anti-DR5 had to be incubated with the fluorescently labeled secondary Ab. Therefore, the cell pellet was resuspended in 1ml PBS with 2% FCS, centrifuged for 8min at 1500rpm and the cell pellet was mixed with 100µl Fbb containing secondary Ab at the concentration of 4µg/100µl. After incubation for 30min on ice, 900µl PBS with 2% FCS were added, the tubes were centrifuged for 8min at 1500rpm, and the cell pellet was resuspended in 500µl PBS with 2% FCS. Cell suspension was pipetted through a filter into a flow tube, and the tubes were kept on ice in the dark before Flow cytometry analysis as described in chapter 2.7.

Table 2.18: Materials used when detected DR4 and DR5 level by Flow cytometry.

Material:	**Company:**	**Cat#:**
Alexa Fluor® 488, goat anti-mouse-IgG_1	Invitrogen, USA	A21121
Alexa Fluor® 647, goat anti-mouse-IgG_1	Invitrogen, USA	A21240
Aluminum foil		
Gammagard S/D	N.V Baxter S.A, Belgium	
HCT116 colorectal adenocarcinoma cell line	ATCC (Manassas, VA)	CCL-247
HeLa cell line	ATCC (Manassas, VA)	CCL-2
IgG_1 antibody	Sigma Aldrich, Switzerland	I5381
Monoclonal Ab to DR5, mouse anti-human	eBioscience	14-9908
Mouse anti-human CD 261/DR4 Alexa 488	Serotec	MCA2332A488
Mouse IgG_1 FITC	BD Pharminogen™	555748

2.10 Evaluation of cell viability following treatment with TRAIL receptor antibodies

Melmet cultures grown as monolayer were tested for survival after treatment with the TRAIL receptor Abs: HGS-ETR 1 and HGS-ETR 2 by MTS assay. MTS is reduced into formazan in metabolically active (i.e. viable) cells. The production of formazan (soluble, colored molecule) is proportional to the number of living cells, and thus the produced color is an indication of the viability of cells. Materials and instruments used when evaluating cell viability after treatment with TRAIL receptor Abs are listed in table 2.19. Untreated cells and cells treated with HGS-IgG were used as controls. Melmet 1 and 5 cells were seeded at densities 3000 cells per well, and Melmet 79 – at density 4000 cells per well, in a 96 well plate on day one. On day two, Ab solutions (at the final concentrations 1µg/ml and 10µg/ml) were added to the cells.

On day five, 20µl MTS (Cell Titer 96®Aqueous Cell Proliferation Assay) was added to each well, and plates were incubated for 2-3hours at 37°C. Absorption was measured at 490nm for 1second by the Wallac instrument, and used to calculate cell viability.

Table 2.19: Materials and instruments used when evaluating cell viability after treatment with TRAIL receptor antibodies.

Materials/Instruments:	**Company:**	**Cat#:**
Cell Titer 96®Aqueous Cell Proliferation Assay (MTS)	Promega (Madison, WI)	G3581
HGS-IgG	Human Genome Sciences	Not available
HGS-ETR 1	Human Genome Sciences	Not available
HGS-ETR 2	Human Genome Sciences	Not available
Victor2 Wallac 1420 multi label counter	Wallac	MR1463

2.11 Spheroid forming assay

A spheroid forming assay, is an assay where cells are tested for the ability to form a new passage of non-adherent spheroids from a single cell i.e. its spheroid forming

capacity (SFC). In many cancer types, including melanoma, SFC seems to reflect tumor initiating capacities of the cells *in vivo*[19]. Materials and instruments used in spheroid forming assay are listed in table 2.20. Melmet cells were tested for their SFC when grown in hESCM4 containing HGS-ETR 1 and HGS-ETR 2. Untreated cells and cells treated with HGS-IgG were used as controls. Single cells from disintegrated spheroids were seeded out at low density, i.e. 1000 cells per 5cm dishes in 4ml hESCM4 containing 10µg/ml HGS-ETR 1 or HGS-ETR 2. Every other day 1ml fresh media was added to the dishes. When "big" spheroids were formed in the control dishes, all samples were evaluated, and spheroids larger than 110µm were counted using a Nikon microscope. A certain inaccuracy was expected, since non-computerized counting will be influenced by a manually variation. Relative sphere formation (RSF) relative to untreated control was calculated from the obtained data.

Table 2.20: Materials and instrument used in spheroid forming assay.

Material/Instrument:	**Company:**	**Cat#:**
HGS-ETR 1	Human Genome Sciences	Not available
HGS-ETR 2	Human Genome Sciences	Not available
HGS-IgG	Human Genome Sciences	Not available
Microscope	Nikon, Japan	

2.12 Evaluating transfection efficiency and toxicity with siRNA complexed to Lipofectamine 2000 or Lipofectamine RNAi MAX.

Different cell lines show different transfection efficiency and toxicity when exposed to different transfection agents. Materials and instruments used when evaluating these two parameters, when transfecting cells with siRNA in complex with lipid based transfection agents, are listed in table 2.21. Complexation and transfection were preformed as described in chapter 2.6. Melmet cells grown as monolayer were tested for down-regulation of the protein XIAP after treatment with anti-XIAP siRNA in complex with LP2000 or LPMAX.

When testing down regulation, $2.0x10^5$ cells of Melmet 1 and 5, and $3.0x10^5$ cells of Melmet 79 were seeded out in a well of a 6-well plate on day one. The cells were transfected on day two. LP2000 volume of 2.5µl and 5µl/1000µl end volume, and LPMAX volume of 2.5µl and 7µl/1200µl end volume were tested. Cells were harvested for western blot analysis on day four (as described in chapter 2.2). Protein lysate was made and analyzed by SDS-PAGE and western blotting (as explained in chapter 2.4). The efficiency of XIAP down-regulation was evaluated comparing the XIAP level in treated samples with XIAP level in untreated control cells.

When testing toxicity, 3000 cells of Melmet 1 and 5 and 4000 cells of Melmet 79 were seeded in a well in a 96-well plate on day one. The cells were transfected on day two with negative control siRNA in complex with a LP2000 at a concentration of 5µl per 1000µl media, or a LPMAX concentration of 2.5µl, 7.5µl or 12.5µl LPMAX per 1200µl media. Untreated cells were used as control. MTS assay were preformed on day three, and cell viability relative to control cells, were calculated (as in chapter 2.10). Toxicity was also tested after three days of incubation, i.e. MTS assay on day five, with LP2000 (5µl/1000µl media).

Table 2.21: Materials and instrument used when evaluating toxicity and transfection efficiency of LP2000 and LPMAX in complex with siRNA.

Material/Instrument:	**Company:**	**Cat#:**
Anti-XIAP siRNA	Ambion	AM16708 (ID 121292)
Cell Titer 96®Aqueous Cell Proliferation	Promega	G3581
Lipofectamine™ 2000, 1µg/ml	Invitrogen, CA	P/N 52887
Lipofectamine™ RNAiMAX	Invitrogen, CA	13778-075
siRNA Silencer® Negative Control	Ambion	AM4611
Victor2 Wallac 1420 multi label counter	Wallac	MR1463

2.13 Combinatorial effects – TRAIL receptor antibodies and siRNA

Melmet cells grown as monolayer were tested for survival, and cells grown as spheroids were tested for their SFC, after combined treatment with HGS-Abs and siRNA against XIAP or survivin. The type and the amount of transfection agent used to make complexes with siRNA, was determined by optimization as described in chapter 2.12 and chosen for each Melmet. Materials and instruments used when testing combinatorial effects are listed in table 2.22.

Cells grown as monolayer were seeded at a density 3000 cells per well in a 96-well plate on day one. (See FIG. 2.9. for illustration.) On day two, the cells were transfected with siRNA as described in chapter 2.6. On day three, 10µg/ml HGS-ETR 1 or HGS-ETR 2 were added together with new RPMI ++. Cell viability was measured by the MTS assay on day five (as in chapter 2.10).

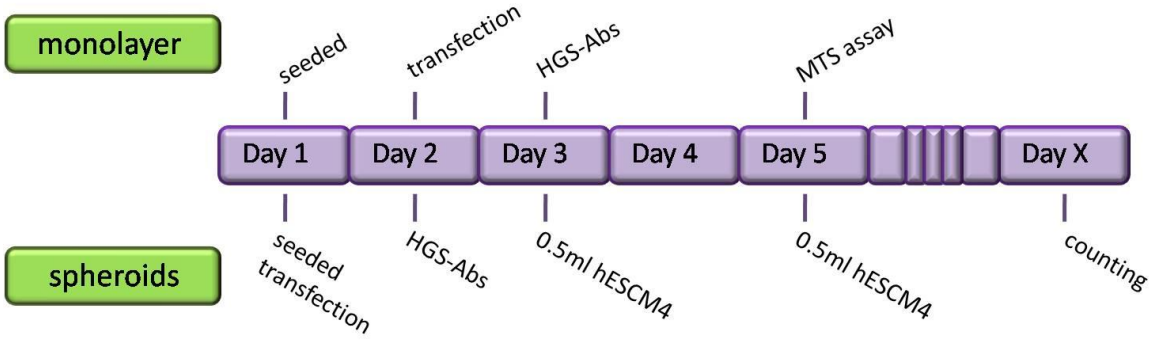

FIG. 2.9: Time based overview of combinatorial treatment of monolayer and spheroids.

On day one, single cells from disintegrated spheroids were seeded at a density 700 cells per well in a 24-well non-adherent plate and transfected as described in chapter 2.6 (see FIG. 2.9. for illustration.), except Melmet 79, which were transfected in half the LP2000 concentration used when transfecting monolayer cells. On day two, the cell and the media were transferred to a 6-well plate, and treated with 10µg/ml HGS-ETR 1 or HGS-ETR 2. 0.5ml hESCM4 was added to the wells every other day until large spheroids were formed in the control well. Spheroids larger than 110µm were

counted manually using a Nikon microscope, and RSF was calculated. Pictures were taken using the GelCount machine.

Table 2.22: Materials and instruments used in combinatorial treatment with TRAIL-like antibodies and siRNA.

Materials/Instruments:	**Company:**	**Cat #:**
24 well non adherent plate	Costar®, USA	3473
Anti-survivin siRNA	Ambion	AM 16708 (ID 121295)
Anti-XIAP siRNA	Ambion	AM16708 (ID 121292)
GelCounter	Oxford Optronix	
HGS-ETR 1	Human Genome Sciences	Not available
HGS-ETR 2	Human Genome Sciences	Not available
HGS-IgG	Human Genome Sciences	Not available
Lipofectamine™ 2000, 1µg/ml	Invitrogen, CA	P/N 52887
Lipofectamine™ RNAiMAX	Invitrogen, CA	13778-075
Microscope	Nikon, Japan	
siRNA Silencer® Negative Control	Ambion	AM4611

3. Results

3.1 Expression of IAPs in metastatic melanoma cell cultures: monolayers *versus* spheroids

Cancer cells tend to have a higher apoptotic resistance compared to healthy somatic cells. One of the reasons for the reduced apoptotic ability could be related to an elevated level of anti-apoptotic proteins, for instance the IAPs. In this study the expression of IAPs in Melmet 1, 5 and 79 was evaluated. The level of seven different IAPs (survivin, XIAP, livin, cIAP-1, cIAP-2, Bruce and NAIP) was evaluated by western blot and/or real time PCR. Cells grown as spheroids and cells grown as monolayers were compared with respect to the levels of IAPs, in order to evaluate if growth conditions influence the IAP expression. To investigate whether melanoma cells, which survive under *in vivo* conditions and manage to seed a tumor, could have enhanced anti-apoptotic properties, the expression level of IAPs in melanoma cells from *in vivo* was also evaluated. For this purpose, melanoma cells isolated from experimental metastases established in rat tibia following systemic injection of Melmet 1 or Melmet 5 cells were analyzed.

Protein levels often reflect a cells status better than mRNA levels. Therefore, the western blot data were considered more reliable than the real time PCR data when conclusions were made about the expression of IAPs in various Melmet cultures. In addition, the known functions of the IAPs are preformed as proteins.

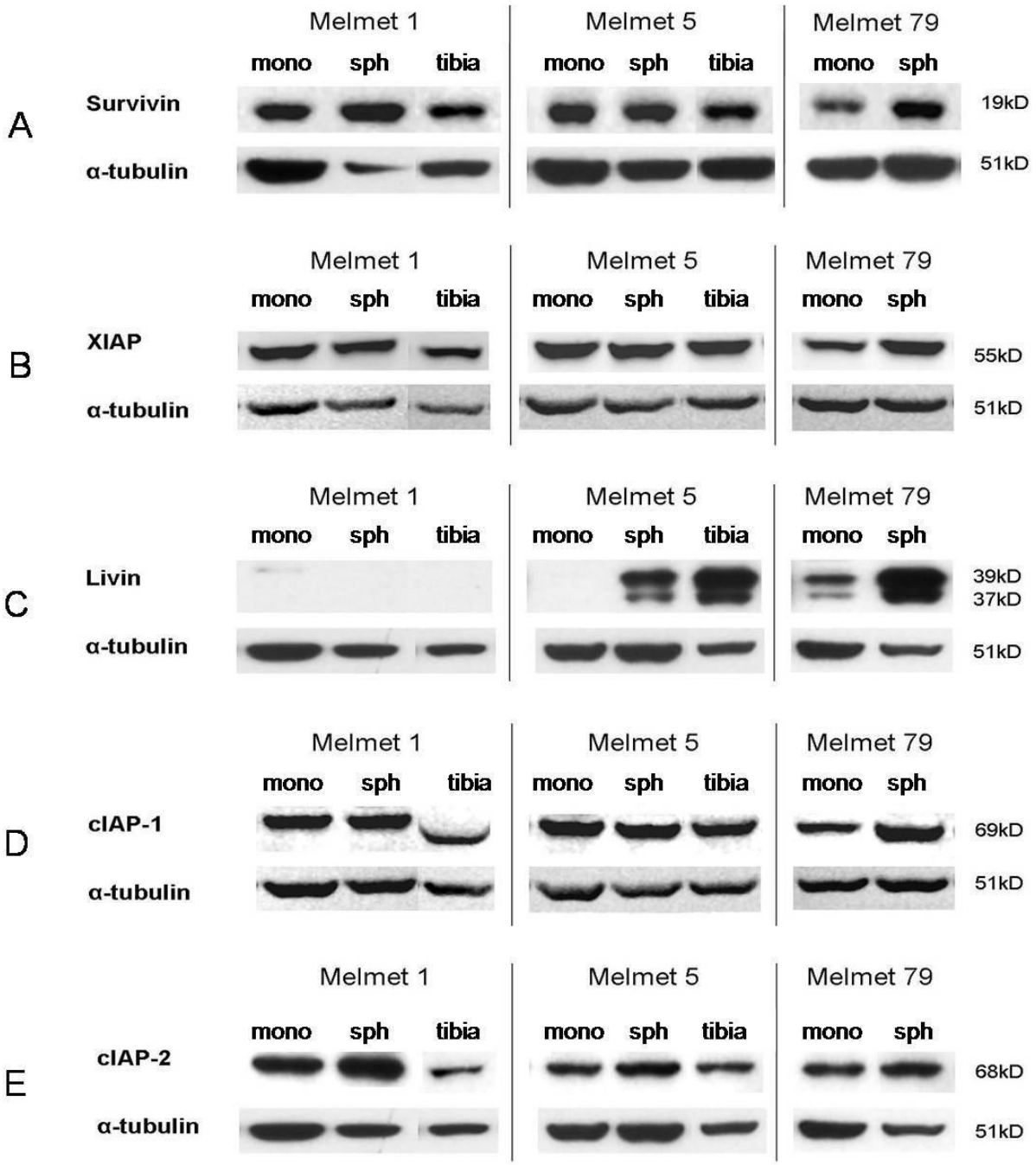

FIG. 3.1: Representative western blots describing (A) survivin, (B) XIAP, (C) livin (α 39kD, β 37kD), (D) cIAP-1 and (E) cIAP-2 protein levels in Melmet 1, 5 and 79 grown as monolayer (mono) or as spheroids (sph). "Tibia" denotes in vivo samples i.e. Melmet 1 and Melmet 5 cells isolated from experimental metastases in rat tibia. α-tubulin was used as a loading control. All IAPs were tested on two biologically independent sets of samples by western blot analysis.

Survivin was clearly expressed in all samples, as shown by western blot (FIG. 3.1 A) and confirmed by real time PCR (data not shown). Both Melmet 1 and 79 showed an elevated survivin level in the spheroids compared to the corresponding monolayers (FIG. 3.1 A), and this elevated expression was verified by quantification of band intensity (data not shown). However, growth condition had no influence on survivin expression in Melmet 5. Also melanoma samples from *in vivo*, i.e. experimental metastases in rat tibia, showed no deviation from *in vitro* cultures with respect to the levels of survivin. .

All three Melmet cell lines expressed XIAP, according to both western blot (FIG. 3.1 B) and real time PCR analysis (data not shown). The XIAP level in Melmet 1 and 5 was independent on growth environment both when analysed by western blot and real time PCR. Both methods pointed, however, towards a higher XIAP expression in the spheroids compared to the monolayer in Melmet 79.

Melmet 1 and Melmet 5 monolayers did not express livin, according to western blots (FIG. 3.1 C) and real time PCR (data not shown). However, livin was detectable in Melmet 5 spheroids, and even higher levels of livin was observed in the Melmet 5 samples from tibia (i.e. experimental metastases originating from injected Melmet 5 spheroid cells), as revealed both by western blots and real time PCR. Also, in Melmet 79 an elevated level of livin in the spheroids compared to the monolayer, was detected by both methods.

All Melmet 1 and Melmet 5 originating samples had similar amounts of cIAP-1, according to western blots (FIG. 3.1 D) and real time PCR (data not shown). Melmet 79 contained, according to western blot, a higher cIAP-1 level in the spheroids compared to the monolayer, but the real time PCR data pointed towards a similar level. A distortion of the cIAP-1 band in the tibia sample from Melmet 1 was probably due to a large amount of an unknown protein seen at ~70kD in the *in vivo* samples (detected by amidoblack staining, data not shown).

cIAP-2 levels in Melmet 5 were considered equal, based on both western blot (FIG. 3.1 E) and real time PCR analysis (data not shown). Melmet 1 and 79 spheroids showed a slightly elevated expression of cIAP-2 compared to the monolayer according to western blots (verified by quantification of intensity, not shown), which, however, was not confirmed by real time PCR data in respect to Melmet 1. The *in vivo* samples from *tibia* showed no increase in the cIAP-2 levels compared to the corresponding *in vitro* samples.

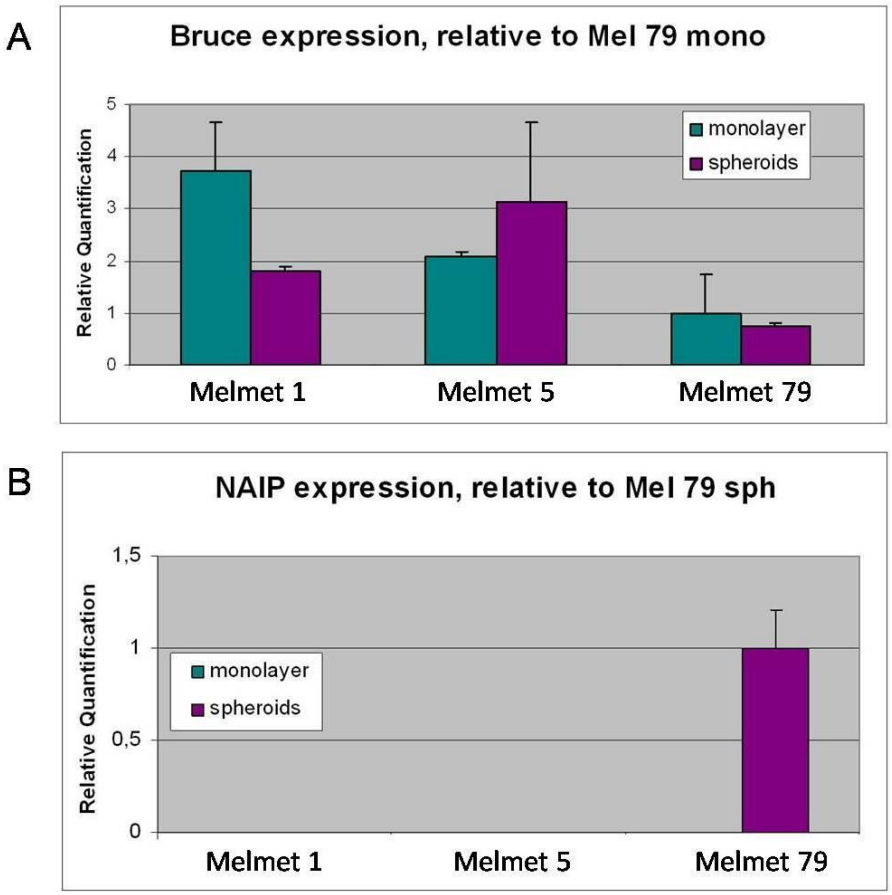

FIG. 3.2: Relative quantification based on real time PCR data for the expression of (A) Bruce and (B) NAIP in Melmet 1, 5 and 79 grown as monolayer and as spheroids. Changes in Bruce and NAIP expression relative to the expression in Melmet 79 monolayer and Melmet 79 spheroids, respectively, are presented. Error bars indicate standard deviations from two parallels in one experiment.

Western blotting was also preformed attempting to evaluate the expression of Bruce and NAIP, but, due to technical problems related to antibodies, no conclusions could

be drawn. Therefore, the real time PCR data constituted a basis when looking at trends of Bruce and NAIP expression in various Melmet cultures.

As shown in FIG. 3.2 A, Bruce was expressed in all samples. Melmet 1 monolayer had an increased Bruce level compared to the spheroids, whereas Melmet 5 tended in the opposite direction. Similar levels of Bruce were observed in both Melmet 79 cultures.

NAIP was not detectable in Melmet 1 or 5 (FIG. 3.2 B). Only Melmet 79 spheroids, but not the monolayer cells, had detectable level of NAIP.

	M1		M5		M79	
	mono	sph	mono	sph	mono	sph
Livin	-	-	-	xx	-	xxx
Survivin	xx	xxx	xx	xx	x *	xx
XIAP	xxx	xxx	xxx	xxx	xx	xxx
cIAP-1	xxx	xxx	xxx	xxx	xx	xxx
cIAP-2	xx	xxx	xx	xx	x *	xx

FIG. 3.3: Relative IAP levels in monolayer (mono) and spheroids (sph) of Melmet 1 (M1), Melmet 5 (M5) and Melmet 79 (M79) based on observations from western blot. The highest detected level within a group of a specific IAP was denoted as "XXX", and the other samples were scored related to this sample: "XXX" (strong expression, "XX" (medium expression), "X" (low expression) and "-"(not expressed), and are not to be compared between different IAPs. Purple boxes indicate an elevated IAP level in spheroids as compared to the respective monolayers. Quantification of band intensity for verification, are indicated by an "".*

In summary, all IAPs, except livin and NAIP, were expressed in all Melmet cultures studied. When comparing IAP levels in monolayers *versus* spheroids (FIG. 3.3), 8 of 15 (~53%) cases studied indicated an increased IAP level in the spheroids. The rest of the cases showed no differences in expression between the spheroids and the respective monolayer cultures.

3.2 Expression of death receptors DR4 and DR5 in melanoma cells cultured as monolayers or spheroids

TRAIL initiates the extrinsic apoptotic pathway via activation of the surface receptors DR4 and DR5. The levels of DR4 and DR5 in Melmet 1, 5 and 79 grown as monolayers and as spheroids were evaluated by staining the cells with anti-DR4/DR5 Abs followed by flow cytometric analysis.

To define an optimal DR4 and DR5 Ab-concentration, the Abs were titrated. The overlapping histograms (as illustrated in FIG. 3.4) indicate that receptor saturation was achieved both for the DR4 and DR5 Ab, and this was observed in all Melmet cultures. As shown in FIG. 3.4, 20µg of DR4 Ab and 2µg of DR5 Ab per 100µl cell suspension was sufficient for receptor saturation, and these Ab concentrations were used in the subsequent receptor analysis (presented in FIG. 3.5 and FIG. 3.6).

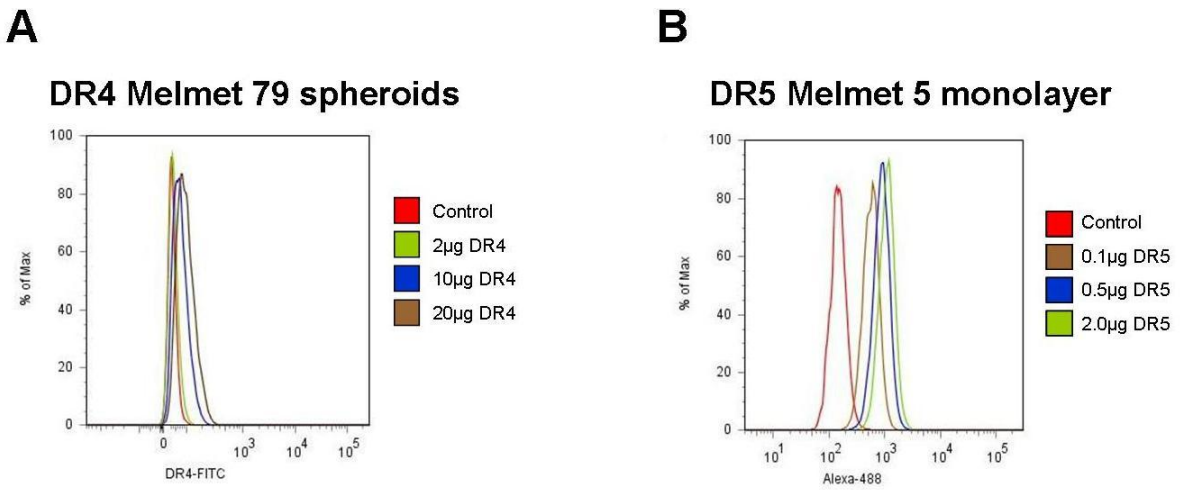

FIG. 3.4: Titration of DR4 and DR5 antibodies to verify receptor saturation. (A) Representative histograms indicating the DR4 antibody titration, here for Melmet 79 spheroids, with 2µg, 10µg and 20µg of the antibody per 100µl cell suspension. (B) Representative histograms indicating the DR5 antibody titration, here for Melmet 5 monolayer, with 0.1µg, 0.5µg and 2.0µg of the antibody per 100µl cell suspension. Amount of cells (% of max) were plotted against light intensity, in a logarithmic fashion.

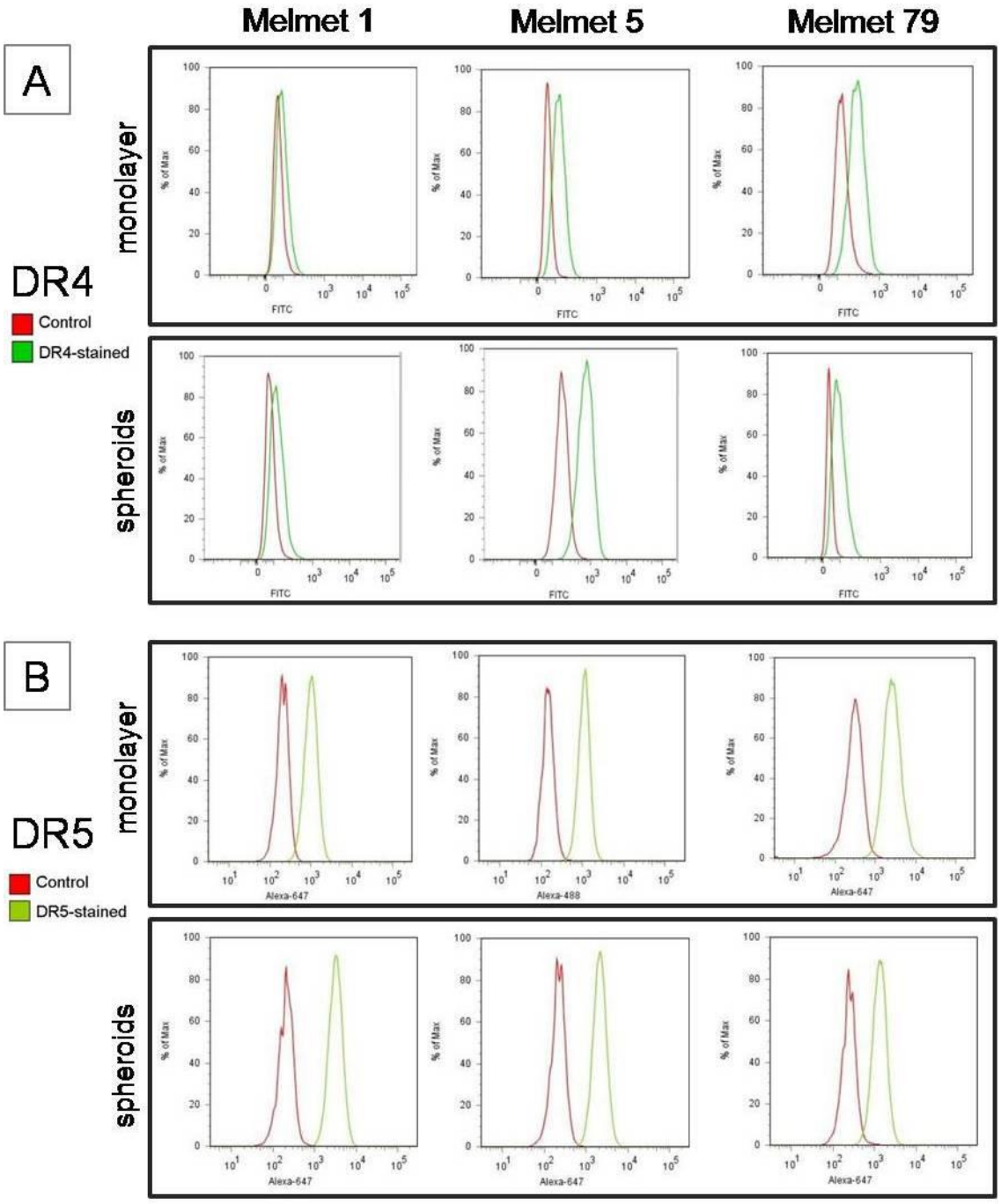

FIG. 3.5: Flow cytometry-based histograms indicating (A) DR4, and (B) DR5 Ab-stained cell populations in Melmet 1, Melmet 5 and Melmet 79 monolayer and spheroids. Amount of cells (% of max) was plotted against light intensity in a logarithmic fashion.

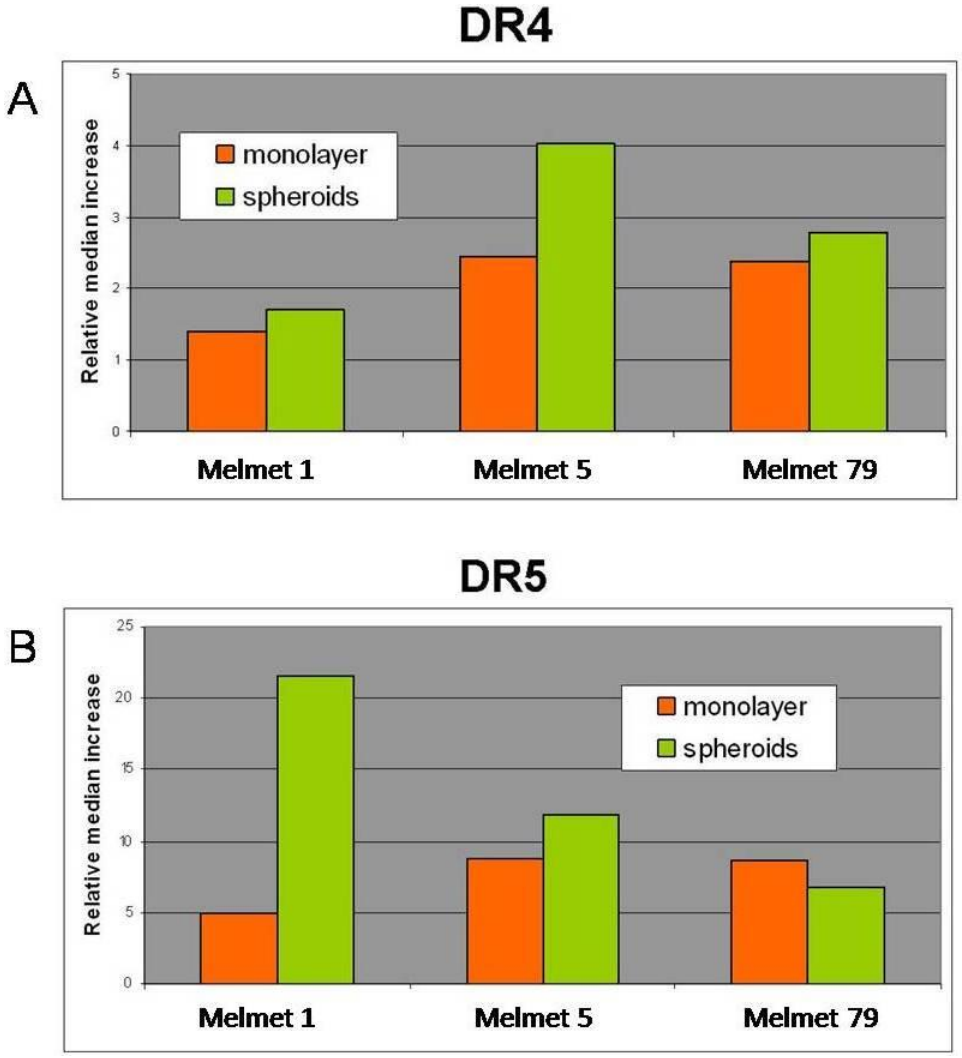

FIG. 3.6 (A) DR4 and (B) DR5 levels presented as relative median increase (i.e. fluorescence median in the test sample relative to fluorescence median in the control sample based on Flow cytometry measurements) in Melmet 1, 5 and 79 cells grown as monolayer and as spheroids.

DR4 positive cells were identified in all Melmet cultures (FIG. 3.5 A), though a relatively weak staining was observed, i.e. only a partial shift of the stained cell population versus the control cells, could be seen, leading to the conclusion that the Melmet cells have a relatively low amount of DR4. Spheroids tended to have a slightly higher level of DR4 than the corresponding monolayers in all Melmets, as shown in FIG. 3.6 A.

All Melmet cell lines were strongly stained with the DR5 antibody (FIG. 3.5 B), suggesting that Melmet cells have a high level of DR5 receptors. As for DR4, Melmet 1 and 5 also had a higher DR5 level in the spheroids as compared to the respective monolayers (FIG. 3.6 B).

Generally, there was not a separate unique cell population with very high or low levels of DR4 or DR5, suggesting that the majority of the cells in the Melmet cultures studied have somewhat similar levels of DR4 or DR5.

3.3 Sensitivity of melanoma cell cultures to the treatment with TRAIL receptor antibodies

Since the Melmet cell lines were concluded to express DR4 and DR5, TRAIL receptor Abs from HGS were employed to activate the apoptotic pathway via the death receptors. As mentioned previously, HGS-ETR 1 targets DR4 while HGS-ETR 2 binds DR5. An HGS-IgG Ab not targeting any specific receptor was used as a negative control. Melmet 1, 5 and 79 grown as monolayers were treated with Ab at concentrations of 1µg/ml and 10µg/ml for 48h and the cell viability was measured by using the MTS assay.

As shown in FIG. 3.7, all Melmets demonstrated a dose-dependent response to the TRAIL receptor Abs. At the highest Ab concentration used i.e. 10µg/ml, Melmet 1 demonstrated a cell viability of ~ 90% and ~70% when treated with HGS-ETR 1 and HGS-ETR 2, respectively (FIG. 3.7 A). Melmet 5 responded primarily to HGS-ETR 2 (10µg/ml), resulting in a cell viability of ~ 70% (FIG. 3.7 B). The best response to both HGS-ETR 1 and HGS-ETR 2, was seen in Melmet 79, where ~75% and ~40% viability, respectively, was observed following the treatment with 10µg/ml Abs (FIG. 3.7 C). HGS-IgG had no noteworthy effect in all three Melmets when compared to untreated control cells.

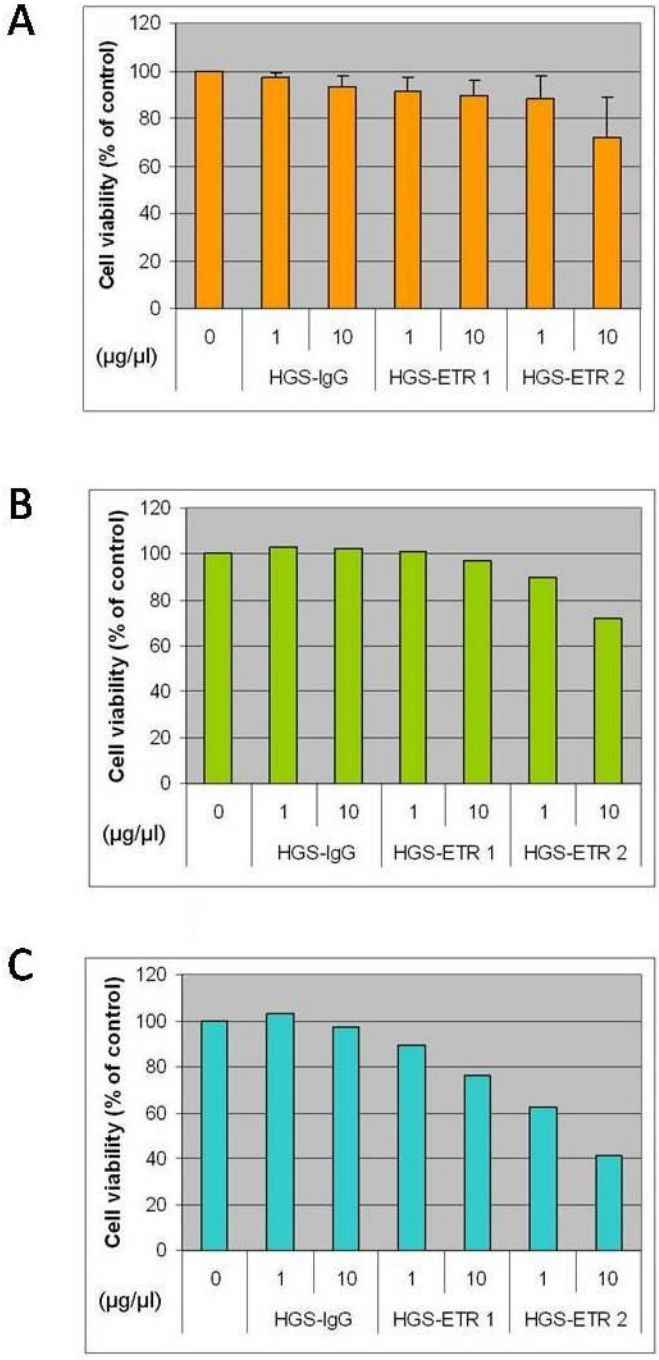

FIG. 3.7: Cell viability of (A) Melmet 1, (B) Melmet 5 and (C) Melmet 79 monolayer treated with TRAIL receptor antibodies from HGS at concentrations 1µg/ml and 10µg/ml. Data presented in (A) describe average values, and standard error of the mean, based on two independent experiments. Data presented in (B) and (C) are based on a single experiment. Each experiment was carried off with three parallels with satisfactory standard errors (not shown).

Melmet 1, 5 and 79 spheroid-derived cells were treated with TRAIL receptor Abs at the concentration of 10µg/ml, to examine whether their spheroid forming capacity (SFC) could be affected by the treatment. Data were related to untreated control and presented as relative spheroid formation (RSF).

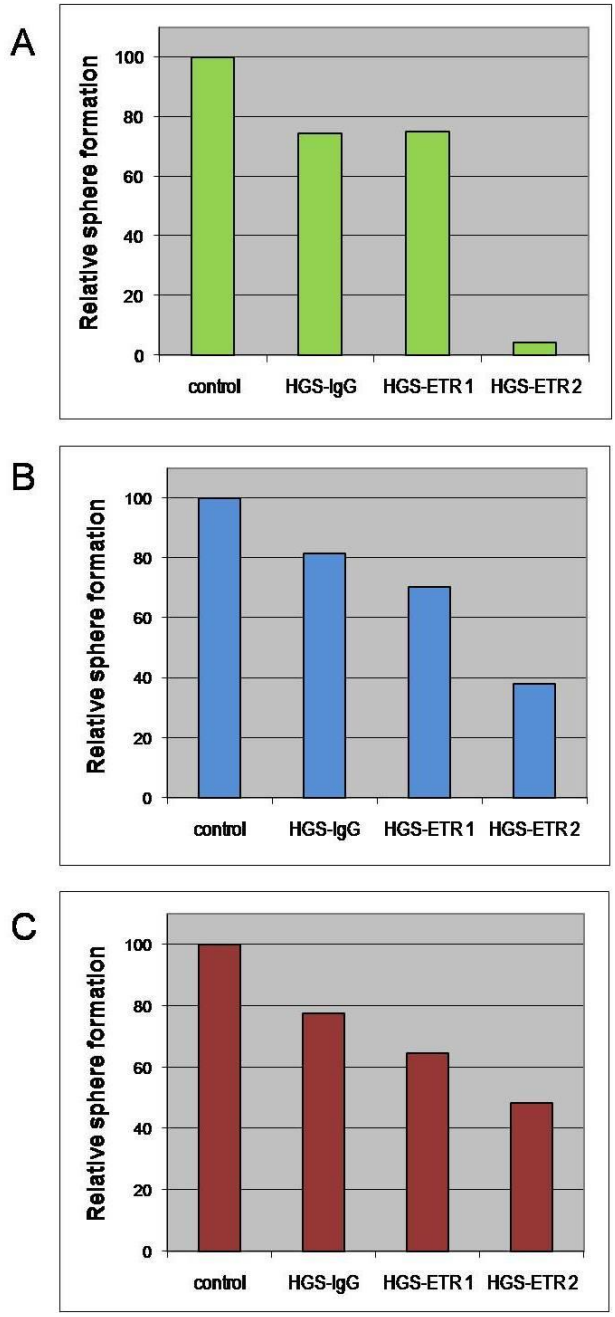

FIG. 3.8: Relative spheroid formation in (A) Melmet 1, (B) Melmet 5 and (C) Melmet 79 after treatment with TRAIL receptor antibodies. Spheroids larger than 110µm were counted, and data are based on one assay with two parallels with satisfactory standard deviations.

Generally, the effect of TRAIL receptor Abs, particularly HGS-ETR 2, was much more pronounced on the spheroid forming cells (FIG. 3.8) than on the monolayer cells (FIG. 3.7) in all Melmet lines. However, also the HGS-IgG had an effect on SFC (FIG. 3.8). Melmet 1 had a similar response to HGS-IgG and HGS-ETR 1, resulting in a ~75% RSF compared to untreated cells, and a strong response to HGS-ETR 2, resulting in ~5% RSF (FIG. 3.8 A). The SFC of Melmet 5 (FIG. 3.8 B) and Melmet 79 (FIG. 3.8 C) were also affected by negative control HGS-IgG (~80% RSF). Still, RSF of ~70% and ~40% were observed in Melmet 5, following treatment with respectively HGS-ETR 1 and HGS-ETR 2. Melmet 79 treated with HGS-ETR 1 or HGS-ETR 2 resulted in ~65%, and ~50% RSF, respectively.

Phase contrast microscopy pictures (FIG. 3.9) illustrate the differences seen in the spheroid formation following the treatment with HGS-IgG and HGS-ETR 2.

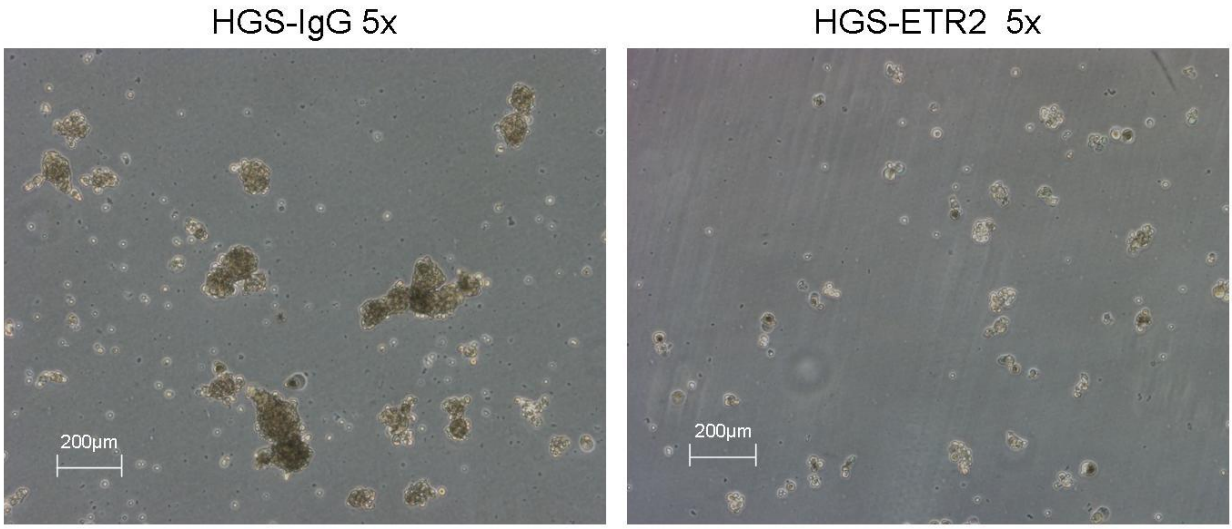

FIG. 3.9: Representative pictures from a spheroid forming assay, here represented by Melmet 1, treated with HGS-IgG (negative control) and HGS-ETR 2. Pictures were taken eight days after initiation of experiment with a 5x objective.

As can be seen in FIG. 3.9, spheroid forming cells treated with HGS-ETR 2 formed not only fewer, but also much smaller spheroids as compared to the IgG-treated control cells.

FIG. 3.10 compares DR4 or DR5 levels with their response to their respective TRAIL receptor Abs in Melmet 1, 5 and 79. Data plotted present percent cell viability relative to HGS-IgG (in blue) and DR4 or DR5 level as relative median measured by flow cytometry in chapter 3.2 (in green).

No obvious trends were seen between DR4 level and response to HGS-ETR 1. On the other hand, DR5 tended to associate to HGS-ETR 2 response, especially in Melmet 1.

All together this indicates that the treatment with HGS-ETR 2, which targets DR5, is more efficient than the treatment with HGS-ETR 1, i.e. HGS-ETR 2 induces higher cell death and stronger inhibition of spheroid forming capacity.

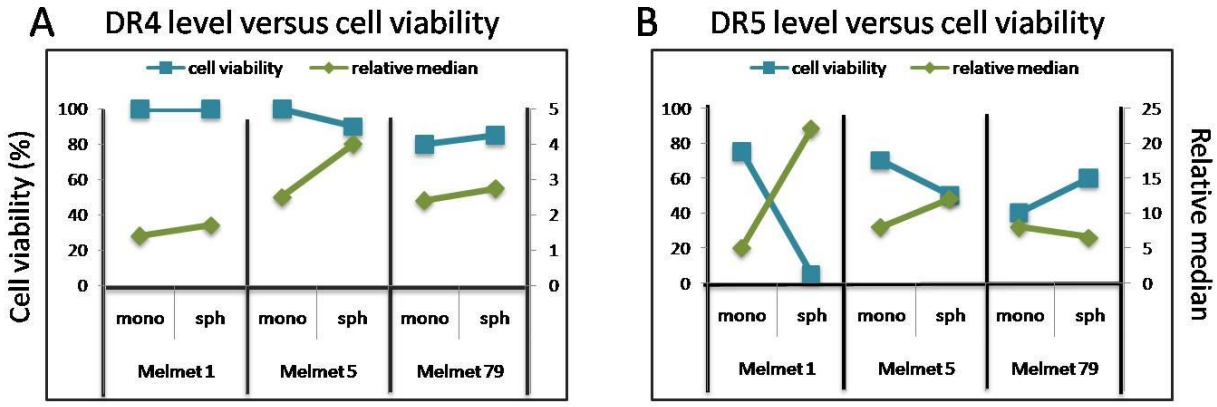

FIG. 3.10: (A) DR4 level presented in relative median in green, right y-axis (as in FIG. 3.6) versus percent cell viability after treatment with HGS-ETR 1 in blue, left y-axis (as in FIG. 3.7 and FIG. 3.8). (B) DR5 level presented in the same way as in (A), after treatment with HGS-ETR 2.

3.4 Uptake of siRNA complexes into melanoma cells cultured as monolayers or as spheroids

Elevated IAP level could inhibit the extrinsic apoptotic pathway. The IAP level in cancer cells could be down-regulated by transfection with anti-IAP siRNA, in this way facilitating apoptosis. Since treatment with Abs from HGS did not result in death of the entire Melmet cell population, we wanted to combine the Ab-based treatment

and transfection with anti-IAP siRNA to try to enhance cell death. Knowing that transfection efficiency is dependent on cellular uptake of siRNA molecules, we first studied the uptake of fluorescently labelled siRNA into Melmet cells cultured as monolayers or spheroids. FAM-labelled siRNA were complexed with Lipofecatmine 2000, and the uptake of the complexes were studied by microscopy. As can be seen in FIG. 3.11, some fluorescent green spots, likely reflecting FAM-siRNA, could be identified in the pictures of both monolayer and spheroid cells.

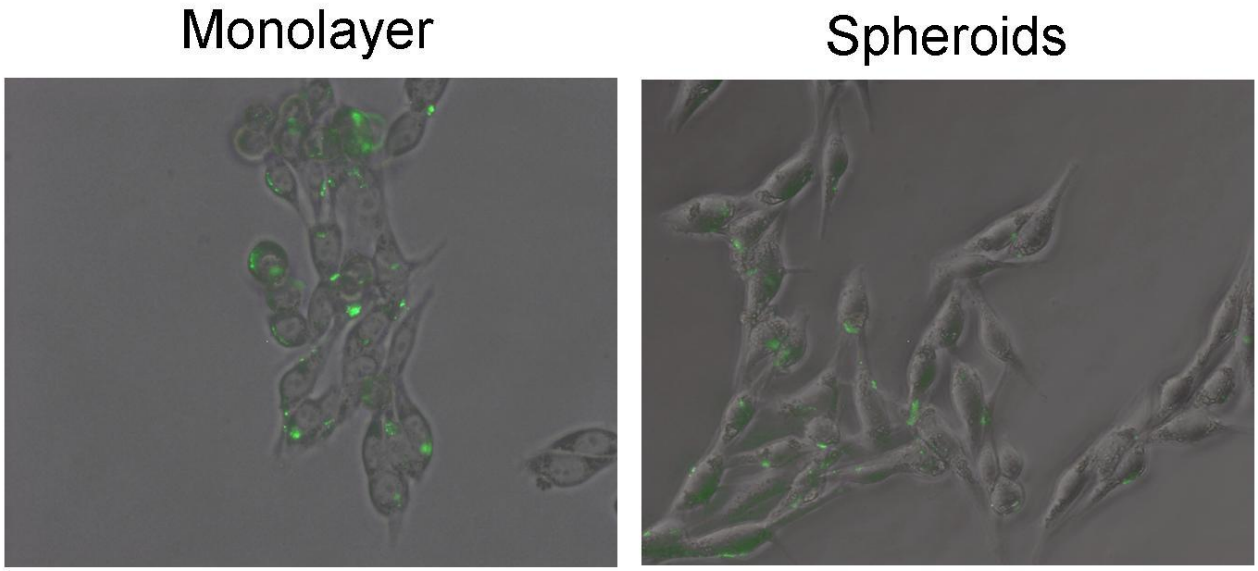

FIG. 3.11: Representative microscopy pictures of monolayer and spheroids transfected with siRNA-FAM, represented by Melmet 1 and Melmet 79, respectively. The pictures display an overlay of fluorescence pictures and phase contrast pictures. After transfection, the spheroids were dissociated into single cells which were allowed to attach to a well bottom before the pictures were taken.

However, due to fast bleaching of the FAM dye and non-three-dimensional images, it was difficult to conclude whether the siRNA complexes localised intracellularly, and whether the uptake was efficient. Thus, the microscopy analysis did not give the required information regarding the transfection efficiency of various Melmet cultures.

To retrieve more accurate data, flow cytometry was used to examine the Melmet cells transfected with the same siRNA complexes, as can be seen in FIG. 3.12.

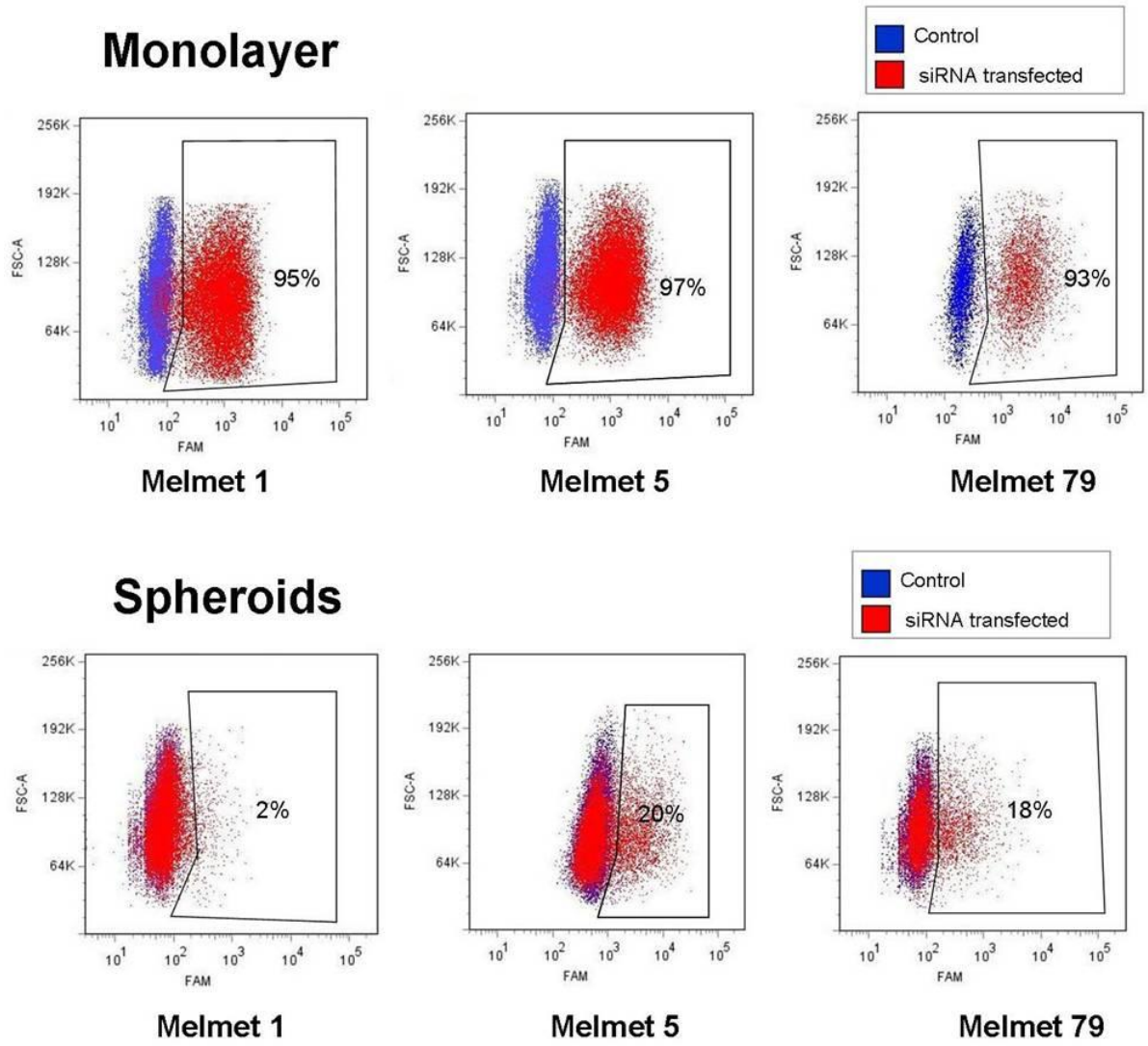

FIG. 3.12: Dot-plots indicating percent of FAM-positive cells in Melmet 1, 5 and 79 grown as monolayer and as spheroids transfected with siRNA-FAM complexes. Forward scatter (FSC-A) were plotted against FAM intensity, in a logarithmic fashion.

All Melmets grown as monolayers resulted in over 90% FAM-positive cells, indicating that the vast majority of the monolayer cells internalized FAM-siRNA. Much fewer spheroid cells were FAM-positive: 2% of Melmet 1, and about 20% of Melmet 5 and 79, indicating that the uptake of the FAM-siRNA complexes was much weaker in the spheroids as compared to the monolayer cells.

We hypothesized that the reason for poor spheroid transfection could be related to spheroid size, i.e. a transport barrier for "big" siRNA complexes. To investigate this, spheroids of different size were treated with FAM-siRNA complexes, separated into "big" and "small" spheroids based on different sedimentation rates, disintegrated into single cells and analyzed by flow cytometry.

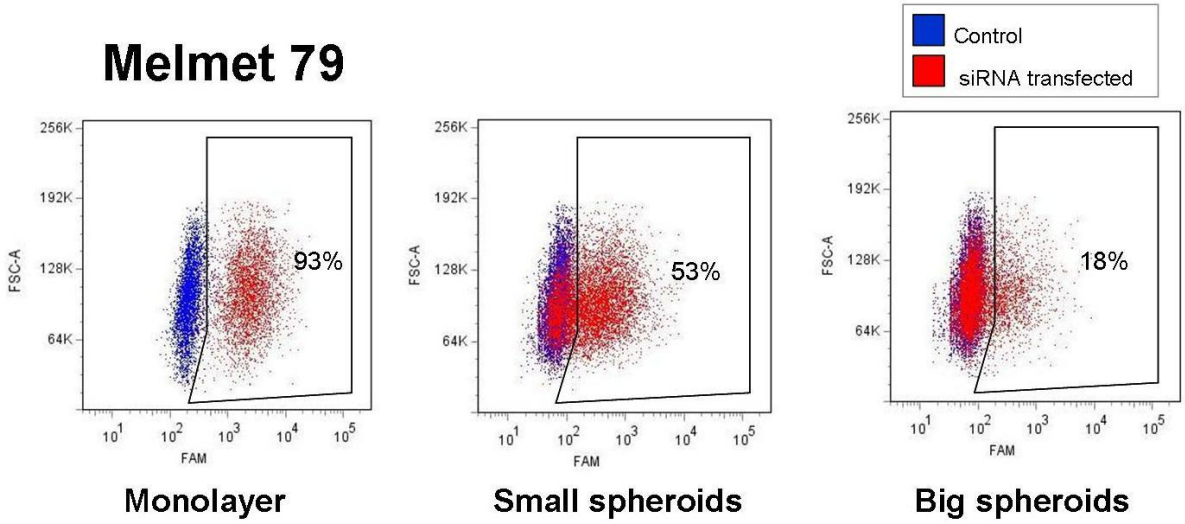

FIG. 3.13: Uptake of FAM-siRNA complexes into Melmet 79 cells from the spheroids of different size (for comparison, uptake into Melmet 79 monolayer cells is presented). Small and big spheroids were separated by exploiting the different sedimentation rates, disintegrated into single cells and analysed by flow cytometry. Forward scatter (FCS-A) was plotted against FAM intensity, in a logarithmic fashion.

As shown in FIG. 3.13, the transfection efficiency of small spheroids from Melmet 79 was notably higher compared to the bigger spheroids, however, lower than in the monolayer cells. Similar results have been obtained also in Melmet 1 and 5 (data not shown), confirming that the spheroid size is a limiting factor for the delivery of siRNA complexes. These observations were very important designing the protocols for treatments of the spheroid-derived cells: Melmet spheroid cells should always be in a single cell manner during the treatment, to enhance the uptake of siRNA complexes or other big therapeutic molecules, i.e. to maximise a possible effect.

3.5 Evaluation of transfection efficiancy and toxicity of the transfection agents Lipofectamine 2000 and Lipofectamine RNAi MAX

The efficiency of LP2000 and LPMAX, two lipid-based transfection agents often used for delivery of siRNA, was tested in Melmet 1, 5 and 79 when grown as monolayer. Cells were transfected with anti-XIAP siRNA in complex with LP2000 or LPMAX at various lipid concentrations, and the efficiency of XIAP down-regulation as well as the toxicity was measured. Anti-XIAP was used, since all Melmets clearly expressed XIAP as detected by western blot analysis (chapter 3.1).

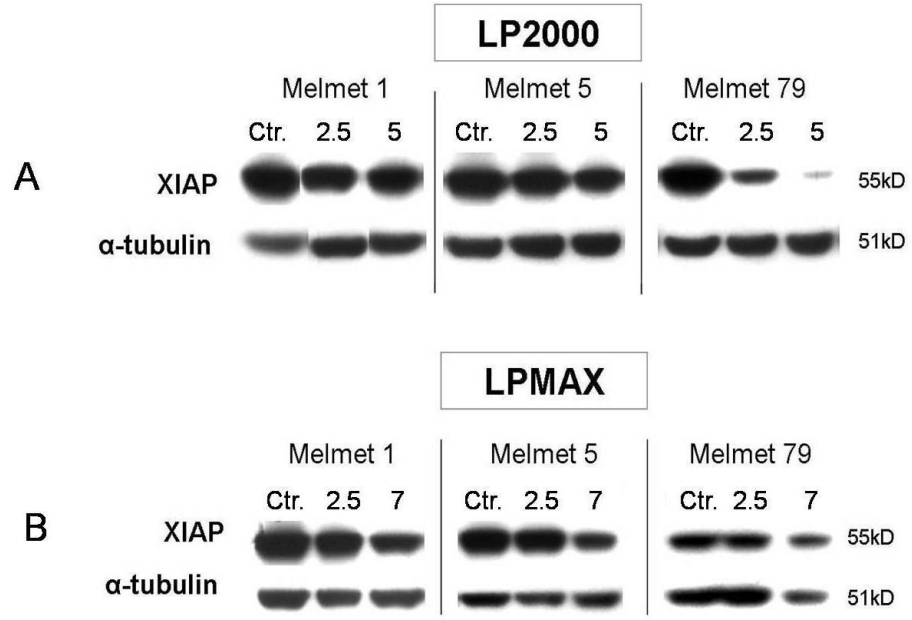

FIG. 3.14: Down regulation of XIAP in Melmet 1, 5 and 79 transfected with anti-XIAP siRNA in complex with (A) LP2000, or anti-XIAP siRNA in complex with (B) LPMAX. Untreated control (Ctr.) was compared to cells transfected with siRNA in complex with 2.5µl or 5.0µl LP2000 per 1000µl final volume, or to cells transfected with siRNA in complex with 2.5µl or 7.0µl LPMAX per 1200µl final volume (details see chapter 2.6). α-tubulin was used as loading control.

Melmet 1 and 5 demonstrated the best down-regulation of XIAP using LPMAX, while LP2000 was the most efficient transfection agent in Melmet 79 (FIG. 3.14). A stronger down regulation was achieved when a higher lipid concentration was used in all Melmets.

Since transfection agents have a tendency to be toxic to some cell lines[69], the toxicity of LP2000 and LPMAX were tested, by transfecting the cells with negative control siRNA in complex with LP2000 or LPMAX at various concentrations (FIG. 3.15). MTS assay were performed one day after the transfection.

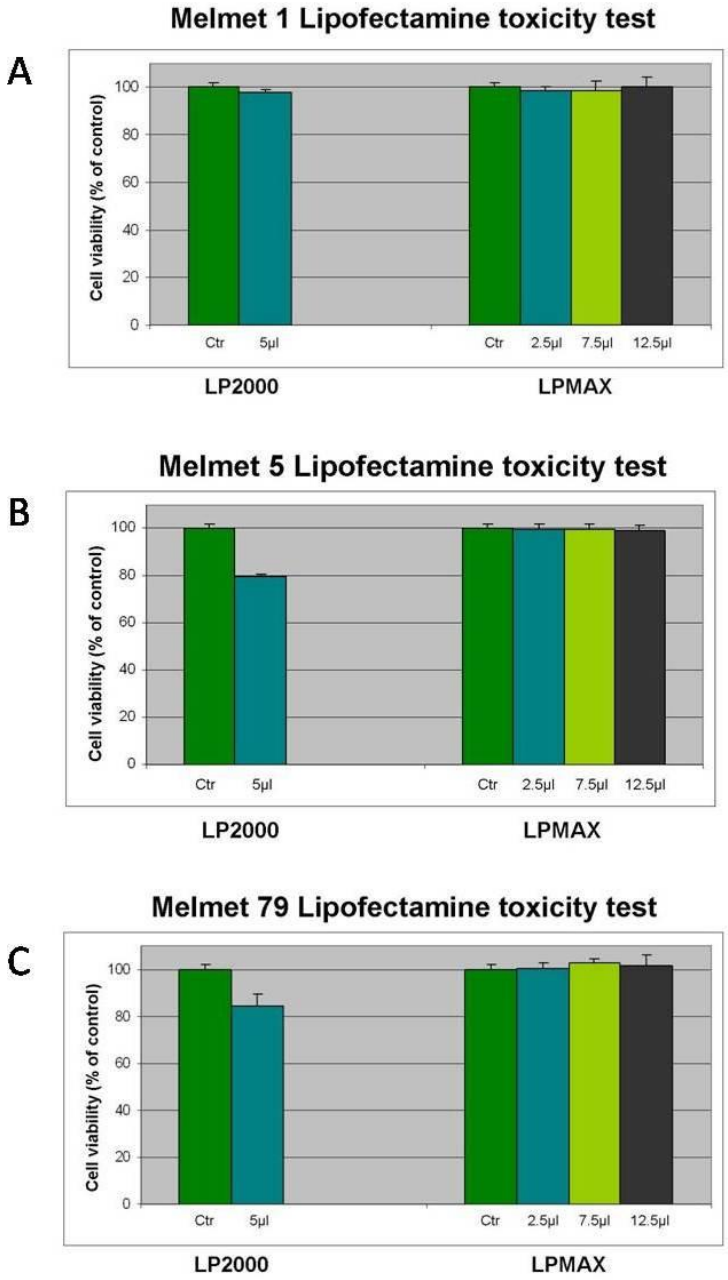

FIG. 3.15: Cell viability (in percent of control) of (A) Melmet 1, (B) Melmet 5 and (C) Melmet 79 transfected with negative control-siRNA in complex with LP2000 (5µl in 1000µl media) or LPMAX (2.5µl, 7.5µl or 12.5µl in 1200µl media), compared to untreated cells (ctr) after 24hour incubation. Standard deviations represent variations from three parallels.

As can be seen in FIG. 3.15, LPMAX gave no toxicity in any Melmet, independent of the concentrations, while LP2000 resulted in some toxicity (~20%) after one day incubation. When cells were incubated with LP2000-based complexes for longer time, i.e. three days, even higher toxicity was observed for Melmet 1 and Melmet 5 (FIG. 3.16).

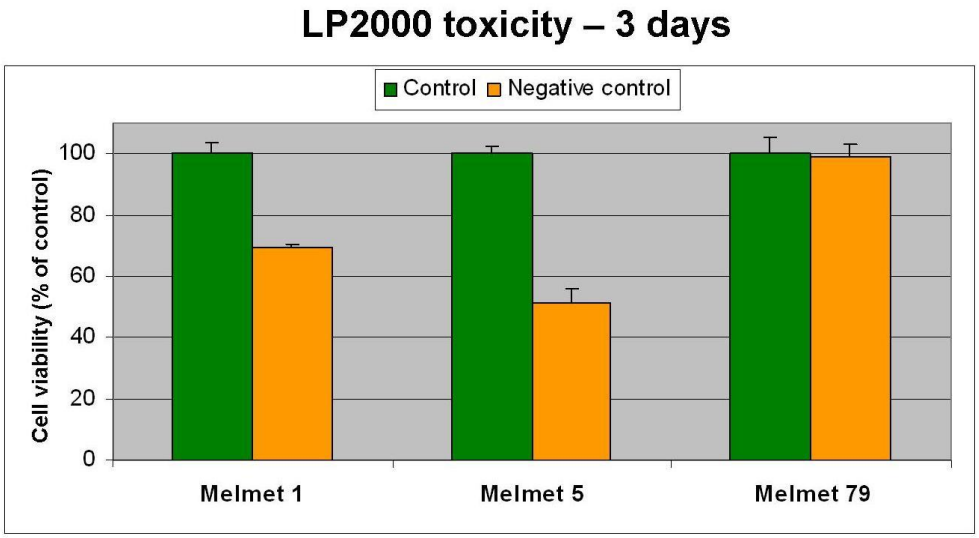

FIG. 3.16: Cell viability (in percent of untreated control cells) in Melmet 1, 5 and 79 transfected with negative control-siRNA in complex with LP2000 (5µl LP2000 in 1000µl media), after three days incubation. Standard deviations represent variations from three parallels.

Thus, LP2000 gave only slight down-regulation of XIAP in Melmet 1 and 5 (FIG. 3.14), and resulted in some toxicity in Melmet 1 and 5 (FIG. 3.15 A and B and FIG. 3.16), indicating that LP2000 is not a good transfection agent for Melmet 1 and 5. Instead, 7.5µl LPMAX per 1200µl media was chosen when transfecting Melmet 1 and 5. 5µl LP2000 per 1000µl media was chosen for transfection of Melmet 79, since LP2000 gave satisfactory down-regulation of XIAP (FIG. 3.14) and relatively low toxicity (FIG. 3.15 C and 3.16).

3.6 Sensitivity of melanoma cell cultures to the combined treatment with siRNA targeting IAPs and TRAIL receptor antibodies

To investigate whether the combined pro-apoptotic treatment could enhance the death of melanoma cells, the Melmet cell lines were tested for treatment with anti-IAP siRNAs and TRAIL receptor Abs. Since all Melmets expressed XIAP and survivin, and since survivin and XIAP are among the most studied IAPs, anti-XIAP and anti-survivin siRNA were chosen to be combined with TRAIL receptor Abs.

3.6.1 Monolayer

Melmet 1, 5 and 79, grown as monolayers, were tested for cell viability after treatment with TRAIL receptor Abs and/or transfection with anti-IAP siRNA. Abs from HGS were used at the concentration of 10µg/ml.

Melmet 1 displayed no effect after treatment with HGS-IgG and HGS-ETR 1, but a 20% reduction in cell viability was observed when treated with HGS-ETR 2 (FIG. 3.17 A), consistent with the results in chapter 3.3. Treatment with negative control siRNA-LPMAX resulted in 10% toxicity, reflecting the toxicity inducible by the transfection agent LPMAX. No obvious effect was observed when treating the cells with anti-XIAP or anti-survivin alone or in combination with HGS-IgG or HGS-ETR 1. Anti-XIAP treatment combined with HGS-ETR 2 was the only treatment strategy, where a down regulation of the IAP tended to contribute to a reduction of cell viability. The XIAP knock-down combined with HGS-ETR 2 resulted in an additional effect of approximately 10%, compared to cells treated with HGS-ETR 2 combined with negative control siRNA-LPMAX.

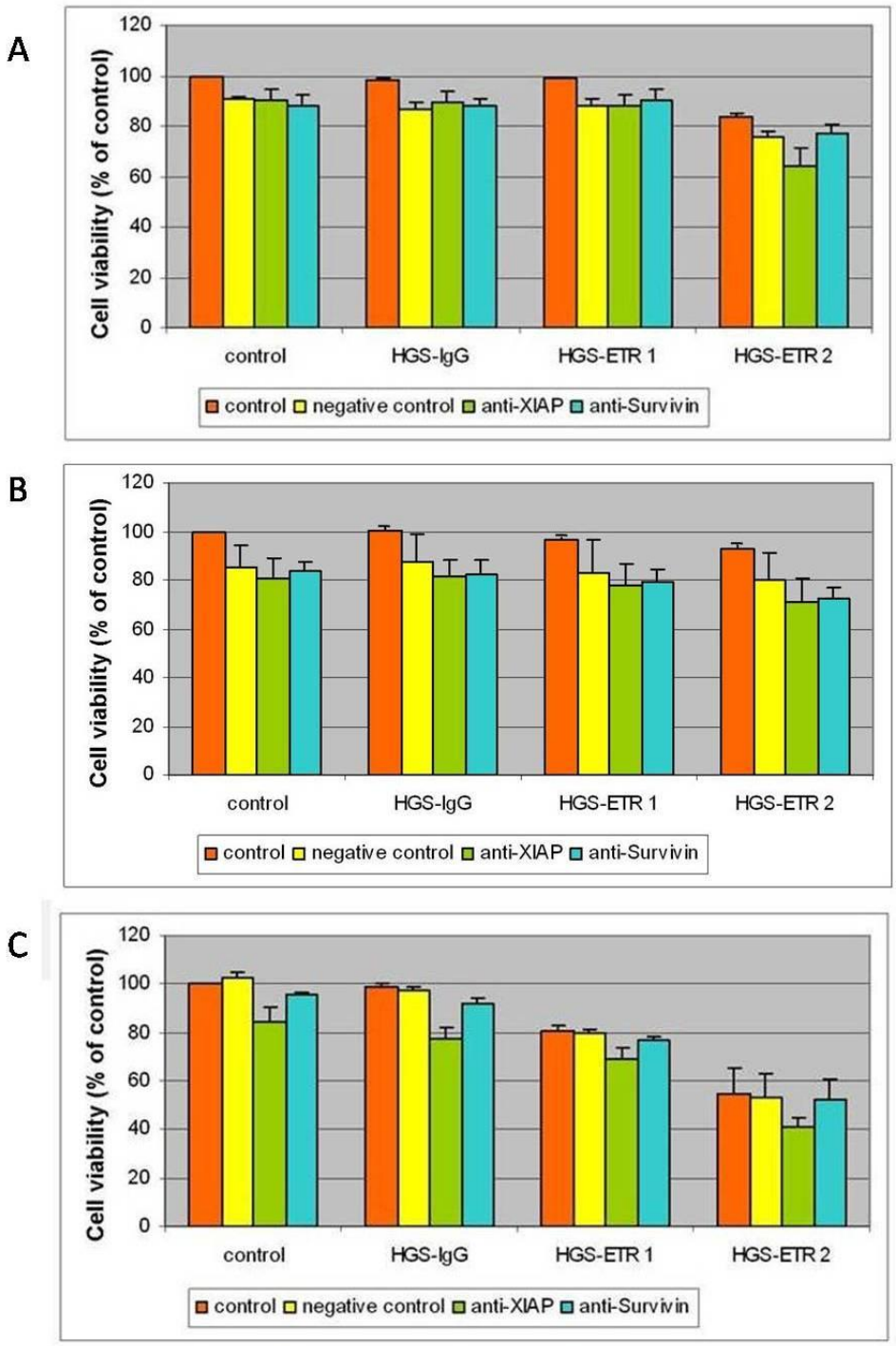

FIG. 3.17: Cell viability (expressed as percent of untreated control) of (A) Melmet 1, (B) Melmet 5 and (C) Melmet 79 grown as monolayer, after treatment with antibodies from HGS and/or transfection with siRNA-lipid complexes (negative control siRNA, anti-XIAP siRNA or anti-survivin siRNA). Cell viability and standard errors of the mean are based on three independent assays for Melmet 1 and Melmet 5, and five independent assays for Melmet79, each assay containing three parallels. MTS assay was preformed 48hours after incubation with Abs.

Melmet 5 was not notably affected by either Ab treatment or siRNA-LPMAX treatment (FIG. 3.17 B). 10-20% reduction in viability was associated to the treatment with the negative control siRNA-LPMAX, and likely was due to LPMAX-mediated non-specific toxicity.

Melmet 79 showed no toxicity following siRNA-LP2000 treatment, and little effect after anti-survivin treatment (FIG. 3.17 C). Anti-XIAP treatment reduced cell viability by 10-20%, when compared to controls in the different Ab groups. HGS-ETR 1 resulted in about 80% and HGS-ETR 2 in about 55% cell viability when comparing to untreated control cells, which is consistent with the results in chapter 3.3. When combining anti-XIAP and HGS-ETR 2, a small additive effect could be measured, resulting in 40% viable cells.

3.6.2 Spheroids

Spheroid cells showed some tendency for up-regulation of IAPs (FIG. 3.3). Therefore, it was of interest to investigate how the down-regulation of IAPs affects the spheroid-derived cells and the spheroid forming abilities. Melmet 1, 5 and 79 spheroid-derived cells were tested for their SFC after treatment with Abs from HGS and/or transfection with anti-XIAP or anti-survivin siRNA. A concentration of 10µg/ml was used when treating with Abs from HGS. Spheroids larger than 110µm were counted, and RSF was calculated. Pictures were taken using the GelCounter machine.

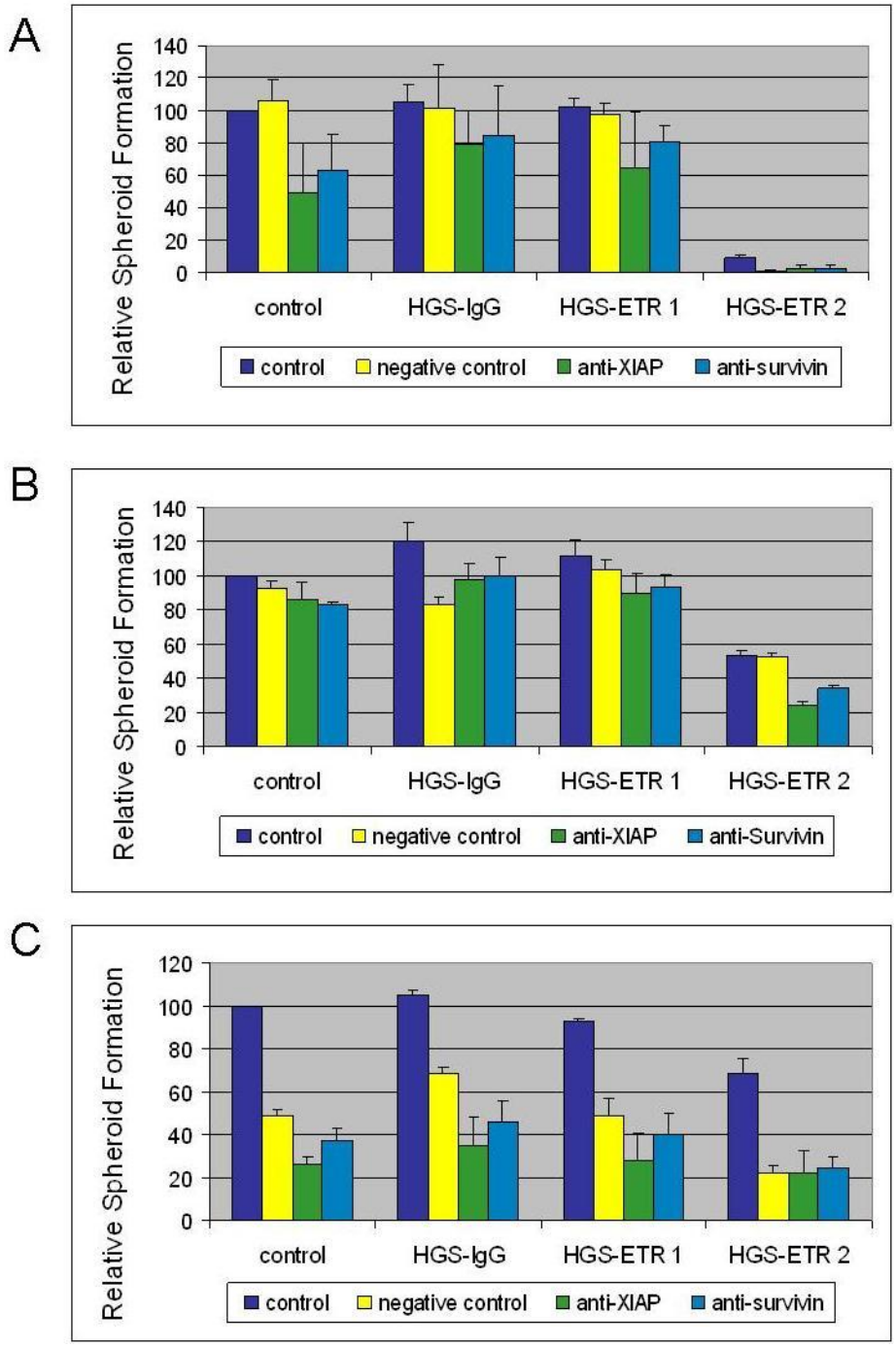

FIG. 3.18: Relative spheroid formation (in percent of untreated control) of (A) Melmet 1,(B) Melmet 5 and (C) Melmet 79 grown as spheroids, after treatment with antibodies from HGS and/or transfection with siRNA-lipid complexes (negative control siRNA, anti-XIAP siRNA and anti-survivin siRNA). Relative spheroid formation and standard error of the mean are based on two independent experiments. Spheroids larger than 110µm were counted after 8-14 days after incubation with Abs.

HGS-ETR 2 treatment resulted in a ~90% down-regulation on RSF on Melmet 1 (FIG. 3.18 A), as observed in chapter 3.3. No change in RSF was seen when treating Melmet 1 cells with HGS-IgG or HGS-ETR 1, or with negative control siRNA. Treatment with anti-survivin or anti-XIAP siRNA tended to reduce the RSF in all Ab treatment groups (FIG. 3.18 A), i.e. 20-50% reduction in RSF was observed. However due to the large HGS-ETR 2 effect, the siRNA effects in the HGS-ETR 2 group were imprecise.

LPMAX resulted in little or no toxicity in Melmet 5, as can be seen comparing untreated control cells with cells treated with negative control siRNA-LPMAX in all Ab treatment groups (FIG. 3.18 B). No clear conclusions could be drawn following the treatments with HGS-IgG or HGS-ETR 1, due to big variations in spheroid formation, suggesting that, probably, there was no considerable effect of the two Abs. Cells treated with HGS-ETR 2 alone showed a RSF of ~55%, basically corresponding with the data in chapter 3.3. The largest reduction in SFC was observed after the combined treatment with HGS-ETR 2 and anti-IAP siRNA, where the combined anti-XIAP treatment reduced RSF by almost 80% and the combined anti-survivin treatment by nearly 65%.

Even though using half the concentration of LP2000 used when treating Melmet 79 monolayer, LP2000 induces 50% toxicity in Melmet 79 spheroids, comparing untreated control groups with groups treated with negative control siRNA (FIG. 3.18 C). No clear Ab effect could be observed in the HGS-IgG or HGS-ETR 1 treatment group data. In this assay, HGS-ETR 2 treatment resulted in ~70% RSF in Melmet 79, not corresponding fully with results from chapter 3.3, which resulted in ~50% RSF. Anti-XIAP or anti-survivin treatment in Melmet 79, resulted in a ~25% and a ~15% reduction in RSF respectively, when compared to cells treated with negative control siRNA (FIG. 3.18 C). An exception was observed in the HGS-ETR 2 group, where all groups of siRNA treatment, resulted in the same RSF (~20% RSF).

For all Melmets, the individual effects of HGS-ETR 2 and of anti-IAP siRNA were confirmed visually in each specific assay, as demonstrated by Melmet 1 in FIG. 3.19 and FIG. 3.20. Cells treated with HGS-IgG or HGS-ETR 1 showed in general similar SFC as control cells regarding both the number (FIG. 3.19), and the size of the formed spheroids (data not shown).

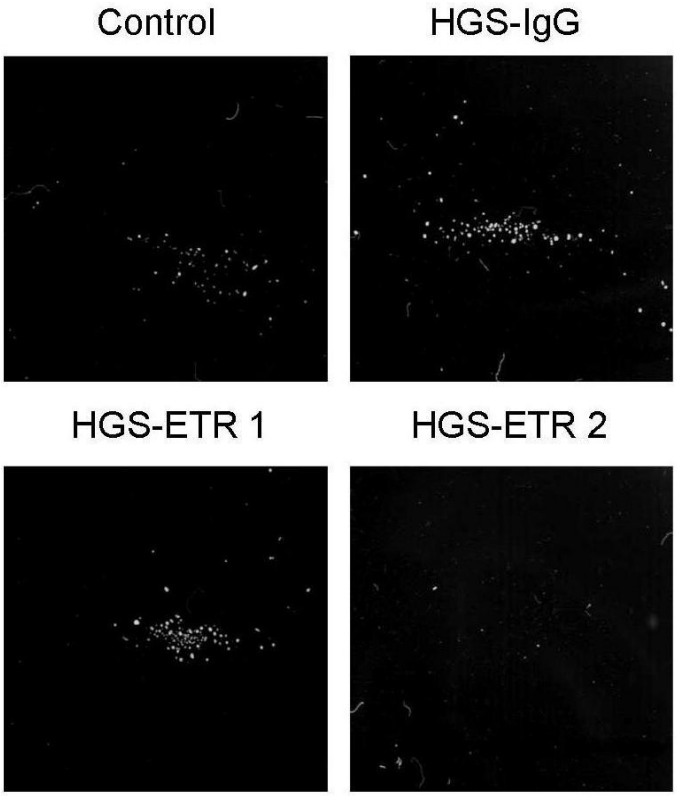

FIG. 3.19: Overview pictures taken by the Gelcounter machine of wells containing untreated Melmet 1 cells, and Melmet 1 cells treated with HGS-IgG, HGS-ETR 1 and HGS-ETR 2 respectively. Pictures demonstrate the visual effect of HGS-ETR 2 treatment, in respect of number of spheroids formed. Spheroids are shown as white dots on a black background.

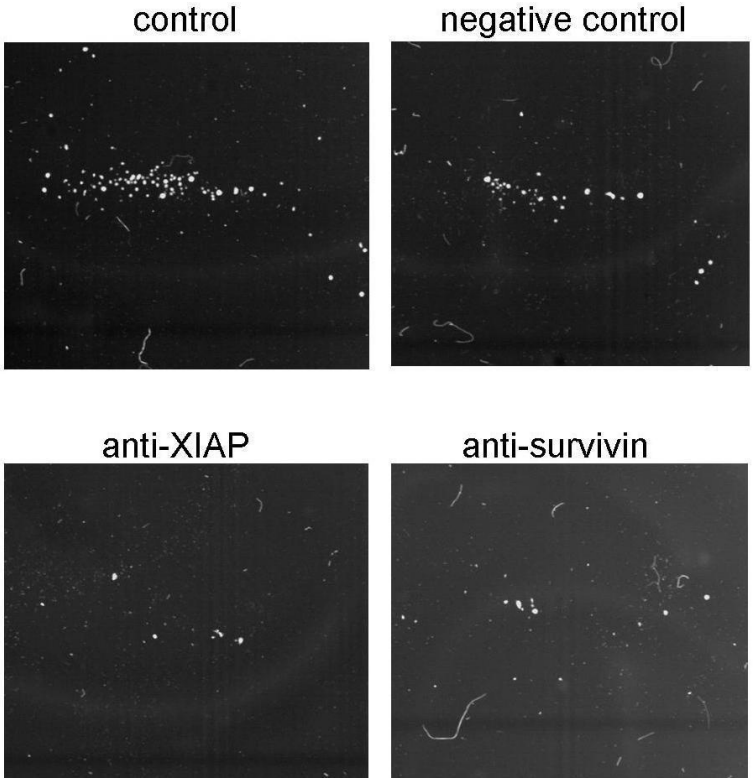

FIG. 3.20: Overview pictures of HGS-IgG treated Melmet 1 cells taken by the Gelcounter machine. Pictures of wells presented, contain non-siRNA treated cells, and cells treated with negative control siRNA, anti-XIAP siRNA and anti-survivin siRNA respectively. Pictures demonstrate the visual effect of anti-XIAP and anti-survivin treatment, in respect to number of spheroids formed. Spheroids are shown as white dots on a black background.

The phase contrast microscopy pictures, shown in FIG. 3.21, illustrate the differences seen in the spheroid formation following treatments. As can be seen, untreated control cells formed many and big spheroids (FIG. 3.21 A). HGS-ETR 2-treated cells formed fewer and much smaller spheroids compared to the control cells (FIG. 3.21 B). When anti-IAP treatment was combined with HGS-ETR 2 treatment, the cells showed a similar appearance as cells treated with HGS-ETR 2 alone (FIG. 3.21 C and D).

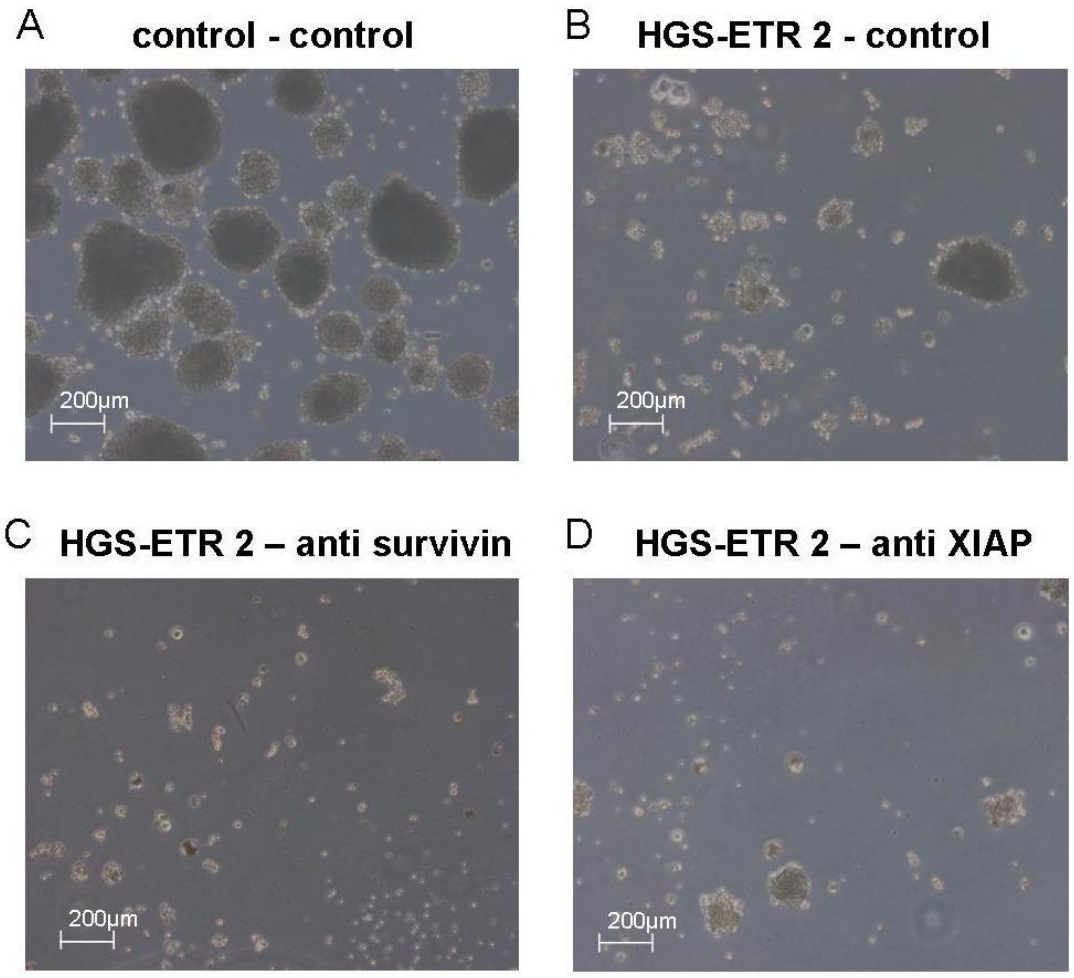

FIG. 3.21: Representative phase contrast microscopy pictures, represented by Melmet 1, of (A) untreated spheroids, (B) spheroids treated with HGS-ETR 2, (C) spheroids treated with the combination HGS-ETR 2 and anti-survivin siRNA, and (D) spheroid treated with the combination HGS-ETR 2 and anti-XIAP siRNA. The pictures were taken 14 days after initiation of experiment with a 5x objective.

Spheroids (and to some extent monolayers) demonstrated a various response to HGS-IgG. The response may to some extent be assay affected, since all Melmets grown as spheroids in the SFA (chapter 3.3) demonstrated a decreased RSF when treated with HGS-IgG compared to untreated cells. Still, different responses have been observed intra-experimentally, which could indicate a complex function of HGS-IgG, which will not be investigated in this study.

4. Discussion

The aim of the project was to investigate the expression of inhibitors of apoptosis (IAPs) and pro-apoptotic death receptors (DR4 and DR5) in malignant melanoma, since these proteins are important in the apoptotic pathway, and consequently, may have an impact on tumor initiation/progression and therapy efficiency. The second aim was to evaluate a treatment based on RNAi mediated down-regulation of IAPs combined with activators of apoptosis via DR4 and DR5 as an option for melanoma therapy in the future. The study was based on the comparison of two different melanoma cell models, i.e. monolayers *versus* spheroids. It has been reported that melanoma spheroid cells growing in stem cell media have higher abilities for tumor-initiation *in vivo* (Fang et. al. and Prasmickaite, manuscript in preparation), supposedly due to the enhanced presence of melanoma CSC. Therefore, it is of importance to find a therapeutic strategy that could efficiently eliminate such cells. Characterization of melanoma spheroids with respect to expression of apoptosis-related molecules, and evaluation of response to apoptosis-inducing therapy is, therefore, an important step in this direction.

This study revealed that all Melmet models expressed IAPs (an exception was livin), and a tendency to increased IAP level was observed in spheroids compared to monolayers (8 out of 15 cases) (FIG. 3.3). Up-regulation of at least one IAP was observed in all Melmets grown as spheroids: Melmet 1 demonstrated an increased level of survivin and cIAP-2, Melmet 5 showed an increased level of livin and Melmet 79 had an elevated level of all five studied IAPs (FIG. 3.3). It should be mentioned that conclusions about the enhanced level of IAPs are based on western blotting data, while real-time PCR data were less conclusive, although they generally confirmed the above mentioned observations with a few exceptions. Since IAPs perform their so far known activity as proteins and not as mRNA, evaluation of the protein levels by western blotting is a reliable strategy and, therefore, was prioritized in this study.

Up-regulation of IAPs suggests that spheroid-derived melanoma cells might have elevated anti-apoptotic machinery (i.e. resistance). This fits well to the assumption that spheroids might be enriched for CSC. Furthermore, enhanced anti-apoptotic properties could contribute to the enhanced tumor-initiating abilities observed for spheroid cells as shown by Fang et. al. and Prasmickaite (FIG. 1.6). However, Melmet 79 spheroids showing up-regulation of all studied IAPs failed efficiently to initiate tumors *in vivo* (FIG. 1.6), indicating that IAPs probably are not a determining factor in tumor initiation. There are, however, several papers showing a correlation between IAP expression and tumor progression[62,55].Thus, an elevated survivin level was shown to correlate with poor survival in melanoma[62,60], suggesting that survivin could be a candidate to characterize aggressiveness in melanoma. In this context, it could be expected that aggressive melanoma cells that manage to establish metastases *in vivo* might have higher levels of IAPs. We, however, did not observe that *in vivo* metastases from tibia had an elevated level of IAPs compared to *in vitro* samples. An exception was livin, which was clearly up-regulated in the metastases from Melmet 5. Having in mind that livin was also strongly up-regulated in spheroids compared to monolayers, it would be of interest to investigate a role of livin in melanoma. Livin is also named melanoma-IAP, ML-IAP, because it is reported to be up-regulated in melanoma when compared to nevus[62,81], but not to differ in level between primary and secondary melanoma[82]. This is also reflected by studies who invalidates livin as a prognostic factor in melanoma patients[59]. Additionally, the importance of livin in apoptosis are unclear, as demonstrated by antisense-mediated down-regulation of livin, which only induces apoptosis in some cell lines[83], (Engesæter, unpublished data).

All together, the IAPs studied revealed that Melmet cells, particularly from spheroids, express resistance-associated anti-apoptotic molecules, IAPs, which might be a hindrance in melanoma therapy aimed to induce apoptosis.

One of the ways to stimulate apoptosis is through the death receptors (DR4 and DR5). To achieve a therapeutic benefit by strategies relaying on DR4 or DR5, the

target cells must express these receptors. Here we show that all Melmet models contain cells expressing DR4 and DR5. DR5 were expressed at a higher degree than DR4, which is in agreement to previous studies on fresh melanoma samples[44]. Furthermore, Melmets grown as spheroids had a slightly elevated level of DR4 and DR5 compared to Melmets grown as monolayer (FIG. 3.6), indicating that spheroid cells might be better targeted by TRAIL receptor Abs. Interestingly, DR4 and DR5 are the only cell surface markers found so far to be up-regulated (particularly in the case of Melmet 1) in spheroids *versus* monolayers, while none of the potential CSC "markers" like CD133, ABCG2, CD20 or p75 showed this tendency (Prasmickaite, manuscript in preparation). Therefore, it is tempting to speculate that DR5 could be associated to tumor initiating cells in melanoma, since, e.g. Melmet 1 spheroids demonstrated high tumor initiating abilities *in vivo* (FIG. 1.6). It can be mentioned, however, that there were no clearly distinct DR4/DR5-positive and DR4/DR5-negative subpopulations, and the majority of cells in population showed a similar expression of the receptors, which might complicate an employment of DR5 as a marker for CSC isolation. Rajeshkumar et. al. has already shown that DR5 up-regulation is associated to pancreatic adenocarcinoma stem cells[84]. On the contrary, Zhuang et. al., has shown that a very high DR5 level in melanoma is correlated with good prognosis[44], arguing against a possible link between DR5 and CSC.

Although DR4/DR5 expression does not necessarily guarantee sensitivity to DR4/DR5 targeted therapy, cells without DR4/DR5 expression will certainly not be valid targets. Here we revealed that, despite the expression of DR4, all the Melmets showed a very weak (if any) response to HGS-ETR 1 (FIG. 3.7 and FIG. 3.8.). Additionally, we showed that the response to HGS-ETR 2 was medium/high in all Melmets, particularly in spheroids (FIG. 3.7 and FIG. 3.8). Treatment with HGS-ETR 2 in Melmet monolayers resulted in 15%-60% reduction in cell viability, indicating that more than 40% of cells survived the treatment. The effect on the spheroids seem to be higher, where HGS-ETR 2 reduced spheroid formation by 50-95%, indicating that $\geq$ 5% of cells were not eliminated by the treatment, and are able to self-renew

and form spheres (i.e. candidate CSC). A higher response to HGS-ETR 2 in the spheroids than in the respective monolayers of Melmet 1 and Melmet 5 correlates to the increased DR5 expression in the spheroids (FIG. 3.10). Likewise, lower DR5 expression in Melmet 79 spheroids corresponds to a lower response to the HGS-ETR 2 treatment, indicating that the level of DR5 might be an important requirement for the efficiency of the treatment. Also, the lower/no effect of HGS-ETR 1 could be explained by lower DR4 expression, or, more unlikely, by low HGS-ETR 1 affinity towards DR4, given that the DR4 Ab has been proven to be effective in non-melanoma cell lines (Engesæter, unpublished data). Additionally, DR4 and DR5 glycosylation pattern or association with lipid rafts could possible control the cells sensitivity to DR4 and DR5 trimerization, and therefore TRAIL receptor Ab therapy[85,86].

It should be noted that also treatment with DTIC resulted in similar (low) efficiency in monolayers, as shown by Engesæter (FIG. 1.7), indicating that Melmet models harbour a large fraction of therapy-resistant cells.

Limited sensitivity of Melmet cells to TRAIL receptor Abs suggest an active anti-apoptotic mechanism[40], which could be mediated by e.g. high levels of various IAPs as discussed above. Theoretically, down-regulation of IAPs could improve a therapeutic effect of the TRAIL receptor Abs. Therefore, two IAPs, survivin and XIAP, were selected for further studies, where the Melmet cells were transfected with anti-survivin or anti-XIAP siRNA. Combining the TRAIL receptor Abs and siRNA, we expected an additive or a synergistic effect. In monolayers, however, only Melmet 79 showed an effect, where XIAP down-regulation contributed with additional 10% reduction of cell viability (additive effect), whereas no additional effect of anti-survivin was observed (FIG. 3.17). In the spheroids, however, the down-regulation of anti-XIAP seems to have a more pronounced effect, reducing spheroid formation on average by 20% in all Melmets (FIG. 3.18). Altogether this indicates that contribution from siRNAs against XIAP or survivin under the conditions used in this study was quite low, and did not notably improve the efficiency of TRAIL receptor Abs. There

could be several explanations for lower than expected effect: i) the down-regulation was not efficient enough (see FIG. 3.14), and the remaining level of the IAP was still sufficient to perform an anti-apoptotic function. Further optimalization of the transfection is needed. ii) The other IAPs, not affected by the specific siRNA, "take over" apoptosis inhibition. In this respect, it would be of interest to combine several siRNA targeting different IAPs. iii) XIAP and survivin confer resistance to TRAIL receptor Ab-mediated apoptosis only in a small subpopulation of the cells, so that down-regulation of these IAPs does not considerably influence the sensitivity of the whole cell population.

The observation that the Melmet spheroids often responded to the TRAIL receptor Abs more efficiently than the respective monolayers, might have important implications for melanoma therapy. Earlier it has been reported that, when grown as 3D spheres, tumor cells demonstrate resistance to apoptosis inducible by e.g. TRAIL, which mimic the chemo resistance seen in solid tumors[87]. Therefore, there is an opinion that spheres are a better model for testing new therapeutic strategies, since they could reflect a more clinically relevant *in vitro* setting. Furthermore, as Fang et. al. and Prasmickaite demonstrated, melanoma cells from spheres seem to be more tumorigenic, thus representing a critical target in therapy. A response of Melmet spheroids to the TRAIL receptor Abs, particularly the response of Melmet 1 cells to the HGS-ETR 2, implies that these antibodies in combination with other drugs might be an interesting strategy for further evaluation, aiming to find a best combination for elimination of tumor initiating cells in malignant melanoma. Likely, cells with stem cell properties might constitute a quite large population, as shown *in vivo* by Quintana[21] and *in vitro* by Prasmickaite (manuscript in preparation). The presence of a big fraction of stem cell-like melanoma cells could explain a generally low effect of treatments in Melmet models and signifies the importance of search for new therapeutic options.

Conclusions

All melanoma cell lines investigated in this study expressed survivin, XIAP, cIAP-1 and cIAP-2 *in vitro*, and spheroids tended to have elevated IAP expression. Livin was also strongly up-regulated in spheroids in the two cell lines where livin expression was detected. HGS-ETR 1 hardly affected the melanoma cells survival. HGS-ETR 2 induced an intermediate response, where down-regulation of XIAP, but not survivin, contributed with a small additive effect in some cases.

Future perspectives

Designing new therapeutic strategies against cancer requires understanding of the biological mechanisms which sustain and promote tumor cell proliferation and resistance to cell death. In this study we have preformed an initial evaluation of the pro-apoptotic treatment including TRAIL receptor Ab and anti-IAP siRNA. The combination resulted in a limited effect, but technical improvements may increase the potency of the treatment. Further optimalization, like changing concentrations of various reagents used in the transfection protocol and varying cell numbers, may improve the IAP down-regulation. Since there is a possibility that one IAP could "fill in" the function of another IAP, a combined study targeting several IAPs at the same time, would perhaps be a more effective treatment strategy, than the single-IAP down-regulation used in this study. It will also be of interest to see the effect of anti-livin treatment in respect to cell viability and spheroid formation, since livin was up-regulated to a large extent when cells were grown as spheres or *in vivo*.

Another interesting aspect is that some cells survive both TRAIL receptor Ab treatment and anti-IAP treatment. These therapy-resistant cells, which are able to form new spheres, should be investigated further in respect to survival mechanisms and stem cell markers. DR5 level could be interesting to study in relation to these therapy-resistant cells, as well as in relation to tumor initiating properties. This can be done by selecting DR5-high and DR5-low populations by flow cytometry, followed by seeding single cells into wells and evaluation of their *in vitro* spheroid forming capacity. If DR5-high cells produced significantly higher amount of spheroids than DR5-low cells, this difference in "tumorigenicity" may be studied further by a limiting dilution assay *in vivo*. Likewise, since survivin is related to outcome in melanoma patients, survivin positive/high cells could be interesting to evaluate against survivin negative/low cells, in respect to spheroid forming capacity.

The therapeutic effect of TRAIL receptor Abs and anti-IAP treatment in this study was measured by cell viability assays and spheroid forming assays. Expanding the

panel of assays to include e.g. TUNEL, JC-1 and annexin staining or western blot of apoptotic markers, could evaluate if these effects actually is a result of the apoptotic process.

In this study an experimental protocol for treatment of single melanoma cells in 3D format has been established. This procedure could be employed for testing the efficiency of various treatments, with the aim to identify, and eliminate, the subpopulation of cells responsible for initiating melanoma growth.

Appendix

Amidoblack solution: 1g Naphtol Blue Black, 450ml methanol, 100ml acetic acid and 450ml ddH_2O.

BSN (Bjerrum – Scäfer – Nilsen) buffer 1X: 50ml 20X BSN (116g Tris, 58g glycin, ddH_2O up to 1000ml.) and 950ml ddH_2O.

Destaining solution: 900ml methanol, 20ml acetic acid and 80ml ddH_2O.

Flow blocking buffer: PBS containing 0.5% FCS and 3% gammablocker.

hESCM4 – human Embryonic Stem Cell Medium 4: 70% MEF conditioned media (hESC media used to culture MEF for 24hours), 30% hESC (80% DMEM-F12, 20% KnockOut Serum Replacer, 1% Non essential amino acids 100x, 2mM Glutamax and 2.3% β-mercaptoethanol and 4ng/ml bFGF.)

Loading buffer 6X: 15% SDS, 50% glycerol, 300mM Tris pH 6.8, 25% β-mercaptoethanol, 0.6% Bromophenyl blue and ddH_2O.

Lysis solution: 1.5ml 5M NaCl, 5ml 0.5M Tris pH 7.5, 50µl NP_40 and ddH_2O up to 50ml.

Lysis buffer: 960µl lysis solution, 10µl PMSF, 10µl Leupeptin, 10µl Pepstatin A and 10µl Aprotinin.

R&D buffer: 25ml 1M Tris pH 7.5, 30ml 5M NaCl, 1ml 20% Tween and ddH_2O up to 1000ml.

Running buffer 1X: 100ml Running buffer 10X (30.2g Tris, 144g glycin in 1L ddH_2O), 5ml 20% SDS and ddH_2O up to 1000ml.

TBST – regular: 20ml 1M Tris pH7.5, 100ml 5M NaCl, 2.5ml Tween 20 and ddH_2O up to 1000ml.

References

[1] Norway, Cancer Registry of, (2007).

[2] Alberts, B. et al., *Molecular biology of the cell*, fourth edition ed. (Garland Science, 2002).

[3] Andersen, A. et al., Work-related cancer in the Nordic countries. *Scand. J. Work Environ. Health* **25**, 1 (1999).

[4] Gray-Schopfer, V., Wellbrock, C., and Marais, R., Melanoma biology and new targeted therapy. *Nature* **445** (7130), 851 (2007).

[5] Gilchrest, B. A., Eller, M. S., Geller, A. C., and Yaar, M., The pathogenesis of melanoma induced by ultraviolet radiation. *N Engl J Med* **340** (17), 1341 (1999).

[6] Miller, A. J. and Mihm, M. C., Jr., Melanoma. *N Engl J Med* **355** (1), 51 (2006).

[7] La Porta, C. A., Drug resistance in melanoma: new perspectives. *Curr Med Chem* **14** (4), 387 (2007).

[8] Shi, J. et al., in *Molecular Therapeutics of Melanoma*, edited by Willard and Ginsburg (Elsevier Inc., 2009).

[9] Gogas, H. J., Kirkwood, J. M., and Sondak, V. K., Chemotherapy for metastatic melanoma - Time for a change? *Cancer* **109** (3), 455 (2007).

[10] Smalley, K. S. M. and Herlyn, M, Integrating tumor-initiating cells into the paradigm for melanoma targeted therapy. *International Journal of Cancer* **124** (6), 1245 (2009).

[11] Nowell, P. C., Clonal evolution of tumor-cell populations. *Science* **194** (4260), 23 (1976).

[12] Jordan, C. T., Guzman, M. L., and Noble, M., Cancer stem cells - Reply. *New England Journal of Medicine* **355** (25), 2703 (2006).

[13] Reya, T., Morrison, S. J., Clarke, M. F., and Weissman, I. L., Stem cells, cancer, and cancer stem cells. *Nature* **414** (6859), 105 (2001).

[14] Visvader, J. E. and Lindeman, G. J., Cancer stem cells in solid tumours: accumulating evidence and unresolved questions. *Nat Rev Cancer* **8** (10), 755 (2008).

[15] Schatton, T. et al., Identification of cells initiating human melanomas. *Nature* **451** (7176), 345 (2008).

[16] Clarke, M. F. et al., Cancer stem cells--perspectives on current status and future directions: AACR Workshop on cancer stem cells. *Cancer Res* **66** (19), 9339 (2006).

[17] Reed, J. A., Finnerty, B., and Albino, A. P., Divergent cellular differentiation pathways during the invasive stage of cutaneous malignant melanoma progression. *Am J Pathol* **155** (2), 549 (1999).

[18] Grichnik, J. M. et al., Melanoma, a Tumor Based on a Mutant Stem Cell? *J Invest Dermatol* **126** (1), 142 (2006).

[19] Fang, D. et al., A tumorigenic subpopulation with stem cell properties in melanomas. *Cancer Res* **65** (20), 9328 (2005).
[20] Monzani, E. et al., Melanoma contains CD133 and ABCG2 positive cells with enhanced tumourigenic potential. *European Journal of Cancer* **43** (5), 935 (2007).
[21] Quintana, E. et al., Efficient tumour formation by single human melanoma cells. *Nature* **456** (7222), 593 (2008).
[22] Keshet, G. I. et al., MDR1 expression identifies human melanoma stem cells. *Biochemical and Biophysical Research Communications* **368** (4), 930 (2008).
[23] Lee, J. et al., Tumor stem cells derived from glioblastomas cultured in bFGF and EGF more closely mirror the phenotype and genotype of primary tumors than do serum-cultured cell lines. *Cancer Cell* **9** (5), 391 (2006).
[24] Bao, S. et al., Glioma stem cells promote radioresistance by preferential activation of the DNA damage response. *Nature* **444** (7120), 756 (2006).
[25] Jacobson, M. D., Weil, M., and Raff, M. C., Programmed Cell Death in Animal Development. *Cell* **88** (3), 347 (1997).
[26] Enari, M. et al., A caspase-activated DNase that degrades DNA during apoptosis, and its inhibitor ICAD. *Nature* **391** (6662), 43 (1998).
[27] Hanahan, D. and Weinberg, R. A., The Hallmarks of Cancer. *Cell* **100** (1), 57 (2000).
[28] Hengartner, M. O., The biochemistry of apoptosis. *Nature* **407** (6805), 770 (2000).
[29] Rao, R. V., Ellerby, H. M., and Bredesen, D. E., Coupling endoplasmic reticulum stress to the cell death program. *Cell Death Differ* **11** (4), 372 (2004).
[30] Bullani, R. R. et al., Selective Expression of FLIP in Malignant Melanocytic Skin Lesions. **117** (2), 360 (2001).
[31] Wiley, S. R. et al., Identification and characterization of a new member of the TNF family that induces apoptosis. *Immunity* **3** (6), 673 (1995).
[32] Mariani, S. M. and Krammer, P. H., Differential regulation of TRAIL and CD95 ligand in transformed cells of the T and B lymphocyte lineage. *European Journal of Immunology* **28** (3), 973 (1998).
[33] Pan, G. et al., The Receptor for the Cytotoxic Ligand TRAIL. *Science* **276** (5309), 111 (1997).
[34] Walczak, H. et al., TRAIL-R2: A novel apoptosis-mediating receptor for TRAIL. *Embo J.* **16** (17), 5386 (1997).
[35] Marsters, S. A. et al., A novel receptor for Apo2L/TRAIL contains a truncated death domain. *Current Biology* **7** (12), 1003 (1997).
[36] Degli-Esposti, M. A. et al., The novel receptor TRAIL-R4 induces NF-kappa B and protects against TRAIL-mediated apoptosis, yet retains an incomplete death domain. *Immunity* **7** (6), 813 (1997).
[37] Emery, J. G. et al., Osteoprotegerin is a receptor for the cytotoxic ligand TRAIL. *J. Biol. Chem.* **273** (23), 14363 (1998).

[38] Daniels, R. A. et al., Expression of TRAIL and TRAIL receptors in normal and malignant tissues. *Cell Res* **15** (6), 430 (2005).

[39] Grosse-Wilde, A. et al., TRAIL-R deficiency in mice enhances lymph node metastasis without affecting primary tumor development. *J Clin Invest* **118** (1), 100 (2008).

[40] Zhang, L. and Fang, B., Mechanisms of resistance to TRAIL-induced apoptosis in cancer. *Cancer Gene Ther* **12** (3), 228 (2005).

[41] Nguyen, T., Zhang, X. D., and Hersey, P., Relative resistance of fresh isolates of melanoma to tumor necrosis factor-related apoptosis-inducing ligand (TRAIL)-induced apoptosis. *Clin Cancer Res* **7** (3 Suppl), 966s (2001).

[42] Zhang, X. D. et al., Tumor necrosis factor-related apoptosis-inducing ligand-induced apoptosis of human melanoma is regulated by smac/DIABLO release from mitochondria. *Cancer Res* **61** (19), 7339 (2001).

[43] Zhang, X. D. et al., Relation of TNF-related apoptosis-inducing ligand (TRAIL) receptor and FLICE-inhibitory protein expression to TRAIL-induced apoptosis of melanoma. *Cancer Res.* **59** (11), 2747 (1999).

[44] Zhuang, L. et al., Progression in melanoma is associated with decreased expression of death receptors for tumor necrosis factor-related apoptosis-inducing ligand. *Human Pathology* **37** (10), 1286 (2006).

[45] Ashkenazi, A., Targeting death and decoy receptors of the tumour-necrosis factor superfamily. *Nat Rev Cancer* **2** (6), 420 (2002).

[46] Johnstone, R. W., Frew, A. J., and Smyth, M. J., The TRAIL apoptotic pathway in cancer onset, progression and therapy. *Nat Rev Cancer* **8** (10), 782 (2008).

[47] Crook, N. E., Clem, R. J., and Miller, L. K., An apoptosis-inhibiting baculovirus gene with a zinc finger-like motif. *J Virol* **67** (4), 2168 (1993).

[48] LaCasse, E. C. et al., IAP-targeted therapies for cancer. *Oncogene* **27** (48), 6252 (2008).

[49] Srinivasula, S. M. and Ashwell, J. D., IAPs: What's in a Name? *Molecular Cell* **30** (2), 123 (2008).

[50] Richter, B. W. et al., Molecular cloning of ILP-2, a novel member of the inhibitor of apoptosis protein family. *Mol Cell Biol* **21** (13), 4292 (2001).

[51] Lagacé, M. et al., Genomic Organization of the X-linked Inhibitor of Apoptosis and Identification of a Novel Testis-Specific Transcript. *Genomics* **77** (3), 181 (2001).

[52] Eckelman, B. P., Salvesen, G. S., and Scott, F. L., Human inhibitor of apoptosis proteins: why XIAP is the black sheep of the family. *EMBO Rep.* **7** (10), 988 (2006).

[53] Conze, D. B. et al., Posttranscriptional downregulation of c-IAP2 by the ubiquitin protein ligase c-IAP1 in vivo. *Mol Cell Biol* **25** (8), 3348 (2005).

[54] Silke, J. et al., Determination of cell survival by RING-mediated regulation of inhibitor of apoptosis (IAP) protein abundance. *Proc Natl Acad Sci U S A* **102** (45), 16182 (2005).

[55] Krajewska, M. et al., Elevated expression of inhibitor of apoptosis proteins in prostate cancer. *Clin Cancer Res* **9** (13), 4914 (2003).

[56] Grossman, D., McNiff, J. M., Li, F., and Altieri, D. C., Expression and Targeting of the Apoptosis Inhibitor, Survivin, in Human Melanoma. **113** (6), 1076 (1999).

[57] Florell, S. R. et al., Proliferation, apoptosis, and survivin expression in a spectrum of melanocytic nevi. *Journal of Cutaneous Pathology* **32** (1), 45 (2005).

[58] Gradilone, A. et al., Survivin, bcl-2, bax, and bcl-X gene expression in sentinel lymph nodes from melanoma patients. *J. Clin. Oncol.* **21** (2), 306 (2003).

[59] Takeuchi, H., Morton, D. L., Elashoff, D., and Hoon, D. S., Survivin expression by metastatic melanoma predicts poor disease outcome in patients receiving adjuvant polyvalent vaccine. *Int J Cancer* **117** (6), 1032 (2005).

[60] Piras, F. et al., Nuclear survivin is associated with disease recurrence and poor survival in patients with cutaneous malignant melanoma. *Histopathology* **50** (7), 835 (2007).

[61] Ding, Y. L. et al., Nuclear expression of the antiapoptotic protein survivin in malignant melanoma. *Cancer* **106** (5), 1123 (2006).

[62] Chen, N. et al., Caspases and inhibitor of apoptosis proteins in cutaneous and mucosal melanoma: expression profile and clinicopathologic significance. *Human Pathology* **In Press, Corrected Proof** (2009).

[63] Chawla-Sarkar, M. et al., Downregulation of Bcl-2, FLIP or IAPs (XIAP and survivin) by siRNAs sensitizes resistant melanoma cells to Apo2L//TRAIL-induced apoptosis. *Cell Death Differ* **11** (8), 915 (2004).

[64] Vogler, M. et al., Small Molecule XIAP Inhibitors Enhance TRAIL-Induced Apoptosis and Antitumor Activity in Preclinical Models of Pancreatic Carcinoma. *Cancer Res* (2009).

[65] Ricci-Vitiani, L. et al., Identification and expansion of human colon-cancer-initiating cells. *Nature* **445** (7123), 111 (2007).

[66] Pampaloni, F., Reynaud, E. G., and Stelzer, E. H. K., The third dimension bridges the gap between cell culture and live tissue. *Nat Rev Mol Cell Biol* **8** (10), 839 (2007).

[67] Colosimo, A. et al., Transfer and expression of foreign genes in mammalian cells. *Biotechniques* **29** (2), 314 (2000).

[68] Friend, D. S., Papahadjopoulos, D., and Debs, R. J., Endocytosis and intracellular processing accompanying transfection mediated by cationic liposomes. *Biochim. Biophys. Acta-Biomembr.* **1278** (1), 41 (1996).

[69] Gao, X., Huang, L., Cationic liposome-mediated gene transfer. *Gene therapy* **2**, 710 (1995).

[70] Fire, A. et al., Potent and specific genetic interference by double-stranded RNA in Caenorhabditis elegans. *Nature* **391** (6669), 806 (1998).

[71] Daneholt, B. and Nobelförsamlingen, RNA interference. *The Nobel Assembly at Karolinska Institutet* (2006).

[72] Rana, T. M., Illuminating the silence: understanding the structure and function of small RNAs. *Nat Rev Mol Cell Biol* **8** (1), 23 (2007).
[73] Meister, G. and Tuschl, T., Mechanisms of gene silencing by double-stranded RNA. *Nature* **431** (7006), 343 (2004).
[74] Soutschek, J. et al., Therapeutic silencing of an endogenous gene by systemic administration of modified siRNAs. *Nature* **432** (7014), 173 (2004).
[75] Zimmermann, T. S. et al., RNAi-mediated gene silencing in non-human primates. *Nature* **441** (7089), 111 (2006).
[76] Shrivastava, N. and Srivastava, A, RNA interference: An emerging generation of biologicals. *Biotechnology Journal* **3** (3), 339 (2008).
[77] Godal, A., Fodstad, O., Morgan, A. C., and Pihl, A., Human melanoma cell lines showing striking inherent differences in sensitivity to immunotoxins containing holotoxins. *J Natl Cancer Inst* **77** (6), 1247 (1986).
[78] Goto, Y. et al., Human High Molecular Weight-Melanoma-Associated Antigen: Utility for Detection of Metastatic Melanoma in Sentinel Lymph Nodes. *Clin Cancer Res* **14** (11), 3401 (2008).
[79] Pfaffl, M. W., A new mathematical model for relative quantification in real-time RT–PCR. *Nucleic Acids Research* **29(9)** (2001).
[80] Leslie, G., Flow Cytometry - A Basic Guide.
[81] Vucic, D. et al., ML-IAP, a novel inhibitor of apoptosis that is preferentially expressed in human melanomas. *Current Biology* **10** (21), 1359 (2000).
[82] Gong, J. et al., Melanoma inhibitor of apoptosis protein is expressed differentially in melanoma and melanocytic naevus, but similarly in primary and metastatic melanomas. *J Clin Pathol* **58** (10), 1081 (2005).
[83] Kasof, G. M. and Gomes, B. C., Livin, a novel inhibitor of apoptosis protein family member. *J. Biol. Chem.* **276** (5), 3238 (2001).
[84] Rajeshkumar, N.V et al., in *Cancer Stem Cells: Therapies and Chemoresistance* (AACR meeting 2009, Abstract # 1069).
[85] Wagner, K. W. et al., Death-receptor O-glycosylation controls tumor-cell sensitivity to the proapoptotic ligand Apo2L/TRAIL. *Nat Med* **13** (9), 1070 (2007).
[86] Song, J. H. et al., Lipid rafts and nonrafts mediate tumor necrosis factor-related apoptosis-inducing ligand-induced apoptotic and nonapoptotic signals in non-small cell lung carcinoma cells. *Cancer Res.* **67** (14), 6946 (2007).
[87] Barbone, D. et al., Mammalian target of rapamycin contributes to the acquired apoptotic resistance of human mesothelioma multicellular spheroids. *J Biol Chem* **283** (19), 13021 (2008).